Pulsed electric field inactivation
in a microreactor

Promotor
Prof. dr. ir. R.M. Boom
Hoogleraar Levensmiddelenproceskunde, Wageningen Universiteit

Co-promotor
Dr. ir. P.V. Bartels
Senior scientist, Agrotechnology & Food Innovations

Promotiecommissie
Prof. dr. ir. A. van den Berg
Universiteit Twente
Prof. dr. T. Abee
Wageningen Universiteit
Prof. dr. A.J.W.G. Visser
Wageningen Universiteit
Drs. D.C. Esveld
Wageningen Universiteit en Research Centrum

Pulsed electric field inactivation in a microreactor

Martijn B. Fox

voor Erik

Contents

Chapter 1

Introduction

1.1 Microtechnology

Microtechnology evolved in the eighties with the lithographical technologies applied in the production of integrated circuits. The rapidly expanding knowledge on materials like silicon and glass and the improvement in micromachining techniques like photographic pattern transfer, etching techniques and deposition techniques made it possible to design highly specific structures with sizes in the range of 0.1 to 100 μm.

These structures have resulted in various devices aimed at micromechanical, microfluidic and microreactor technological applications. Typical applications in micromechanics are accelerator detectors, which are applied in air bags, and optical applications like the arrays of canting mirrors in a beamer for optical switching.

Microfluidics is the field of research where fluid dynamics is combined with microengineered structures, which introduces several specific characteristics related to the small dimensions. The flow characteristics in microchannels are mainly determined by the surface properties, in contrast to laboratory or larger scale equipment, where bulk fluid properties are more important. The small sizes are very advantageous for analytical applications, since surface phenomena prevail, which can be utilised in for example electroosmotic flow. In addition, small samples are required, separation efficiencies increase and thus separation times decrease. This resulted in the introduction of the μTAS (micro total analysis systems) concept and the Lab-on-a-chip concept, which basically aim to integrate several steps in sampling and analysis, on a single microtechnological chip. This reduces the costs, and since the chips are relatively small it is possible to apply these chips for point-of-care testing, where for example analysis of blood properties is done within a short time at the place where a patient resides.

The prevalence of surface phenomena is for example exploited for electroosmotic driven fluid flow. The wall of a microchannel is often charged and as a result charge separation will occur in the fluid at the wall. When an electric field is applied in the flow direction of a microchannel, the ions near the wall will move and drag the rest of the bulk fluid with it. This is for example utilised for the activation of flows in microfluidic chips (Haswell, 1997; Schasfoort, 1999; Valero *et al.*, 2005).

Microtechnology offers several specific advantages to reactor technology in comparison to common laboratory or larger scale equipment. First of all, the small size causes the fluid flow almost always to be laminar. Since the characteristic dimensions of microtechnological devices are very small, Reynolds numbers in microtechnological structures are often below one. This means that viscous forces are dominant over inertial forces and turbulent mixing is not possible, which makes the flow patterns highly predictable. This phenomenon can for example be exploited in highly controlled extraction processes in microfluidic chips as two (miscible) flows can be brought together in a region where mass transfer of a certain component can take place, while the two phases can be

separated afterwards without need for extra equipment like membranes to keep the two phases separated (Brody *et al.*, 1997).

However, it should be noted that the laminar flow also implies that mixing of fluids in microtechnological structures is not as obvious as in larger equipment. Therefore different microtechnological based mixers have been developed, e.g. (Bessoth *et al.*, 1999; Lin *et al.*, 2005), dedicated to mixing fluids in microtechnological structures. In these mixers, the two fluids are brought in close proximity by stacking and folding of the separate streams.

Secondly, mass transfer by diffusion will be very fast. The diffusivity itself is not affected, but as the distances over which components have to travel are very short, the transfer of the components will be very rapid. This advantage is also utilized in the mixer described above.

A similar advantage is the fast heat transfer in microtechnological structures. The smaller structures become, the larger the surface-to-volume ratio will be. This, and the fact that the distances are very small, is advantageous for addition or removal of heat and therefore also for control of the temperature. This has been applied in microtechnological heat exchangers aimed at chemical process industry (Ehrfeld *et al.*, 2000) as well as in microfluidic glass chips. Guijt *et al.* (Guijt *et al.*, 2003) for example introduced a special design where a temperature sensitive reaction in a microtechnological channel could be controlled by introducing a parallel channel in which an exothermic reaction took place to increase the temperature. However, heat can also be removed quickly by the large surface area, as was demonstrated by Schneider *et al.*, who studied highly exothermic reactions in a microfluidic device (Schneider *et al.*, 2004).

1.2 Pulsed electric fields technology

Shelf stable fluid foods are usually heat pasteurized or sterilized to inactivate pathogenic and spoilage microorganisms and enzymes. As a result of this thermal treatment, the taste, texture and nutritional quality of the food product are unfortunately also degraded. New pasteurization methods like ultra high pressure (UHP) or pulsed electric field (PEF) inactivation have a low thermal impact on the product and therefore preserve the intrinsic quality of the product better. These technologies are under development and are gaining more and more interest as an alternative to conventional thermal preservation methods.

The PEF process relies on the electroporation of microorganisms by short, high electric field pulses. Sale and Hamilton (Hamilton *et al.*, 1967; Sale *et al.*, 1967; Sale *et al.*, 1968) were the first authors to report the inactivation of microorganisms using high electric field pulses. Since that time much research has been conducted, concentrating on the technological aspects (Yin *et al.*, 1997) and microbial inactivation kinetics (Peleg, 1995), as well as on the implications for the food product, like by-product formation (Reyns *et al.*, 2004) and metal ion release from the electrodes (Roodenburg *et al.*, 2005; Roodenburg *et*

al., 2005). This recently resulted in the first commercial application for PEF in the summer of 2005 (The Associated Press, August 18, 2005).

In PEF, short (typically in the microsecond range), high electric field (10 to 60 kV cm^{-1}) electric field pulses are applied to a food sample (Knorr *et al.*, 2001). Since the electric field pulses need to be conducted through the food sample, especially fluid foods like juices or milk are suitable for PEF pasteurization. These fluid foods can be transported through channels with suitable electrode configurations while being treated in a continuous way. Besides microbial inactivation, PEF can also be used to increase extraction yields of intracellular components from cells, like the extraction of sugar from sugar beets (Belghiti *et al.*, 2004).

When an electric field is applied over the food sample, the potential drop over a microbial cell will be mainly focused over the cellular membrane as the fluid food matrix and the intracellular matrix are very conductive compared to the cellular membrane. This will create a high electric field strength over the very thin cellular membrane.

Figure 1.1 Schematic representation of pore formation in a cellular membrane. A hydrophobic pore (left) is formed first, followed by a hydrophilic pore which eventually becomes irreversible.

The membrane itself consists of a phospholipids bilayer, which has already very small short-lived defects due to random thermal fluctuations. The high electric field causes these defects to form small hydrophobic pores (Fig. 1.1). When the electric field strength is increased even more, these pores can grow and become hydrophilic, a process known as electroporation. Small hydrophilic pores can be reversible; i.e. they can reseal when the electric field is removed. This reversible electroporation is often used in biotechnology for the introduction of foreign molecules like DNA to a cell. In this case the cell has to be electroporated, but reseal afterwards to stay alive with the included foreign molecules. At a certain pore size, the pores become irreversible, which leads to cell death (Chang *et al.*, 1992).

PEF makes use of irreversible electroporation of the cellular membrane to inactivate microbial cells. However, this mechanism does not apply to microbial spores which cannot be inactivated by PEF and the technique is therefore yet unsuitable for sterilization (Barbosa-Canovas *et al.*, 1999).

1.3 Microtechnology and PEF

At the moment, PEF faces a few challenges, associated with the use of high electric fields in fluids. First of all, the applied voltage pulses have to be very high (tens of kilovolts), in order to reach the high electric field strengths. The pulses have to be short (few microseconds) and preferably square to limit the total amount of applied energy. These requirements can only be met by dedicated electrical pulsers, which have to be especially designed to apply the pulses in a controlled way. As the electrical breakdown in a gas happens at much lower electric field strengths than the breakdown of water, gas bubbles should be kept outside the treatment chamber, since arching can seriously damage the PEF treatment chamber and the product. The temporal high electric current can also cause deterioration of the electrodes by electrolysis. When the electrodes are corroded, the electric field distribution inside the PEF reactor will be disturbed, resulting in a less optimal treatment of the fluid. This introduces an increasing chance of arching and thus further electrode damage, while dissolved electrode material will contaminate the product.

Secondly, the temperature of the fluid increases during PEF treatment. Since electrical pulses are given to the fluid, the temperature will rise due to ohmic heating. Application of electrical pulses at higher temperatures improves the inactivation of microorganisms (Sepulveda *et al.*, 2005), but the increase should not be too high, as too high temperatures can change food properties this technology aims to preserve.

Microtechnology can be an aid in eliminating these challenges. Because of the small electrode distances, only low voltages need to be applied to get high electrical field strengths. If the electrode distance is 10 μm, a 10 V pulse will already give a 10 kV cm^{-1} electric field strength. Therefore, generally available equipment can be used and more defined pulseforms (which are hard to generate at high voltages) can be applied. Secondly, the large surface-to-volume ratio will make temperature control much easier, thereby making it possible to distinguish electric field related effects from temperature effects, which is a great advantage in the research of PEF kinetics.

1.4 Project aim and cooperation.

The overall aim of this thesis is to obtain more insight in the specific characteristics and the potential of the PEF process in a microtechnological reactor. First of all, a microreactor needed to be designed and validated with existing process equipment. The developed PEF microreactor offers some unique opportunities, like fast heat exchange and the possibility of online observation, which will be explored in the study of the PEF process in a way which is not possible with laboratory scale equipment. This thesis will focus on the application of the microreactor where these features will be investigated in more detail. Differences between these microreactors and conventional cells will yield information on the mechanisms (e.g. the influence of heat).

The required combination of expertises in this research project was made possible due to the close cooperation established with both MESA+ at Twente University and the institute for Agrotechnology and Food Innovations in Wageningen. The experience in microfluidics and microtechnological laboratory facilities in the group of Prof. A. v. d. Berg lead to the design and manufacturing of the PEF microdevice. The parallel study in this project conducted by A. Valero in Twente made it possible to compare the inactivation in a flow trough and static device. The experience in PEF processing of Dr. H. Mastwijk and the laboratory PEF equipment at the Food Safety group at A&F accumulated in the set-up and validation of the microdevice. The project was initiated by Dr. P. Bartels. The project was financed by both the graduate school VLAG and Agrotechnology and Food Innovations.

1.5 Outline of this thesis

In **chapter 2**, an overview on already existing microtechnological devices for electroporation of cells will be given. The different devices are reviewed based on their application; for analysis of components or the electroporation process itself, for transfection of cells with foreign molecules or for inactivation of cells. Subsequently, the different design approaches are compared, discussed and recommendations for future designs are given. **Chapter 3** introduces the new PEF microreactor. The electric field distribution and flow patterns within the microreactor are modelled to investigate the functionality of the device. A comparison with a laboratory setup is made to validate the microreactor. This comparison is done with a model system, consisting of artificial vesicles.

The PEF microreactor described in chapter 3 is used in **chapter 4** to study the inactivation of the microorganism *L. plantarum*, where membrane permeation is studied by flow cytometry and related to inactivation. The most important parameter to be studied is the effect of temperature as this is one of the first devices where electric effects and temperature effects can be separated.

Chapter 5 discussed the effect of electric fields on yeast in a combined study in the PEF microreactor and a single cell trapping device. The process is followed by studying membrane permeation and cell inactivation. Qualitative measurements in the trapping device are linked with quantitative measurements in the PEF microreactor.

In **chapter 6**, the potential application of microtechnological PEF in pilot scale productions is discussed. Considerations for a (conceptual) design of a microfluidic PEF system are discussed.

Chapter 2

Electroporation of cells in microfluidic devices

In recent years several publications about microfluidic devices have been published to study the process of electroporation, resulting in the poration of the biological cell membrane. The devices have been designed for analysis, transfection or pasteurization. High electric field strengths were created by the close proximity of the electrodes or by creating a constriction in between the electrodes which focuses the electric field. Detection is usually done by fluorescent labelling or impedance measurement. Most devices have been focussing at the electroporation process itself, but integration with separation and detection processes is expected. Especially single cell content analysis is expected to be a valuable addition to the microfluidic chip concept. Furthermore, microdevices can enhance the research in intracellular electroporation by using advanced pulse schemes.

2.1 Introduction

Microfluidics has been one of the fastest growing fields of research in recent years, as illustrated by the correspondingly large increase in the volume of publications on the subject (Schasfoort, 1999; Prins, 2001; Andersson, 2004). One of the exciting aspects of using microfluidics in combination with life sciences is the application of electric fields to treat, manipulate and analyse biological cells (Andersson, 2003; Andersson, 2004). When they are directed into the channel of a microfluidic device and an electric field is applied, cells can be affected by various different phenomena, depending on the strength and direction of the electric field, the time span that the electric field is applied for, the properties of the materials that the microfluidic chip is constructed from, the properties of the fluid in the channel and the characteristics of the biological cell itself.

When an electric field is applied to a fluid, the temperature of the fluid increases due to ohmic heating. This effect is related linearly to the conductivity of the fluid but quadratically to the electric field strength that is applied. One of the processes that is observed when fluid is exposed to electric fields in narrow channels is electroosmosis (Hunter, 1980; Wong *et al.*, 2004). Since many microfluidic devices have charged walls, a charge distribution develops in the fluid near the wall. An electric field directed along the channel will therefore cause the movement of charge within the fluid, resulting in fluid motion. Electroosmosis is used in many microtechnological applications as the driving force for fluid movement (electroosmotic flow, EOF) (Haswell, 1997; Schasfoort, 1999; Bruin, 2000; Prins, 2001; MacInnes, 2002). The controlled fluid movement by EOF has been used to direct biological cells by bulk fluid motion within microfluidic chips (Valero *et al.*, 2005; Washizu, 2005). In addition to bulk transport, an electric field will also cause the electrophoretic movement of cells suspended in a liquid, since the cells themselves are charged due to the composition of the cell membrane. Thus, the cells will be pulled towards the electrode with the opposite polarity to that of the cellular membrane by coulombic forces (MacInnes, 2002). This well-known phenomenon is used in single-cell capillary electrophoresis (Stuart *et al.*, 2002), to control bacterial concentrations in microdevices (Cabrera *et al.*, 2001) or to control the movement of cells within a microdevice (Li *et al.*, 1997). A third effect that can be used to manipulate biological cells with electric fields is dielectrophoresis. Since the electric field induces a dipolar charge distribution over the cell, the cell will be attracted to an electrode where the electric field converges. This effect has been used for cell manipulation (Doh *et al.*, 2005), as well as for other applications such as separating DNA molecules (Nedelcu *et al.*, 2004) or other macromolecules (Clague *et al.*, 2001).

Another effect that can be obtained using an electric field in the vicinity of biological cells is electroporation. This review will focus on the electroporation of cells in microfluidic devices, although cell electroporation is often combined with electroosmosis, electrophoresis and dielectrophoresis. When high electric fields strengths (> 1 kV cm^{-1}) are used and the field is pulsed, the integrity of a mammalian cell is comprised; an effect

known as electroporation (Chang *et al.*, 1992). Hamilton and Sale (Hamilton *et al.*, 1967; Sale *et al.*, 1967; Sale *et al.*, 1968) discovered that the application of high electric field pulses at typical field strengths of 10 kV cm^{-1} also affects the viability of bacterial cells. Upon the brief application of an electric field, an extra transmembrane potential (V_{TM}) is developed across the poorly conducting cellular membrane (Fig. 2.1). The V_{TM} is linearly proportional to the electric field strength and the cell radius. The lateral mobility of the phospholipids in the membrane causes hydrophobic pores to appear randomly in the membrane. It is demonstrated that these hydrophobic pores grow under the stress from the V_{TM} and become hydrophilic pores at a threshold V_{TM} of 0.5–1 V (Chang *et al.*, 1992; Ho *et al.*, 1997).
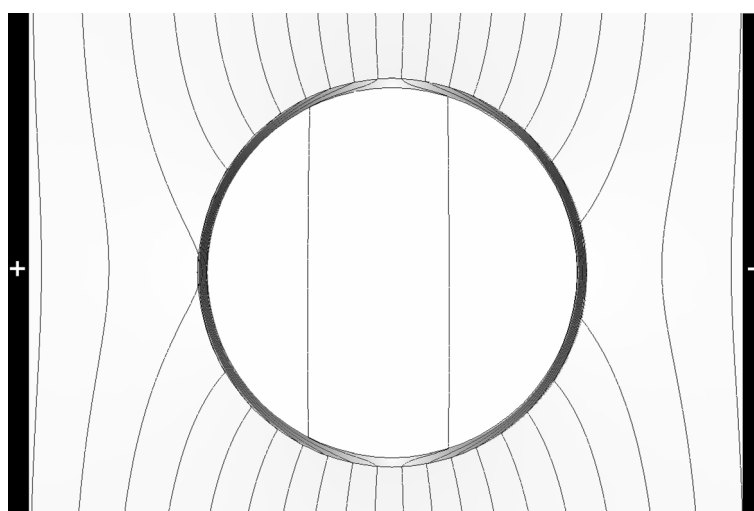
Figure 2.1 Schematic representation of a cell in an electric field. Black depicts high electric field strengths, white depicts low electric field strengths. The lines are equipotential lines.

Inducing a V_{TM} around the threshold V_{TM} in a mammalian cell results in reversible electroporation: the pores reseal given time (Chang *et al.*, 1992). It is assumed that the same picture applies to bacteria. Application of a TMP far above the threshold results in irreversible electroporation (the pores do not reseal) which leads to cell inactivation. Reversible electroporation is used to introduce foreign molecules into cells while the pores are open. Typical electric field strengths used for transfection are 1 kV cm^{-1}, often with long (milliseconds) exponential decay pulses. Although the literature is ambiguous about the exact mechanism of exchange between components in the surrounding medium and the contents of the cell, it is thought that local electroosmosis plays an important role (Dimitrov *et al.*, 1990). Electroporation has been used to introduce various components into cells, including proteins (Ho *et al.*, 1997), DNA (Prasanna *et al.*, 1997) Rb+ ions (Serpersu *et al.*, 1984; Serpersu *et al.*, 1985; Tsong *et al.*, 1985) and drugs (Tsong *et al.*, 1985). In contrast to reversible electroporation, where the cell viability is maintained, irreversible electroporation is used in a low-thermal pasteurization technique called pulsed electric field

(PEF) processing. Here, short (typically in the microsecond range), high electric field strength (typically more than 10 kV/cm) pulses are applied to a food product to inactivate the microorganisms in it (Wouters, 1999; Knorr *et al.*, 2001). When used on a large scale of 1000 L hr^{-1} or more, PEF provides a particularly good alternative to the usual heat pasteurization of pumpable foods (Barbosa-Canovas *et al.*, 1999) like fruit juices (Min *et al.*, 2003; Mastwijk *et al.*, 2004) or dairy products (Yeom *et al.*, 2004), and it can also aid the release of intracellular content from plant cells, for example during the extraction of sugar from sugar beet cells (Eshtiaghi, 2002; Belghiti *et al.*, 2004).

The use of microfluidic devices for cell electroporation applications offers clear advantages compared to common electroporation set-ups. First of all, by applying microelectronic pattern techniques, the distances between the electrodes in the microchips can be made very small, which means that relatively low potential differences are sufficient to give high electric field strengths in the regions between the electrodes. The electrical design of the pulser is therefore much simpler, which permits us to choose from a wider range of pulsers. This allows pulse forms other than the common block or exponential decay pulse shapes to be used (Schoenbach *et al.*, 2001). Cell handling and manipulation are also easier, as the channels and electrode structures are comparable to the sizes of the cells. As the hydrodynamic regime used in microfluidics is very different to that used in large scale equipment, it is possible to make use of specific hydrodynamic effects associated with this regime. The coupling between cell electroporation and separation or detection of the released components is also more direct, as it can be integrated onto the same device. This even makes it even possible to trap single cells and to determine intracellular content or other properties, which is hardly feasible using laboratory-scale equipment. In addition, only small amounts of cells and difficult-to-produce reagents, such as specific plasmids, are needed. On top of this, in situ optical inspection and real-time monitoring of the electroporation process (using fluorescent probes for example) also become possible, as the microdevices can be made transparent. However, the experimental results published so far have been mainly qualitative because the field of microtechnology is relatively new.

Finally, the area-to-volume ratio in microdevices is relatively large, which results in faster heat dissipation per unit surface area. This makes it possible to distinguish between heat and electric field effects, in contrast to the usual PEF experiments, where temperature increases of 10 °C and more are observed (Pol, 2000; Lelieveld, 2005), although this advantage is less important in transfection and analysis microdevices.

2.2 Overview of existing designs

One of the first single-cell electroporation devices was made by Lundqvist (Lundqvist *et al.*, 1998; Ryttsen *et al.*, 2000; Nolkrantz *et al.*, 2001; Olofsson *et al.*, 2003), who studied the electroporation of individual cells using two carbon fiber microelectrodes. These microelectrodes, which had diameters of 5 μm, were moved to within 2–5 μm of the cellular membrane with a micromanipulator. Single cells could be selected from a solution and successfully electroporated with 1 volt-millisecond square wave pulses. This set-up

gives a high degree of freedom when selecting cells, even in a complex multicellular system, and even for organelles, as was demonstrated by staining only the exonuclear cytoplasmic region with fluorescein. Gene transfection with GFP (green fluorescent protein) plasmids has also been accomplished (Lundqvist *et al.*, 1998). Although this design demonstrated the possibilities of single-cell electroporation, it is a labour-intensive technique, comparable to existing patch clamp techniques. Moreover, the cell is not brought into a confined geometry, which makes it unsuitable for automation.

Therefore, a more common approach is to use a microfluidic system which can handle small amounts of cells, combined with an electrical treatment based on integrated, fixed electrodes. These electroporation microdevices can be roughly divided into three categories, depending on their application:
1. Devices for analysis of cellular properties or intracellular content
2. Devices for transfection of cells
3. Devices for inactivation/pasteurization of cells

We now consider each of these in turn.

2.2.1 Devices for analysis of cellular properties or intracellular content

Electroporation microdevices are mainly used in the field of analysis, as the advantages of doing so are numerous, including the very small sample size needed, the high separation efficiencies obtained, and the ability to combine the technique with sensitive measurement methods. Applications of electroporation microdevices to analysis vary from those devices which measure true electroporation properties, like the pore formation process, to those where electroporation is only an aid to further analysis of the cell content, notably by capillary electrophoresis (CE). Another application involves measuring the cell concentration in a bulk fluid.

CE is a technique that has evolved significantly due to the use of microtechnology (Zabzdyr *et al.*, 2001). The capillary structures are relatively simple to make in several materials, the devices are suitable for coupling to sensitive detection methods, and they are cheap to produce (Jankowski *et al.*, 1995; Yeung, 1999; Zabzdyr *et al.*, 2001; Vrouwe *et al.*, 2004). In conventional CE of cell content, a batch of cells is lysed after which a small sample is analyzed (Verpoorte, 2002). However, since the average properties of a larger group of cells are measured, valuable information is lost. Therefore, one of the most important challenges in CE (and microtechnology in general) is to be able to analyze the contents of a single cell (Munce *et al.*, 2004). Whereas cell lysis can be accomplished using methods like chemical lysis (Wheeler *et al.*, 2000), electroporation has the advantage that no chemicals need to be added to the system, which could disturb the measurements. Gao *et al.* (Gao *et al.*, 2004) used electroporation in a microfluidic device to release the cellular content. Their design consists of a simple crossed channel, in which erythrocyte cells are loaded using a pressure gradient (Fig. 2.2a). When a cell arrives at the crossing, an EOF is used to direct the cell into the separation channel, after which the flow is stopped for 15 s to allow the cell

to attach to the wall. The cell is then electroporated using a one-second 1400 V pulse. In this way, the single-cell glutathione content was measured in a reproducible way without the need to use disturbing lysing agents. McClain *et al.* (McClain *et al.*, 2003) also reported on a CE chip for single-cell analysis, in which continuous 450 V m^{-1} square wave pulses with a DC offset of 675 V m^{-1} were used. The DC offset provides the necessary potential for separation, while the pulses are used for electroporation. A nonpulsed but high DC current would result in too much ohmic heating. Using this device, cells which were previously loaded with several fluorescent stains were electroporated, which was followed by the separation and measurement of the stains.

Although these are effective demonstrations of single cell electroporation coupled to separation and analysis, more advanced designs have been proposed for the electroporation of biological cells. In a series of articles (Huang *et al.*, 1999; Davalos *et al.*, 2000; Huang *et al.*, 2001; Huang *et al.*, 2003), Huang and Rubinsky presented a microfluidic device in which a single cell is captured and electroporated for analysis purposes. This chip (Fig. 2.2b) (Huang *et al.*, 1999; Huang *et al.*, 2001) consists of two chambers in n+ polysilicon, separated by a 1 μm thick silicon nitride membrane with a hole. The hole diameter (2 to 10 μm) in the membrane is smaller than the cell diameter. Pulses are applied via the conducing n+ polysilicon layer. Since the thin polysilicon layer is translucent, it is possible to observe the chip while treating biological cells. Cells are pumped through the top chamber, followed by the immobilization of one cell in the hole by lowering the pressure in the bottom chamber. The electrode distance is 900 μm, but the electric field is focused in the pore of the silicon nitride membrane. Therefore, only pulses of 0 to 120 V are needed for cell electroporation. The electroporation and resealing process can be followed in time via impedance measurements as the cell plugs the hole (thereby strongly changing the impedance). With this chip, Huang *et al.* were able to show the natural difference in electroporation behaviour between human prostate adenocarcinoma and rat hepatocyte cells.

The n+ polysilicon electrode was replaced in later publications (Huang *et al.*, 2001) by an Ag/AgCl electrode, since the polysilicon electrodes hindered the precise characterization of the electrical properties of the cell membrane. This was caused by the complicated electrochemical behaviour at the electrode–electrolyte interface, particularly for DC and low-frequency pulses. By staining human prostate adenocarcinoma cells with YOYO-1 (a membrane-impermeable fluorescent DNA stain), it was possible to combine an impedance measurement with an optical measurement (Huang *et al.*, 2003). This combination showed that impedance measurement is a suitable way of measuring cell electroporation behaviour in the microdevice. With the same design, it was also demonstrated that it was possible to study the responses of cells to specific chemical substances, in this case Triton X-100, which is a cell lysis reagent.
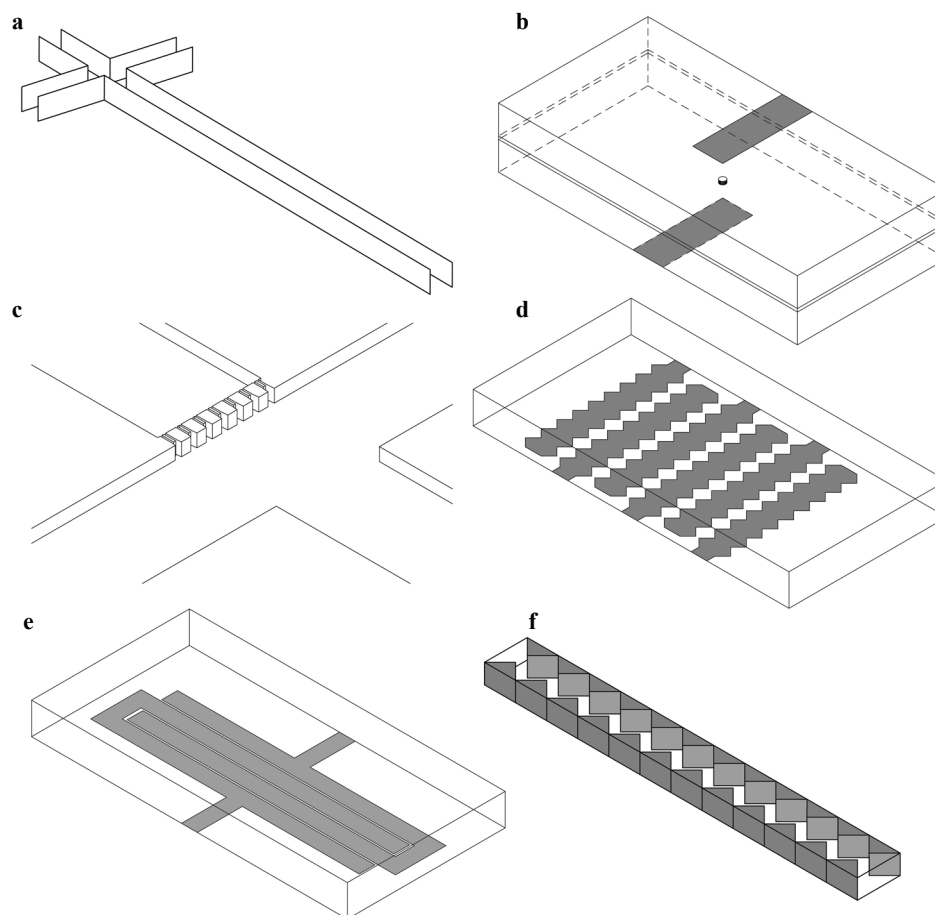
Figure 2.2a–f Schematic representations of different analytical microfluidic electroporation devices. Not to scale. a Gao *et al.* (Gao *et al.*, 2004); b Huang and Rubinsky (Huang *et al.*, 1999; Davalos *et al.*, 2000; Huang *et al.*, 2001; Huang *et al.*, 2003); c Valero *et al.* (Valero *et al.*, 2005); d Lee and Tai (Lee *et al.*, 1999); e Suehiro *et al.* (Suehiro *et al.*, 1999); f Lu *et al.* (Lu *et al.*, 2005).

Valero *et al.* (Valero *et al.*, 2005) used a different geometry to trap cells and subsequently electroporate them in order to study the electroporation behaviour. Their design consists of a chip with two crossing channels, where one side of the crossing is partially blocked; leaving special designed trapping sites with small flow channels behind the trapping sites (Fig. 2.2c). The trapping sites have a size which is approximately the size of a cell (10–12 μm), whereas the subsequent flow channel is 3 μm wide, preventing the cells from flowing any further than the trapping site. Gold wires inserted in the entrance reservoirs are used as electrodes. Using electroosmotic flow, human promyelocytic leukemic (HL-60) cells were directed towards the trapping sites, where they were trapped and subsequently

23

electroporated as the electric field was focused at the trapping sites. This device was applied to the study of apoptosis (controlled cell death), where the cells were observed visually while they were stained in the trapping site with fluorescent FLICA and propidium iodide.

As well as the aforementioned trapping devices, several flow-through devices have also been reported. Lee and Tai (Lee *et al.*, 1999) reported on a microdevice used for the lysis of cells for analysis, consisting of a straight, 30 μm-high microchannel with an electrode structure at the bottom perpendicular to the fluid flow (Fig. 2.2d). The electrode structure consists of interdigitated gold electrodes with a saw-tooth structure to enhance the electric field gradient. The tips of the saw-tooth structure are separated by 5 μm. Cells are introduced by pressure-driven flow and dielectrophoretically directed towards the tips of the electrode, where 20 V, 100 μs pulses were used to electroporate the cells. Various cell types, such as yeast cells, plant protoplasts and E. coli, could be electroporated. Although the design could be further optimized, the authors showed the ability of the device to electroporate small numbers of cells on the microscale, while concentrating the cells near the electrodes in order to increase electroporation efficiency.

Suehiro *et al.* (Suehiro *et al.*, 1999) used a variation of the device designed by Lee and Tai to measure the cell concentration. The device used by Suehiro has straight 12 μm-wide electrodes at a glass wafer (Fig. 2.2e), with a 5 μm clearance between the electrodes, instead of the saw-tooth structure used by Lee and Tai. Yeast cells from the pressure-driven fluid flow are directed dielectrophoretically towards the surface between the interdigitated electrodes using a 5 V, 100 kHz AC voltage, thereby changing the impedance between the electrodes. Since the impedance change is correlated to the time allowed for the cells to migrate towards the electrode structure and the cell concentration, it is possible to use the device to measure cell concentrations. However, the impedance changes are relatively small, which limits the sensitivity to 10^4 CFU ml^{-1} for yeast cells. In order to increase the sensitivity, Suehiro *et al.* (Suehiro *et al.*, 2003) increased the dielectrophoretic voltage stepwise to 20 V in order to electroporate the trapped cells. The electroporated cells have an improved conductivity because of the fractured membrane, which causes the lowest sensitivity limit to jump to 10^2 CFU ml^{-1}. This method has also been applied to bacterial E. coli cells (Suehiro *et al.*, 2005). As the sensitivity decreased, the form of the pulses used for electroporation had to be improved to make them continuous block pulses of a limited time, in order to avoid contamination by products generated by electrode degradation.

Lu *et al.* (Lu *et al.*, 2005) also used the advantageous saw-tooth structure for their more advanced microelectrode structure in order to enhance the electric field strength. A straight, 50 μm-high microchannel was constructed on pyrex glass, where the side-walls consisted of gold saw-tooth-shaped electrodes with a tip distance of 30 μm (Fig. 2.2f), supported by the polymer SU-8. Using pressure-driven flow, cells are directed through the channel and electroporated at the place where the electrodes are closest to each other (where the electric field strength is the highest). To avoid electrolysis in the channel, a continuous alternating voltage of 6–8.5 V at 5–10 kHz is applied to electroporate the cells. It was possible with this device to electroporate human carcinoma (HT-29) cells, as assessed using fluorescent acridine orange and propidium iodide staining. Although this design was designed to induce

cell lysis and therefore the release of intracellular content for further analysis, it could be used for transfection purposes as well, since transfection could take place in the channel and then the transfected cells could be sampled for further culturing.

2.2.2 Transfection designs

Transfection of cells with foreign DNA is often accomplished by reversible electroporation (Neumann *et al.*, 1989). However, the treatment protocols are often suboptimal (Chang *et al.*, 1992) and based upon the application of long-duration pulses (milliseconds) with relatively low electric field strengths, which results in an excess amount of inactivated cells. Furthermore, cells exposed to electric fields can be sensitive to substances in the medium such as Al^{3+} ions, which can become solubilized from the electrodes (Loomis-Husselbee *et al.*, 1991). It is possible to control the circumstances better in microfluidic devices, and hence increase the efficiency of transfection. Besides this advantage, only small amounts of transfection material are needed, and it is possible to make structures where the transfection of more cells in a parallel fashion is possible. Several microfluidic designs have been published, some aiming at single-cell transfection, others at the transfection of larger amounts of cells.

Lin *et al.* (Lin *et al.*, 2001) constructed a device made of PMMA that consisted of a 0.2 mm-high, 5 mm-wide channel with integrated gold electrodes at the top and the bottom of the channel at the electroporation spot (Fig. 2.3a). Since the electrode distance was relatively small, only 10 ms pulses of 10 V were required for electroporation. The efficiency of this simple design was proven by transfecting human hepatocellular carcinoma cells (*Huh*-7) with β-galactosidase and green fluorescent protein genes.

While Lin *et al.* used a small electrode distance to focus the electric field, it is also possible to do this by introducing a constriction between the two electrodes. Khine *et al.* (Khine *et al.*, 2005) used this concept in their design (Fig. 2.3b), which was originally developed as a multiple patch clamp array (Seo *et al.*, 2004). Although the constriction itself increases the electric field strength, this effect is enhanced in this design by applying a gentle underpressure and sucking a cell partially into the constriction, thereby blocking the constriction completely. The cell cannot pass the constriction because the cell diameter (12–17 μm) is approximately four times larger than the constriction (3.1 μm). Low potentials of less than 1 V could be applied using an Ag/AgCl electrode. The release of calcein and the uptake of trypan blue from HELA cells after electroporation was followed visually, although transfection with DNA has not yet been accomplished in this device type.
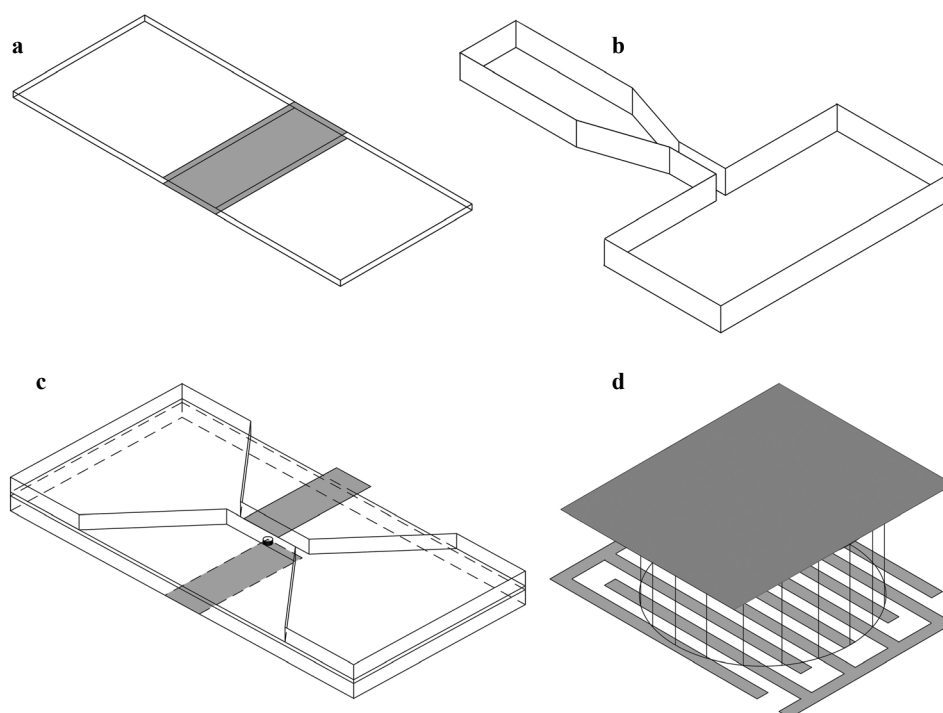
Figure 2.3a–d Schematic representation of various different transfection microfluidic electroporation devices. Not to scale. a Lin *et al.* (Lin *et al.*, 2001); b Khine *et al.* (Khine *et al.*, 2005); c Huang and Rubinsky (Huang *et al.*, 2003); d Lin *et al.* (Lin *et al.*, 2001; Lin *et al.*, 2003; Lin *et al.*, 2004).

Huang and Rubinsky, who designed an electroporation analysis device with a microhole in a silicon nitride membrane, also adapted this analysis-oriented design (Huang *et al.*, 2003) to make it applicable to cell transfection. They did this by creating a flow-through channel on top of a silicon nitride membrane that was approximately 1.5 times the size of a cell (Fig. 2.3c). The hole in the membrane is situated in the middle of the channel. Once a cell is brought into the microchannel, it is captured in the microhole by a backside pressure, electroporated, uploaded with the desired foreign molecules and then released, exiting the channel on the other side. The microhole in the silicon nitride membrane provides the necessary enhancement of the electric field. Using this design, it was possible to stain cells with fluorescent YOYO-1 using 100 ms, 10 V pulses and transfect them with an enhanced green fluorescence protein-gene.

While all the transfection-oriented designs above were aimed at cells in solution, Lin *et al.* (Lin *et al.*, 2001; Lin *et al.*, 2003; Lin *et al.*, 2004) created a microfluidic design aimed at the transfection of animal cells growing on a solid surface (Fig. 2.3d). The chip consists of a glass wafer with a gold interdigitated electrode structure, which is sealed with a PDMS mould to form a cavity. Cells grow on the glass surface. The interdigitated electrode

structure can be used to electroporate the surface-bound cells. In this way, it was possible to transfect Huh-7 cells, human embryonic kidney cells and HUVEC primary cells with GFP DNA. By adding an extra anode electrode above the interdigitated structure, negative DNA plasmids were directed to the cathodes by an electrophoretic potential (Lin *et al.*, 2004) prior to electroporation, creating a local high concentration of plasmids near the cells at the cathodes. Improved cell transfection was demonstrated by the relatively high concentration of transfected cells near the cathodes as compared to experiments where no electrophoretic forces were used.

2.2.3 Pasteurization design

In the food processing industry, electroporation is used for the pasteurization of liquid foods in what is known as pulsed electric field (PEF) processing (Knorr *et al.*, 2001). Pasteurization is used to render all spoilage bacteria present in the liquid foods inactive. Therefore, irreversible electroporation of all of the cells needs to take place. Because of this, and due to the fact that bacterial cells are generally significantly smaller than eukaryotic cells (1–5 μm), higher electric fields are required in PEF than in electroporation for transfection and/or analysis purposes.

Although microtechnology seems a less obvious choice for PEF applications because voluminous flows are processed, the use of microdevices avoids the risks involved with using high voltages and causes any heat generated to be rapidly dissipated. Because of this, microdevices should aid the exploration of other possibilities in the field of PEF.

The first PEF microreactor was presented by Fox *et al.* (Fox *et al.*, 2005), which consisted of a 50 μm-deep channel with a 10 μm-deep, 30 μm-long constriction to focus the electric field between the two electrodes (Fig. 4). It was possible to make a comparison with a pre-existing laboratory set-up (Pol, 2000), with a typical constriction size of 1×2 mm, using artificial vesicles loaded with carboxyfluorescein as a model system. This comparison showed that, despite the difference in length scales, the two devices were comparable when 2 μs square wave pulses of 0 to 800 V were used. Vesicle electroporation in both devices was studied using the transmembrane potential and the total amount of energy added as criteria for comparison. The total amount of energy added did not turn out to be a good parameter for comparing the laboratory set-up to the microtechnological set-up, as this criterion is mainly determined by the device. However, the transmembrane potential was a good parameter to use when comparing vesicle breakdown, as it describes effects happening in the vesicle itself, which eliminates structural effects.
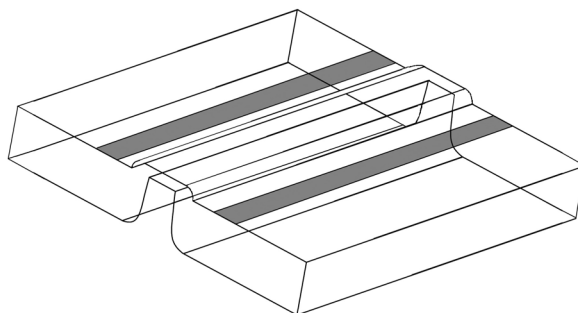
Figure 2.4 Schematic representation of the PEF microreactor (Fox *et al.*, 2005). Not to scale.

2.3 Technical comparison between the microfluidic devices

2.3.1 Electrode properties

The properties of the microdevices discussed above have been summarized in Table 2.1. High electric field strengths are required for electroporation. Two different strategies are used to achieve this in the discussed microdevices: the electrodes can be positioned in close proximity, or the electric current can be focused into a small flow constriction. The first approach has been applied by several authors (Lee *et al.*, 1999; Lin *et al.*, 2001; Suehiro *et al.*, 2003; Lu *et al.*, 2005). However, depending on the pulse scheme and pulse duration, this will inevitably lead to electrode degradation due to electrolysis. Electrolysis occurs when the potential difference is larger than the redox potential of the liquid and the pulse duration is longer than the time taken to charge the electrical double layer. Since the pulses applied in electroporation are usually higher than the redox potential, electrolysis will often take place. The close proximity of the electrodes will result in the contamination of the load with electrode material. Moreover, the local electric field will degrade as the electrodes corrode. Nevertheless, this approach is suitable for analysis-oriented designs, where single-cells must be electroporated in a controlled way with a limited number of pulses. However, in designs where pulses must be applied continuously, such as those intended for transfection or pasteurization, this approach has some serious drawbacks. The stronger electric field strengths present at the electrode surface might result in the formation of gas due to the electrolysis of water. Gas bubbles should be avoided in these microdevices as the breakdown potential of the gas is much lower than that of water, and so arcing can occur, which can seriously damage the electrode. If the average electrical current is low, the rate

of electrolysis is also low and the gas dissolves and is transported away. In many cases this is not sufficient.

The rate of electrolysis can be reduced by applying shorter pulses and thus reducing the current or by applying bipolar pulses instead of unipolar pulses, which makes the time-averaged current zero. If bipolar pulses are applied, electrolytic reactions still occur, but are then partially reversed during the successive pulse. Electrolysis can also be reduced by increasing the resistance between the electrodes, as the total current will also be reduced.
The other approach, taken in several devices (Huang *et al.*, 1999; Fox *et al.*, 2005; Khine *et al.*, 2005; Valero *et al.*, 2005), is more promising for designs where long intervals of pulses or continuous pulses are required. These designs make use of a constriction of the channel, which results in a high electrical resistance. The main potential drop in these devices is not in the vicinity of the electrode, which therefore prevents electrode degradation. Another option for decreasing the resistance would be to use low-conductivity fluids. However, the composition of the fluid is restricted by biological constraints in many cases.

Although the design and properties of the electrodes are more important in high than in low current applications, it is crucial to have a good electrode structure. Various materials have been used so far, including different metals, polysilicon and Ag/AgCl electrodes. For impedance measurements where high accuracy is needed, Ag/AgCl electrodes offer the best choice, since there is no polarization at the electrode surface. Polysilicon, which has elusive electrode surface properties, is a less obvious choice of electrode material. Metal electrodes seem to be the best choice for other applications, as the electrodes are easy to incorporate into the production process and the behaviour at the surface is well-known, although complex. The electrodes used in the microdevices reported here are unprotected electrodes, except in one case (Lee *et al.*, 1999), which makes them more susceptible to degradation by electrolysis. As discussed above, electrolysis can result in corrosion of metal electrodes (Roodenburg *et al.*, 2005) and degradation is even observed in the case of noble metal electrodes, as large fragments can break from the electrode at high electric field strengths, as reported by Lee (Lee *et al.*, 1999) and Fox (Fox *et al.*, 2005). Lee (Lee *et al.*, 1999) proposed a solution to this where a very thin Teflon layer was applied onto the electrodes. The electrode was therefore separated from the fluid. This technique has also been proposed in large-scale PEF equipment (Dunn *et al.*, 1987; Mazurek *et al.*, 1995; Lubicki *et al.*, 1997; Efremov *et al.*, 2000). It would be logical to think that such an approach should be copied in future microtechnological structures, for example by applying dedicated coatings (Baer *et al.*, 2003). However, care is required here, as the isolating layer will alter the form of the pulse form. It will act as a high-pass filter, blocking low frequencies and the DC component and therefore complicating the analysis and interpretation of the results.

Table 2.1 Technical specifications of the different electroporation microdevices

Publication	Materials	Focussing: mechanism	Typical size (μm)	Electrode material	Electrode distance	Movement mechanism	Flowthrough static
(Huang *et al.*, 1999)	n+ polysilicon siliconnitride	Constriction	2-10	n+ polysilicon Ag/AgCl	900 μm	PDF	Static
(Valero *et al.*, 2005)	silicon	Constriction	8-12	Au wires, not integrated	Very large	EOF	Static
(Gao *et al.* 2004)	Soda-lime glass	No focussing	-	ND, not integrated	Very large	PDF & EOF	Flow through
(McClain *et al.*, 2003)	White crown glass	No focussing	-	ND	Very large	EOF	Flow through
(Lee *et al.*, 1999)	Silicon	Electrode	+/ 16	Au	5 μm	PDF & DEP	Flow through
(Suehiro *et al.*, 2003)	Glass	Electrode	5 μm	Cr	5 μm	DEP	Flow through
(Lu *et al.*, 2005)	Pyrex glass & SU-8	Electrode	130	Au	30 μm	PDF	Flow through
(Lin *et al.*, 2001)	PMMA	Electrode	0.2	Au	0.2 mm	PDF	Flow through
(Khine *et al.*, 2005)	PDMS	Constriction	4*3.1	Ag/AgCl, not integrated	Very large	PDF	Static
(Lin *et al.*, 2001)	Glass, PDMS	Electrode	100	Au	100 μm	-	Static
(Huang *et al.*, 2003)	Silicon. siliconnitride	Constriction	6	Pt	ND	PDF	Flow through
(Fox *et al.*, 2005)	Glass	Constriction	30	Pt	70 μm	PDF	Flow through

PDF: pressure-driven flow, EOF: electroosmotic flow, DEP: dielectrophoresis, N.D. Not determined

2.3.2 Cell handling

A clear distinction can be made between static devices and flow-through devices, as summarized in Table 2.2. Static designs are most commonly used for single-cell measurements, as they facilitate sample introduction, treatment and analysis. To analyze single-cell content, it is essential to restrict the released cell content to a small volume in order to prevent dilution beyond the detection limit. Secondly, the separation of cellular debris and cellular content is required for many analysis methods. The biological cell is retained at a defined location, for example via suction at a small channel opening, and the extracted cell content can then be separated into a very narrowly defined volume. To study single-cell properties like impedance, the cell should be directed towards one place and immobilized there.

Flow-through devices are generally used for analysis devices where many cells are electroporated, as well as transfection devices, as it is important to collect a sample of the transfected cells for replication. This is even more important for a PEF device, as larger quantities of cells need to be treated in a production environment. To treat large quantities, a commercial PEF microreactor might be scaled-up by mass parallelization instead of by scaling-up by size.

2.3.3 Detection

While some researchers have just begun to look into the development of microdevices that perform both single-cell electroporation and subsequent analysis of the cell content (McClain *et al.*, 2003; Gao *et al.*, 2004), most of the electroporation microdevice research performed so far has focused on analyzing and understanding the electroporation process itself. Membrane integrity analysis is often performed optically, by measuring the uptake or release of fluorescent markers such as YOYO-1, PI, acridine orange, FLICA, calcein AM or CF. Measuring impedance is another technique that is often used to follow electroporation; this has the advantages of a fast, online response and a non-invasive nature. Transfection analysis has been performed with GFP genes and β-galactosidase genes. Once again, the GFP genes were used because they make optical detection easier.

Table 2.2 Electroporation and cell properties of the different electroporation microdevices

Publication	Purpose	Potential (V)	E-field (kV cm^{-1})	Pulse time	Tested cells	Cell size	Measurement method
(Huang *et al.*, 1999)	Analysis	0-60	N.D.	2 µs-100 ms	Human prostate adenocarcinoma cells Rat hepatocytes	20	YOYO-1
(Valero *et al.*, 2005)	Analysis	100	N.D.	Continuous DC	Human promyelocytic leukemic cells (HL-60)	10	PI/FLICA
(Gao *et al.*, 2004)	Analysis	1400	N.D.	1 s	Erythrocytes	10	CE
(McClain *et al.*, 2003)	Analysis		0.6	Continuous DC&block pulse	Jurkat	ND	OG, CF, Calcein AM
(Lee *et al.*, 1999)	Analysis	20	≈2	100 µs	*S. cerevisiae, E. coli,* plant protoplasts	2-35	Cell counting
(Suehiro *et al.*, 2003)	Analysis	20	N.D.	+/- 20 s AC	*S. cerevisiae*	5	Impedance
(Lu *et al.*, 2005)	Analysis	6-8.5	≈1-2	5-10 kHz AC	HT-60 cells	10	AO/PI
(Lin *et al.*, 2001)	Transfection	10	0.5	5 ms	*Huh-7* (human hepato-cellular carcinoma cells)		GFP/β-galactosidase plasmids
(Khine *et al.*, 2005)	Transfection	1	N.D.	6.5 ms	HELA cells	10	Calcein AM trypan blue
(Lin *et al.*, 2001)	Transfection	100	0.1-0.4	ND	Several endothelian cells	~ 10	GFP
(Huang *et al.*, 2003)	Transfection	10	≈2.5	100 ms	Human prostate adenocarcinoma cells (ND-1)	ND	YOYO-1 Enhanced GFP plasmids
(Fox *et al.*, 2005)	Inactivation	800	100	2 µs	Artificial vesicles	0.2	CF

PI: propidium iodide, CE: capillary electrophoresis, AO: acridine orange, GFP: green fluorescent protein, CF: carboxyfluorescein, OG: Oregon green, N.D. Not determined.

2.3.4 Cell types

Almost all of the devices reported have been tested with animal cells, or at least with cells that are relatively large in size, such as yeast and plant cells. Because the transmembrane potential over a cellular membrane is linearly related to the size of the cell, relatively low electric field strengths are sufficient for the electroporation of large cells, which makes testing easier. Secondly, the large cell size makes it easy to visually inspect the effects of the electric fields on the cells. This approach has been applied in most microdevices, and fluorescent markers have been used to study the cellular response microscopically in situ. An additional advantage of using large cells is that they are in the same size regime as the microtechnological devices. Hence, it is possible to trap them at certain locations in the microdevice, which is preferred for single-cell measurements. To perform single-cell measurements on smaller cells, for example bacterial cells, smaller structures with sizes on the order of 1 μm or even smaller are required. It is much more challenging to make microfluidic structures with these sizes, and so the development of devices aimed at bacterial electroporation has been retarded. Secondly, observing with a microscope becomes less feasible as the dimensions of a cell become comparable to wavelengths associated with light. Hence, more research is needed to improve single-cell bacterial electroporation measurements.

2.4 Future trends

2.4.1 Materials

Microchips are expensive to produce because of the costs of the substrate material and the many steps involved in the production process, such as photolithography, etching and cleaning (Becker *et al.*, 2000). This is not an issue for research prototypes or for devices that can be cleaned and then reused. However, such costs are a major issue for disposable devices intended for routine analysis. The need to reduce the costs has driven the general trend towards the production of polymeric microfluidic devices (Reyes *et al.*, 2002). Polymers are cheap compared to glass or silicon substrate and applicable for mass production technologies such as injection moulding, hot embossing, and the phase separation micromoulding process. Since many different types of polymers are available, which differ in their mechanical, optical and temperature properties as well as in resistance to chemical attack, polymer-based devices can be tailored to any application. A similar trend can be expected for microfluidic electroporation devices, as some devices are already polymer-based (Lin *et al.*, 2001; Khine *et al.*, 2005) or partially polymer-based (Lu *et al.*, 2005). One point to consider is the fabrication of the electrodes, which sometimes requires different techniques than glass-based microdevices. The deposition can often only be done with a shadow mask, which limits the dimensional accuracy (Becker *et al.*, 2000).

2.4.2 Integration of detection

As well as nonsilicon chips, we also expect the progressive integration of electroporation with subsequent measurements in future electroporation microdevices. Most existing analysis designs are able to monitor phenomena like fluorescence uptake of impedance changes at the area of electroporation. Gao (Gao *et al.*, 2004) and McClain (McClain *et al.*, 2003) showed that it was possible to combine electroporation with intracellular content analysis based on CE. However, the electroporation process itself in these devices is relatively rough, and more sophisticated devices with full control over the electroporation process as well as cell debris separation and subsequent intracellular cell content analysis have not been reported yet. Therefore, it is expected that integrated devices where combinations of electroporation, separation and analysis occur will emerge, such as devices with integrated chromatography, electrophoresis or isoelectric focusing steps for separation, and mass spectroscopic, electrochemical and fluorescent methods for analysis. Secondly, the present designs usually require multiple manual steps in order to insert the cells, electroporation them and measure the effects. Until now, no devices have been reported where all of these steps have been integrated in an automated way, preferably with multiple samples in parallel, which could greatly enhance the application of microtechnological analysis.

2.4.3 Intelligent handling

If the analysis and operation are integrated onto a microfluidic device, it becomes possible to manipulate the cell or fluid flow based on a previously measured signal. The electroporation process can then be triggered by the detection of a single or a sufficient number of cells between the electrodes. This can be combined with concentration methods that are used to reduce the volume, such as specially designed flow structures (Lettieri *et al.*, 2003), electric field methods like dielectrophoresis (Voldman *et al.*, 2001) or electrophoresis, which has been demonstrated by transfecting surface-bound cells in a local high concentration of plasmids (Lin *et al.*, 2004). It is also possible to select suitable cells prior to electroporation or to use a fluorescent or electrical response to separate the cells after electroporation.

2.4.4 Beyond simple pulses

The use of microtechnology allows the voltage required to reach sufficiently high electric field strength to be lowered. This makes it easier to use more advanced pulse forms then those currently provided by commercial high-voltage pulsers. Until now, mainly exponential decay and square wave pulses have been used, with pulse lengths of the micro- and milliseconds. However, recent publications (Mueller *et al.*, 2001) show that more advanced pulse forms can produce very different effects. The group of Schoenbach (Schoenbach *et al.*, 1997; Schoenbach *et al.*, 2001; Stacey *et al.*, 2003; Chen *et al.*, 2004;

Pakhomov *et al.*, 2004) demonstrated that high-frequency pulses with pulse durations of 10–100 ns can cause intracellular damage but they allow the extracellular membrane to remain intact. This opens up new possibilities in the field of apoptosis induction (Beebe *et al.*, 2003), gene delivery to the nucleus, or altered cell function, depending on the electrical pulse duration. Microtechnology offers the ability to study these effects.

2.5 Conclusions

Many microfluidic designs for electroporation aimed at the analysis, transfection or pasteurization of biological cells have been reported in recent years. This range of applications has resulted in a variety in designs: microchips in which cells move through a treatment zone, microchips in which cells are trapped at a specific location, and devices in which the cells are surface-bound. Relatively low voltages are required in such systems due to the close electrode spacing employed, which is even enhanced further in some cases by applying a constriction between the electrodes. This approach reduces electrolytic damage to the electrodes. Detection is usually performed by fluorescent visualization or via non-invasive impedance measurements.

Most of the devices reported so far have focused on just the electroporation process itself, but integration with separation and detection processes is expected to add further value to the concept of an integrated electroporation microfluidic chip in the near future. The field of single-cell content analysis—where the cell content is released by electroporation—is particularly promising, as it is difficult to accomplish in larger structures. Polymeric chips are expected for single-use electroporation devices. Furthermore, microfluidic devices can facilitate research into intracellular electroporation by applying advanced pulse schemes.

Chapter 3

A new pulsed electric field microreactor

This paper presents a new microreactor dedicated for pulsed electric field treatment (PEF), which is a pasteurization method that inactivates microorganisms with short electric pulses. The PEF microreactor consists of a flow-through channel with a constriction where the electric field is focussed. Compared to a laboratory-scale setup 25 times lower voltages were needed to obtain the same electric field strength due to the close electrode spacing. A finite element model showed that the electric field intensity is very homogeneous throughout the channel, which is crucial for pasteurization processes. Experiments where artificial vesicles, loaded with carboxyfluorescein, were electroporated showed that the maximum transmembrane potential adequately described the processes both in the microreactor and the laboratory-scale setup, although the length scales are different. Electroporation started at a transmembrane potential of 0.5 V, reaching a maximum fraction of electroporated vesicles of 51% at a transmembrane potential of 1.5 V. The partial electroporation is not a result of the heterogeneity of the vesicles or the electric field. With this new PEF microreactor it is possible to study the PEF process in more detail.

3.1 Introduction

The development of new, low thermal food preservation methods are of great interest to the food industry (Knorr *et al.*, 2001), because appearance, taste and nutritional value can be better retained (Barbosa-Canovas *et al.*, 1999). One of the novel low thermal technologies for pasteurization of fluid foods is pulsed electric fields (PEF). With this method, short (typically 2-300 μs), high (typically 20-60 kV cm^{-1}) electric field pulses are continuously applied through the food stream to inactivate the microorganisms. The resulting temperature increase is minimal compared to heat treatment.

Inactivation of microorganisms by PEF relies on electroporation of the cellular membrane (Sale *et al.*, 1967). When an external electric field is applied across a cell, a potential develops over the cellular membrane, the transmembrane potential (V_{TM}). Above voltages of 0.5-1 V, the membrane integrity is compromised and aqueous pores are formed. At low voltages these pores are reversible, which is for example used in molecular biology for gene transfer, where DNA has to enter the cell, but the cell should not be inactivated (Prasanna *et al.*, 1997). At higher voltages pore formation is irreversible, which is used for PEF, where the food has to be pasteurized.

Both in transfection and PEF, the high electric field strength is applied in pulses to limit the temperature rise due to ohmic heating. Pulses should be short to reduce the total energy dissipation and the residence time of the food sample should be short to maximize the heat removal. In electroporation for transfection purposes, batch processes are generally used, whereas in PEF continuous processes are applied.

Present PEF laboratory-scale equipment uses treatment chambers with a size in the order of a few millimetres and a residence time of a few milliseconds. However, the optimization of production and laboratory-scale PEF equipment is hampered by the instantaneous temperature rise of the product in the treatment chamber. A miniaturized PEF process unit has a number of specific advantages. First of all heat is removed more quickly due to the significantly larger surface to volume ratio of a microreactor, so it is possible to distinguish between electric and temperature effects during continuous flow processing. Secondly, a reduced electrode distance allows a lower voltage. The electric pulse can thus be controlled better, which opens possibilities for alternative pulse forms, such as shorter pulse forms and higher frequencies. Finally, the use of glass wafers to construct a PEF microreactor has the advantage that in situ visual inspection of electroporation and flow effects in the treatment chamber is possible.

Electroporation studies at microtechnological scale are focussed at the electroporation of single cells, either for gene transfection of micro organisms (Huang *et al.*, 2003), measurement of the electroporation kinetics (Huang *et al.*, 1999) or for the extraction of cellular content (Khine *et al.*, 2005). Until now, a few microtechnological flow-through devices have been reported that can be used for the transfection of cells (Huang *et al.*, 1999;

Huang *et al.*, 2001; Huang *et al.*, 2003; Khine *et al.*, 2005). However, the amount of fluid that can be treated is small, which is good for transfection, but for food preservation purposes larger amounts of fluid have to be treated in a continuous way.

Lin *et al.*(Lin *et al.*, 2001) constructed a microchannel flow through device made of PMMA in which fluid is treated by an electric field generated by two electrodes perpendicular to the flow direction. The electrode distance and thus channel height is 0.2 mm. The chip was designed for transfection purposes, but seems also applicable for PEF purposes. A disadvantage may be the low resistance between the electrodes, causing a high current density and hence promoting electrode damage by electrolysis.

We present a new PEF microreactor, based on the principle of focusing an electric field at a specific location in the fluid channel (Fig. 3.1). The microreactor consists of a channel with a constriction (Fig. 3.1b) with electrodes placed before and after the constriction to provide the electric pulses. In the constriction, the electric resistance is high compared to the larger channel sections, thereby focussing the electric field. Fluid flows through the channel driven by a pressure gradient and cells passing the constriction are continuously electroporated by the strong electric field. Since the electric field is focused, all the fluid that passes the constriction is exposed to it. Hence there are no spots with low electric field strengths where fluid can pass without treatment, which is crucial for pasteurization where typically a 99.99% reduction in microbial activity is required. This microreactor design allows having multiple constrictions in series to treat the fluid several times.
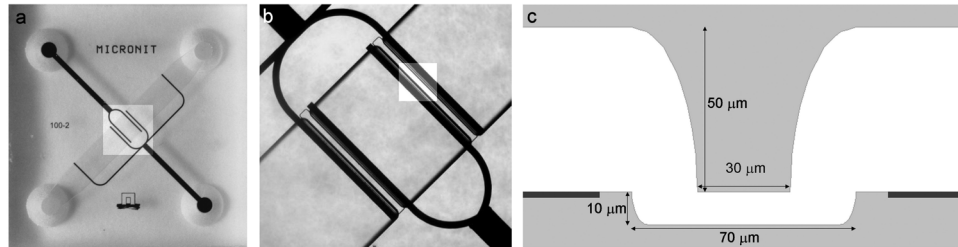
Figure 3.1 The PEF microreactor (a) with a close up (b) and a schematic side view (c) of the constriction (not to scale) with the electrode configuration. Fluid flows from left to right through the channel. Electrodes are shown in black.

The PEF microreactor will be compared to a standard laboratory-scale setup, which is currently used in PEF research. The electric field properties of both devices are compared using a finite element model, where a straight microchannel without a constriction will be examined as well. The treatment efficiency is compared for the PEF microreactor and the laboratory-scale PEF setup using artificially made vesicles loaded with a fluorescent indicator.

3.2 Materials and methods

3.2.1 PEF microreactor

The microreactor is constructed of two Borofloat glass wafers, with an entrance and exit hole powderblasted in the top wafer to enter a 50 μm deep, 1 mm wide HF etched channel. The constriction is created by leaving a barrier in the top wafer and by subsequently etching the 10 μm deep channel in the bottom wafer. The length of the constriction is 30 μm, which is determined by the not-etched-away barrier in the 50 μm deep channel (Fig. 3.1c). The platinum electrodes, 200 nm thick and 30 μm long, are placed at 30 μm of the constriction. Chips with two treatment chambers in series were used for experiments. The flow rate was 0.15 ml s^{-1}, using a syringe pump (Harvard Apparatus, Holliston, USA). The voltage was supplied by a pulser (HFDA, Malaga, Spain), measured with an oscilloscope (Tektronix, USA) and a 1000x probe (Tektronix, USA).

3.2.2 Laboratory PEF design

The reference Wageningen University laboratory-scale PEF device (Pol, 2001) consists of three stainless steel tubes with an inner diameter of 2 mm. In between the tubes two coaxial isolating rings with a slanted orifice are placed acting as treatment chambers with a radius of 1 mm and a length of 2 mm. High voltage pulses were applied to the middle stainless steel tube, whereas the outer two tubes were grounded. A vesicle solution (see section 3.2.4) was pumped through the setup at a flow rate of 1.17 ml s^{-1}.

3.2.3 Computer model analysis

The electric field distribution and the flow properties were compared for the PEF microreactor, a straight micro channel without a constriction and the laboratory-scale PEF setup (Table 3.1), using a finite element model in Femlab 3.0 (Comsol, Stockholm, Sweden). The electric field distribution was calculated for a DC field solving Gauss' law, with voltages chosen such that the minimum electric field strength was 14 kV cm^{-1}. The flow profile was calculated using an incompressible Navier-Stokes flow model with a Poiseuille flow profile at the entrance.

The electric field distribution was analyzed by following 20 equally spaced flow streamlines at the entrance. The maximum electric field strength (Fig. 3.4) and the total amount of added energy for each streamline were determined (Table 3.1). Using the volume fraction for each streamline, a cumulative distribution plot was made for the maximum electric field strength.

Table 3.1 Properties of the modelled PEF setups. With results used in further calculations.

	ΔV (V)	Flow (ml s^{-1})	V/E (μm)	ΔH_{min} (J ml^{-1})	d_{pef} (μm)
PEF microreactor	98	$0.15 \cdot 10^{-3}$	70	1.1	140
Laboratory-scale PEF	2524	1.16	$1.7 \cdot 10^3$	0.3	460
Straight channel	201	$0.15 \cdot 10^{-3}$	144	10.6	N.D.

3.2.4 Model system – vesicles

The efficiencies of the PEF microreactor and the laboratory-scale PEF setup were tested using vesicles as a model system. The vesicles were filled with carboxyfluorescein (CF) and were unilammelar and homogeneous in size. To prepare the vesicles, the procedure according to Hope (Hope *et al.*, 1985) and Mayer (Mayer *et al.*, 1986) was followed. The vesicles were made from dioleoyl phosphatidyl choline (DOPC) (Avanti polar lipids, Alabaster, USA), filled with 100 mM CF, 10 mM N-2-Hydroxyethylpiperazine-N'-2-ethanesulfonic acid (HEPES) solution (pH=7.4) in a 10 mM HEPES (pH=7.4), 16 mM NaCl and 268 mM sorbitol buffer.

The vesicle size was measured using dynamic light scattering (DLS). Vesicles without CF inside were used for these measurements, because the emission wavelength of CF (520 nm) interferes with the laser wavelength of the DLS setup (524.5 nm). Using the 90 degrees measuring angle, the diameter of the vesicles was determined to be 152 nm with a small distribution.

The bulk fluorescence was used to measure the amount of vesicle electroporation efficiency. At the used high concentrations of 100 mM CF inside the vesicles, quenching will take place (Fig. 2). The vesicle suspension therefore exhibits low overall fluorescence. Electroporation of the vesicles results in release of the CF and thus strong dilution to concentrations below 2 μM, where quenching does not occur anymore. As a result the fluorescence of the solution becomes a measure of the total amount of CF released and hence of the amount of vesicles electroporated. At low intensities, this correlation is linear (insert Fig. 2) and therefore the fraction of electroporated vesicles (X_v) was defined as:

$$X_v = \frac{I(t) - I_0}{I_{total} - I_0} \tag{3.1}$$

with I(t) being the intensity at time t, I_0 being the intensity at the beginning of the experiment and I_{total} being the total intensity of the bulk after chemical breakage of the vesicles using Triton X-100.
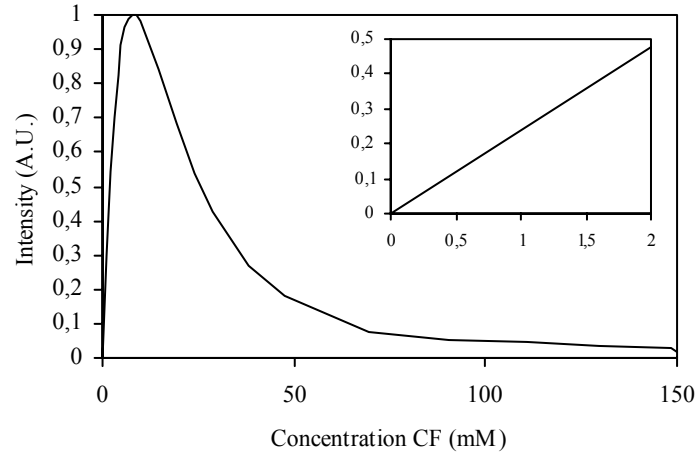
41

Figure 3.2 Fluorescent intensity of carboxyfluorescein as a function of its concentration.

The fluorescent intensity of the PEF microreactor was measured offline, while it was measured online in the laboratory-scale PEF setup, using a flow-through cuvette (Hellma, Müllheim, Germany) in a spectrofluorimeter (Perkin-Elmer, Wellesley, USA).

3.2.5 Treatment intensity analysis

In order to compare processes and systems, one requires equipment independent parameters to characterise the PEF treatment. The treatment intensity in the PEF microreactor and laboratory-scale PEF setup was compared on basis of both the maximum applied transmembrane potential and the amount of energy added per volume.
The transmembrane potential for a cell with a radius r, can be described in a simplified way for a DC field by

$$V_{TM} = k \cdot E \cdot r \cdot \cos(\varphi) \tag{3.2}$$

where k is a shape factor (1.5 for spheres), E is the electric field strength and φ is the angle between the applied electric field strength and the point of interest on the membrane. Equation 2 shows that the applied electric field strength and the cell radius are the most important parameters in describing the maximum transmembrane potential that can be developed. It is independent of the medium conductivity (σ), which is typically 0.1 to 3 S m^{-1} for a food product. The conductivity determines the dissipated energy density (Pd) in the fluid:

$$Pd = \sigma E^2 \tag{3.3}$$

The maximum voltage was measured during the experiments. An E/V scaling parameter was determined (Table 3.1) using the finite element model to calculate the maximum electric field strength (E) from this measured voltage (V).

For one pulse, the amount of added energy equals

$$\Delta H_{puls} = \frac{1}{R} \int_0^\tau V^2 dt = \sigma d_{pef} \int_0^\tau V^2 dt \tag{3.4}$$

The integral of $V^2 dt$ is determined numerically by taking for each pulse (with pulse length τ) the values of $V^2 > 0.05 \times V^2_{max}$ into account because of signal processing causes. From measurements it follows that the PEF cell is ohmic. Therefore the resistance of the treatment cell (R) follows from the cell constant (d_{pef}) and the conductivity of the fluid (σ). The total dissipated energy per volume of fluid (ΔH) is:

$$\Delta H = \frac{\Delta H_{puls} \, f \, n}{\phi} \tag{3.5}$$

where f is the pulse repetition frequency (Hz), ϕ is the fluid flow ($m^3 s^{-1}$) and n is the amount of treatment chambers in series.

3.3 Results and discussion

3.3.1 Electric field analysis

The electric field distribution was analysed with a finite element model for the laboratory-scale PEF device, for the PEF microreactor and for a straight microchannel without constriction (Fig. 3.3). Due to the increased electrical resistance in the constriction of the PEF microreactor and the laboratory-scale setup, the voltage drop is concentrated, causing high electric field strengths (Fig. 3.3a&b).

At the sharp edges of the constriction in the microreactor, local high electric field strengths occur, but this does not hamper the functionality of the chip. However, at the edge of the electrode a local high field strength of 18 kV cm^{-1} can be observed as well. This is an inherent disadvantage of the design, as the electrode material can get damaged. This problem is even more severe in the straight microchannel design (Fig. 3.3c) where the field strength at the edge of the electrode will be 54 kV cm^{-1}. Therefore a straight microchannel

without constriction is not a suitable design for the PEF process. The disadvantage of the peak electric field at the electrode edge was also confirmed by the observation that the electrodes slowly dissolved, starting from at the edges closest to the treatment chamber. Nevertheless, the PEF microreactor was able to operate at electric field strengths of 120 kV cm^{-1}, which far exceeds the values commonly obtainable with PEF equipment. Moreover, due to the small electrode spacing, 25 times lower voltages are required to obtain a similar electric field strength as compared to the laboratory-scale PEF equipment.
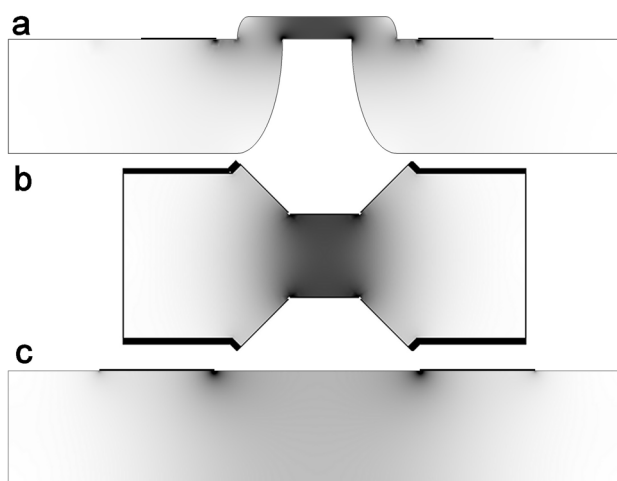

Figure 3.3 Electric field distribution in the PEF microreactor (a), the laboratory-scale PEF setup (b) and a straight microchannel without constriction (c) with the electrodes in black (not to scale). High electric field strengths are depicted blacker.

For a PEF unit to be used for pasteurization purposes, it is important that no volume fraction can pass with very low or no treatment. Therefore, the maximum electric field strength for the three designs has been analysed using a cumulative distribution plot (Fig. 3.4).

The voltages (Table 3.1) have been chosen such that all the fluid which enters the channel is treated with at least 14 kV cm^{-1}. This makes all the three designs a priori suitable for pasteurization. The model showed that the maximum electric field strength was lowest in the middle of the channel. The fraction of fluid that is over-treated at higher electric field strengths passed the electrode or the wall at a close distance. The distribution in the laboratory-scale PEF is steeper than in the two microtechnological designs because of the coaxial design with electrode material at all sides, whereas the PEF microreactor has a planar design with an electrode only at the upper side of the channel. Hence, the laboratory-scale PEF has a better distribution of the electric field than the PEF microreactor. The straight microchannel has a worse distribution than the PEF microreactor because there is no field focussing. This shows that the design of the microreactor can be further optimised

in terms of homogeneity of the electric field, e.g. by optimizing the electrode design. A comparison between the energy efficiencies of the different setups (Table 3.1), also shows the higher efficiency of the laboratory-scale PEF setup. The efficiency of the laboratory-scale PEF setup is approximately a factor 3 higher than the PEF microreactor.
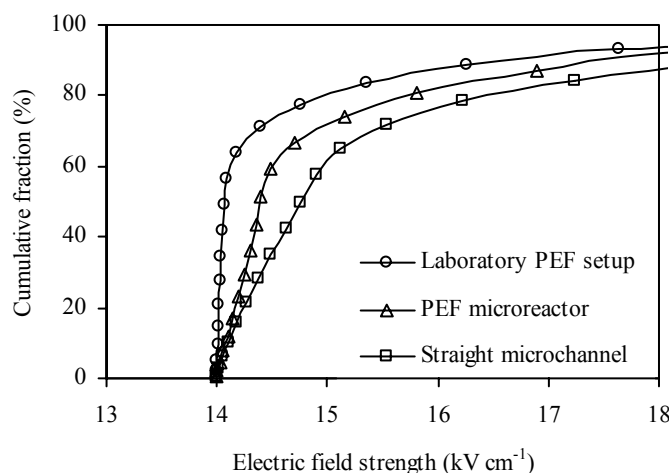

Figure 3.4 Cumulative distribution plot of the maximum voltage for the PEF microreactor, the laboratory-scale PEF setup and the straight microchannel. The plots go to 100% at higher electric field strengths.

3.3.2 Electroporation process

One of the major advantages using a miniaturized PEF setup in glass is the fact that the treatment chamber is visible. This makes the treatment chamber accessible for online optical inspection during experiments. Despite the fact that the vesicles are smaller than the wavelengths of visible light, they can be individually monitored under a microscope due to the strong fluorescent signal. In figure 3.5, the break-up of a vesicle loaded with CF was followed in time. In figure 5a, a vesicle was observed as a bright mark approaching the two electrodes (dark). The vesicle was breaking in figure 3.5b, releasing the CF and thereby causing a bright plume, which flows away (Fig. 3.5c).
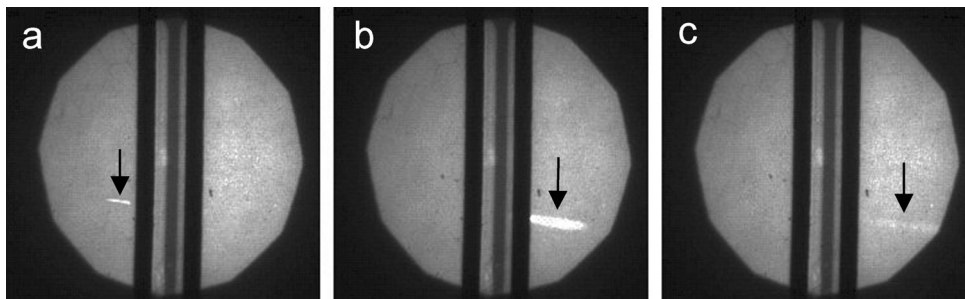
Figure 3.5 Breaking of a vesicle in time (from left to right) due to an electric field. The flow is oriented from left to right. The two dark lines are the electrodes with the treatment chamber in dark grey in between. The vesicle is the bright particle.

The treatment intensity in the PEF microreactor and the laboratory-scale PEF was also compared quantitatively using the bulk fluorescent signal. The vesicle electroporation was related both to the amount of applied energy and to the maximum transmembrane potential that was reached during the pulses (Fig. 3.6).

Due to the small size of the vesicles (a factor 10 smaller than cells), relatively high electric field strengths are needed to obtain electroporation. Therefore, we were able to electroporate maximally 12% of the vesicles with a maximum energy density of 30 J ml^{-1}. Using the PEF microreactor, we were able to reach energy densities of 240 J ml^{-1}, which is a factor 8 higher than the laboratory-scale PEF setup. As a result, we were able to electroporate a fraction of vesicles up to 51%.
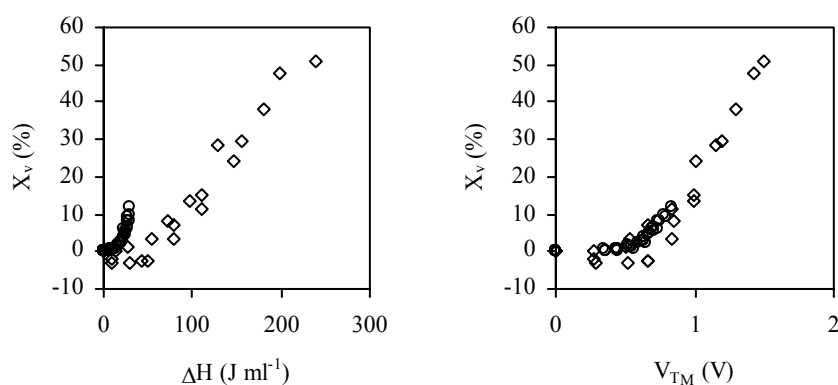

Figure 3.6 Vesicle electroporation in a laboratory-scale PEF setup(o) and PEF microreactor (◊) as a function of the total amount of added energy and maximum transmembrane potential.

The energy efficiency of the PEF microreactor was lower than the energy efficiency of the laboratory-scale PEF. To electroporate 10% of the vesicles, the laboratory-scale PEF setup needed approximately 28 J ml^{-1}, whereas the PEF microreactor needed approximately 100 J ml^{-1}. This is approximately a factor 3 higher, which is similar to the efficiency difference which follows from the simulations (Table 3.1).

A comparison on basis of the calculated maximum V_{TM} (Fig. 3.7b) clearly showed that vesicle electroporation in the laboratory-scale PEF setup and PEF microreactor behaved equal. Opposed to a comparison based on the energy density, the transmembrane voltage can adequately link the two processes at different size scales. The reason for this is that the maximum transmembrane potential does not describe behaviour of the treatment system, but only the response of the vesicular membrane to the electric field. The threshold for vesicle electroporation was approximately 0.5 V, which compares well to values reported in literature where it is stated that electroporation starts at a transmembrane potential between 0.5 and 1 V (Ho *et al.*, 1996).

Above the threshold transmembrane potential we observe a gradual increase of the electroporated fraction with increasing applied transmembrane potential. Such behaviour is always observed for electroporation of microorganisms, which is generally attributed to the heterogeneity in the microbial population and/or the heterogeneity in treatment intensity. However, in our specific set-up these complicating heterogeneities are absent and hence one would expect a very steep increase of the electroporated fraction above a threshold transmembrane potential. After all, the DLS indicated that the vesicles size distribution is mono-disperse with a mean diameter of 152 nm and certainly not differ so much to explain a factor 3 in threshold transmembrane potential. Also the analysis of the maximum electric field strength showed a very narrow distribution, by which only less than 10% of the vesicles would be electroporated at a V_{TM} 0.2 V below the rest.

This contradiction leads us to two hypotheses that might explain the gradual increase of electroporation. If the electroporation is not catastrophic for the vesicle integrity and the pore formation is reversible, only a fraction of the internal CF would be exchanged with the surrounding. As a result, only a fractional electroporation would be observed. Alternatively, it might be caused by the stochastic nature of the PEF process itself. As a result of the lateral mobility of the phospholipids, hydrophobic pores are by chance appearing in the membrane. These are essentially defects and serve as the onset for hydrophilic pore formation during the electric field pulse (Glaser *et al.*, 1988). Therefore the distribution in magnitude and angular positions of the hydrophobic pores will be reflected in stochastic nature of the electroporation process.

3.4 Conclusion

We demonstrated a new microtechnological microreactor design for the pulsed electric fields process, in which cells can be inactivated with electric fields. The chip has a flow-through configuration where the electric field is oriented parallel to the fluid flow and focussed in a constriction. The electrodes are placed as close to the constrictions as possible to prevent unnecessary energy loss.

The comparison between the PEF microreactor, a straight microchannel and a laboratory-scale PEF setup showed that a constriction was necessary to enhance the electric field and protect the electrodes from locally high electric fields and thus corrosion. In the PEF microreactor, the electric treatment was guaranteed in the complete channel, thereby making the design suitable for pasteurization purposes. The electric field strength in the PEF microreactor is 25 times higher than in the laboratory-scale PEF, which makes it possible to use notably shorter pulse forms.

Using artificially prepared vesicles, it was possible to observe the electroporation process online, which makes the online optical study of electric field effects with other fluorescent dyes for specific cellular processes also possible (Valero *et al.*, 2005). A quantitive comparison showed that the energy efficiency of the laboratory-scale PEF setup is higher than the PEF microreactor, but electroporation in both devices can very well be compared with the transmembrane potential. Electroporation of the small vesicles started at a transmembrane potential of approximately 0.5 V, which is confirmed by literature (Ho *et al.*, 1996). At higher electric field strengths, electroporation increased only gradually, which was is presumably to be linked partial, reversible electroporation or with the stochastic nature of membrane pore formation.

This transmembrane potential dependent electroporation opens possibilities in making the PEF process more compact with a higher energy efficiency by using shorter pulses and higher flow rates. Using the newly designed PEF microreactor, undesired side effects such as heat production and control problems can be minimized.

3.5 Acknowledgements

Chapter 4

Inactivation of L. *plantarum* in a PEF microreactor

This article describes the inactivation of L. plantarum by pulsed electric fields (PEF) in a microfluidic reactor. The microreactor has the specific advantage that the field intensity can be extremely high with accurate control and measurement of the pulse shape, combined with good temperature controllability. It is demonstrated that the temperature increase due to the ohmic heating of the fluid during treatment is marginal, thereby making this an excellent device for decoupling the temperature and electric field effects of PEF. Flow cytometry measurements showed that the electroporation of cells by PEF is a gradual effect. Reducing the pulse width at equal energy inputs did not show a change in inactivation. Higher temperatures showed higher inactivation rates. The effect of the temperature and the electric field strength could be described by a model that combines an Arrhenius equation for temperature dependency with either a Huelsheger or an activation energy based model for electric field dependency.

4.1 Introduction

Pulsed electric fields (PEF) is a low temperature, non-thermal based pasteurization method, which inactivates microorganisms without affecting the flavour, colour or nutritional components of food products to a great extent (Barbosa-Canovas *et al.*, 2001; Knorr *et al.*, 2001). The method is based on the application of short, high electric field pulses to a food sample, which inactivates microorganisms by damaging the cellular membrane. The cellular membrane is virtually non-conductive in comparison to the intracellular content and the medium and therefore is the potential drop over the cell from an externally applied electrical field mainly concentrated over the cellular membrane at the poles (Ho *et al.*, 1996). This transmembrane potential (V_{TM}) can be described for spherical cellular microorganisms by the cell radius (r) and the electric field strength (E)

$$V_{TM} = 1,5 \, r \, E \hspace{5cm} (4.1)$$

When the transmembrane potential reaches a value of approximately 1 V, the membrane integrity is affected (Hamilton *et al.*, 1967). The high electric field will initiate the formation of small pores, which can be reversible at low transmembrane potentials. At higher transmembrane potentials that are used in PEF, irreversible pores are formed, which results in cell inactivation (Sale *et al.*, 1967).

At the moment the application of PEF faces a few challenges. The analysis of the inactivation kinetics is inherently complicated by the characteristics of the PEF equipment. Because of the high electric field densities and the conductivity of the foods, ohmic heating will cause the fluid temperature to rise. Although inactivation levels increase at higher temperatures, the temperature increase should be minimized to prevent adverse effects to other product properties. Until now, it was experimentally very difficult to decouple the temperature effect and inactivation by the electric field treatment. Secondly, the control of the pulse shape is difficult as short, high voltage pulses are needed. This limits the degrees of freedom in electronic circuitry.

These problems can be circumvented by using microfluidics. In recent years, the field of microfluidics has seen a strong growth as techniques became readily available to make small, highly defined structures in a range of materials. Microfluidic electroporation devices offer a great advantage with regard to heat transport. Because of the high area-to-volume ratio, generated heat will be removed much faster, making a distinction between temperature and electric field effects possible. As the electrode distances will be much smaller, the required voltages are also much lower, making a more defined control of the pulses much easier.

The microfluidic PEF reactor designed for this study (Fox *et al.*, 2005) makes PEF possible at tenfold lower electrode potentials compared to laboratory equipment. The microreactor (Fig. 4.1) has been designed specifically so that all the fluid must pass the high electric field

zone. The PEF microreactor has several small constrictions that serve as an electrical resistance where the field is focused. With this setup, electric field strengths could be obtained up to 120 kV cm^{-1} although gradual electrode degradation was observed at these extreme electric field strengths.
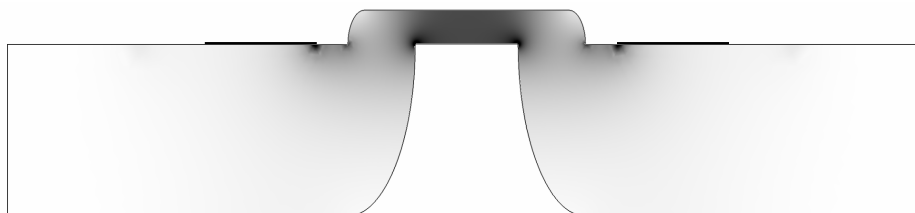

Figure 4.1 Schematic side-view of the PEF microreactor treatment chamber, with the electric field distribution. The black wide lines are electrodes, while the electric field is depicted in grey-scale (high electric field in black, low electric field in white)

In this article we study the effect of several process parameters on the inactivation of *L. plantarum* in the PEF microreactor. These parameters are the number of pulses combined with the pulse duration, but most important the temperature as this microreactor is one of the first designs which can separate temperature and electric field effects.

4.2 Materials and methods

4.2.1 Growth of bacteria and sample preparation

Lactobacillus plantarum DSMZ 20174 (Orla-Jensen, 1919) was grown at 30 °C on MRS medium (Merck, Germany). Cells were grown for two days and harvested in the stationary growth phase, washed twice and resuspended in 10mM N-2-hydroxy-ethylpiperazine-N-2-ethanesulphonic acid (HEPES) and 8 mM NaCl buffer (pH = 7, $\sigma \approx 0.1$ Sm^{-1}) to an OD$_{660}$ of approximately 0.2 (1 cm light pathway). Samples were filtrated through 5 μm pore size membranes (Sartorius, Germany) for removal of particles and stored on ice until further use.

4.2.2 Pulsed electric field microreactor

The used PEF microreactor, which has been described previously (Fox *et al.*, 2005), consists of two glass wafers with a 1 mm wide, 50 μm deep channel with two 10 μm deep, 30 μm long constrictions in series (Fig. 1). Pressure driven flow is used to pump the cells through the channel, using a syringe pump (Harvard Sciences, USA). Square wave pulses were applied by an Avtech AVR-4-B-WUA pulser which can give 100 ns to 100 μs, 0 V to

400 V pulses with a rise time of 20 ns. Electronic measurements were done with a Tektronix TDS 1012 oscilloscope wit a P5100 100x passive probe and a P220 1x/10x passive probe.

The electrical setup is depicted in Fig. 4.2. In this setup both the voltage is recorded and the current. The current is determined as a voltage across a resistor of 1 kΩ that is added in series. The chip and ohmic resistance are connected in series with a capacitor of 470 pF to eliminate low frequency currents that are present. This reduces the rate of electrolysis that deteriorates the electrodes contained in the microstructure. By introducing the capacitor, the pulse will switch polarity at shut off to obtain a zero time averaged current. If the capacitor is omitted, a time average non-zero current will be present. In this case one electrode will act as an anode where reducing reactions will take place, while the other will act as a cathode where oxidative reactions take place (Fox *et al.*, 2006).
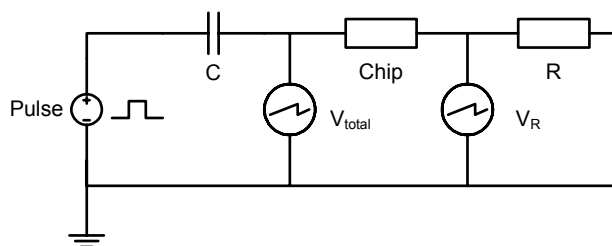
Figure 4.2 Electrical setup for the microfluidic chip

4.2.3 Temperature measurements

The temperature development inside the channel was measured using the temperature dependent fluorescence of the dye Rhodamine B. At higher temperatures, the intensity of Rhodamine B decreases with 1.95 % K^{-1} (own results and Ross *et al.*, 2001; Guijt *et al.*, 2003). The temperature was recorded at increasing electric field strengths from 0 to 43 kV cm^{-1}, and thus at increasing energy inputs of 0 to 140 J ml^{-1}. At each energy input, 10 pictures were taken and afterwards averaged, using Matlab with the image toolbox (version 7.0.0.19920, The MathWorks, Inc.). The temperature (T) was found in a range starting at room temperature of 23 °C (T_{23}), using the measured fluorescent intensity (I) and the intensity at 23 °C (I_{23})

$$T = 23 + \frac{(I_{23} - I)/I_{23}}{0.0195} \qquad (4.2)$$

4.2.4 Flow cytometry

Cells were stained with the BacLight bacterial viability kit (Invitrogen, USA), containing the nuclear stains propidium iodide (PI) and SYTO 9. Cells were incubated for 10 minutes after which flow cytometry (FCM) analysis was conducted. The FCM analyses were performed on a FACSCalibur flow cytometer (Becton Dickinson, USA), equipped with a 15 mW, 488 nm air-cooled argon ion laser. A band pass filter of 515 to 545 nm was used to collect green fluorescence (FL1), a band pass filter of 564 to 606 nm was used to collect the yellow-orange fluorescence (FL2) and a long-pass filter of 670 nm was used to collect red fluorescence (FL3). Forward scatter was collected with a diode detector; side scatter and fluorescence were collected with photomultiplier tubes. All signals were collected with logarithmic amplifications and the side scatter was used to distinguish cells from noise. Data were analysed using CellQuest (Becton Dickinson, USA).

4.3 Results and discussion

4.3.1 Temperature

Most PEF reactors at laboratory scale or pilot scale show an almost instant temperature increase after pulsing, caused by ohmic heating. Abram *et al.* (Abram *et al.*, 2003), for example, report that their experiments are performed at an inlet temperature of 30 °C and the outlet temperature never exceeded 40 °C. Although this temperature is below the inactivation temperature of *L. plantarum*, the instant temperature increase might add an extra stress to the cells, thereby increasing the inactivation rate especially since heating is done at an extremely fast rate. Until now, this temperature effect could not be separated from the electric field effect.

Using a PEF microreactor, the surface to volume ratio is much larger, resulting in fast heat dissipation. Therefore it is expected that only a marginal temperature increase will be recorded. This was verified by measuring the temperature inside the channel using a heat sensitive fluorescent dye, Rhodamine B of which the intensity decreases at increasing temperature (Fig. 4.3).
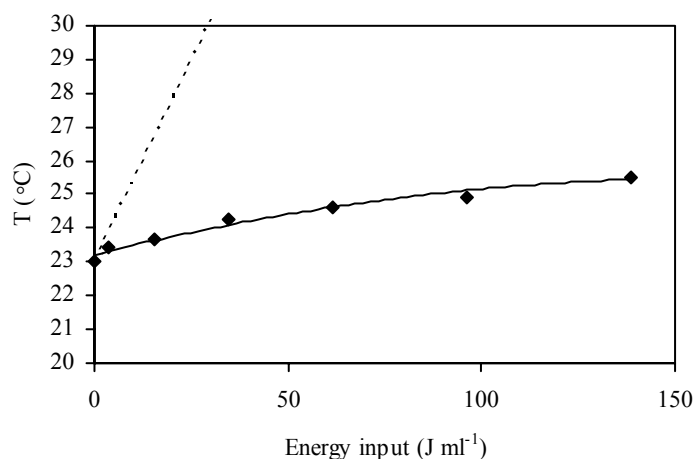
Figure 4.3 Temperature increase after the last treatment chamber in an 8 chamber PEF microreactor after addition of 1 kHz, 2 μs pulses with a fluid flow of 540 μl hr^{-1}. The case of adiabatic heating is depicted with the dashed line.

The measurement was determined after the last constriction of a chip consisting of 8 constrictions in series. The measurement at this spot shows that the temperature is higher with a larger energy input. This temperature increase is linear with the square root of the energy input. An energy input of 138 J ml^{-1} results in a temperature increase of 2.5 K (from 23 °C to 25.5 °C). In the theoretical case of adiabatic heating, the fluid temperature at this energy input would increase with 33 °C. This shows that the heat is indeed dissipated very fast. Besides this small temperature increase, it was also observed that the temperature difference of the fluid before and after the treatment chamber is negligible, which indicates that the dissipated energy is distributed very fast. These measurements show that the PEF microreactor is very suitable for temperature controlled PEF experiments.

4.3.2 Flow cytometry

In addition to regular viability measurements by plating, the membrane integrity of treated cells was also investigated using flow cytometry. Cells were stained with the fluorescent PI and SYTO-9 stains after treatment. PI is a membrane impermeable stain. When the membrane integrity is damaged, PI can enter the cell and intercalate with the DNA, thereby increasing the fluorescent intensity. SYTO-9 is a membrane permeable stain, generally showing a decrease in fluorescent intensity after membrane damage.

To make a distinction between inactivated and viable cells, heat inactivated cells and viable cells were compared on the flow cytometer as a reference, using the two stains. Two

distinct groups were observed where the inactivated cells showed a decrease both in PI and SYTO intensity (region L and D in Fig. 4.4). When cells were inactivated using PEF (Fig. 4.4), the same decrease in PI and SYTO intensity was observed. This is in contradiction to the general observation where PI intensity increases after membrane damage. Wouters *et al.* (Wouters *et al.*, 2001) and Abram *et al.* (Abram *et al.*, 2003), who also studied *L. plantarum* inactivation in a laboratory-scale PEF setup combined with PI flow cytometry, observed an increase of PI intensity after electroporation, although another strain of *L. plantarum* was used. However, a pattern similar to these measurements is found more often, for example for *Staphylococcus aureus* (Rice *et al.*, 2003).
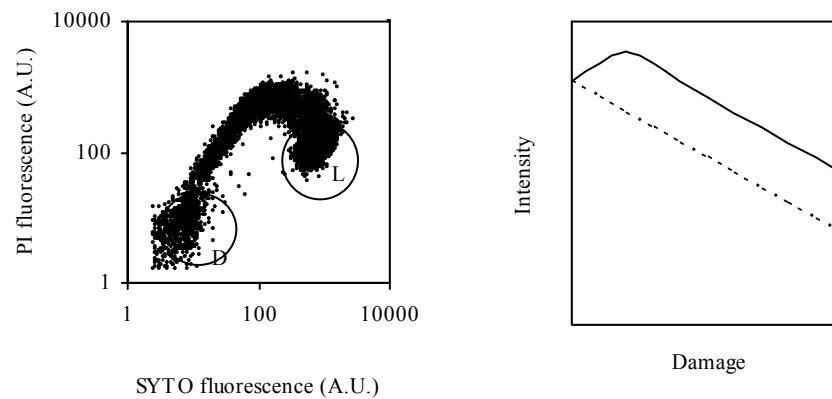

Figure 4.4 Typical flow cytometry result after inactivation with PEF with a schematic representation of the response of PI (solid line) and SYTO (dashed line). The living cells population (L) and the dead cells population (D) after heat inactivation are designated.

PEF treated samples show viable and inactivated cells, with an increase in inactivated cells at increasing treatment intensity. In contrast to heat treatment, a large group of cells was visible between the viable and inactivated cells after PEF treatment. PEF treatment gave a steady decrease in SYTO 9 intensity, but the PI intensity increased for a small fraction of cells, whereas it decreased for the rest of the cells. This gradual change in PI intensity was also observed by Wouters *et al.* (Wouters *et al.*, 2001). As PI and SYTO 9 are membrane integrity probes, the gradual shift might indicate that a PEF treatment induces formation of small pores in the cellular membrane. This prevents the relatively large PI and SYTO 9 molecules to enter in large amounts, as is possible after heat inactivation, where the membrane is more damaged. In the below-mentioned experiments, the group between the viable and inactivated cells had been counted as inactivated. However, it can be concluded that only using PI as a membrane integrity indicator after PEF treatment is insufficient in this case. A dual staining method gives a better overview as the PI intensity alone does not necessarily increases or decreases with membrane damage.

4.3.3 Number of pulses and pulse width

Since the inactivation increases with the number of pulses in an approximate log linear fashion, it is generally assumed that the electroporation process has a stochastic nature, resulting in a first order kinetics (Huelsheger *et al.*, 1981; Barbosa-Canovas *et al.*, 1999). In these experiments (Fig. 4.5), the number of 2 µs pulses was increased at a constant electric field strength of 38 kV cm^{-1}. Higher inactivation rates were reached by applying more pulses up to a reduction of 97% (1.6 log reduction) with a reduction of 76% in flow cytometry using 24 pulses. The viability measurements show a steady decrease in viability, whereas flow cytometry measurements seem to reach a steady state situation. The latter shows the limited accuracy of the measurement method of flow cytometry at levels lower than 10% of living cells.
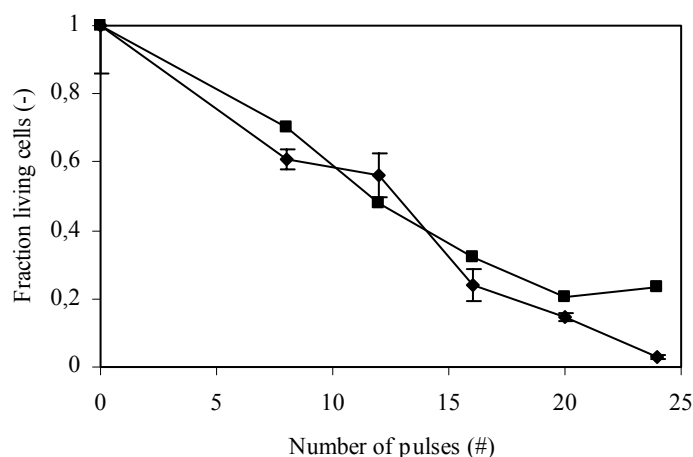
Figure 4.5 *L. plantarum* inactivation (♦) after application of 2 µs, 38 kV cm^{-1} pulses at different pulse numbers, compared to PI uptake measured with flow cytometry (■).

The effect of the pulse width has been investigated, since pulses with a shorter pulse width add less energy to the fluid. The total amount of applied energy was kept constant; i.e. a shorter pulse length was compensated by a higher average number of pulses. The average amount of added energy was 131 J ml^{-1} at an electric field strength of 47 kV cm^{-1}. The results in figure 4.6 show that decreasing the pulse length from 2 µs to 300 ns does not lead to a significant change in inactivation.
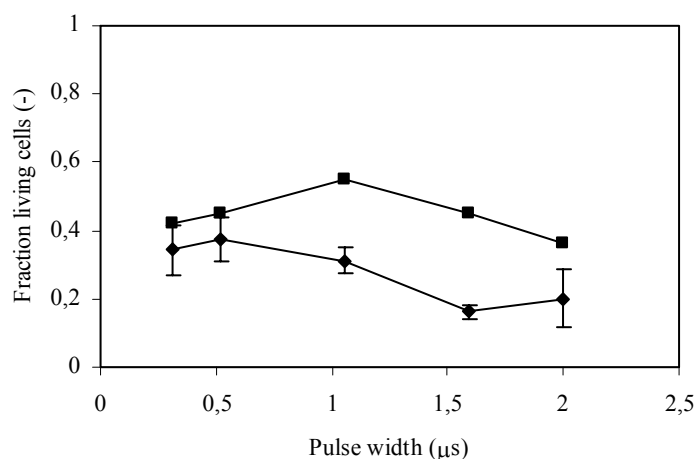
Figure 4.6 *L. plantarum* inactivation (♦) after application of 40 kV cm^{-1} pulses at different pulse durations, but an equal amount of added energy, compared to PI uptake measured with flow cytometry (■).

This proves that within this range, shorter pulses do not have any added value, since an equal amount of energy has to be added to get an equal inactivation. The characteristic parameter is the pulse width times the number of pulses (t = τ·n) which is the total time that pulses have been applied. This parameter has also been observed as crucial by other authors (Huelsheger *et al.*, 1981), although reported at a range of larger pulse widths.

4.3.4 Temperature dependency

The temperature dependency of the *L. plantarum* inactivation is investigated in the range of 25 to 45 °C (Fig. 4.7). Experiments were conducted where the electric field strength has been varied at different temperatures. The inactivation starts at electric field strengths of 20 to 30 kV cm^{-1} with an increasing inactivation rate at higher temperatures. This increase in inactivation rate has also been observed by other authors, e.g. by Heinz *et al.* (Heinz *et al.*, 2003) or Sensoy e*t al.* (Sensoy *et al.*, 1996).
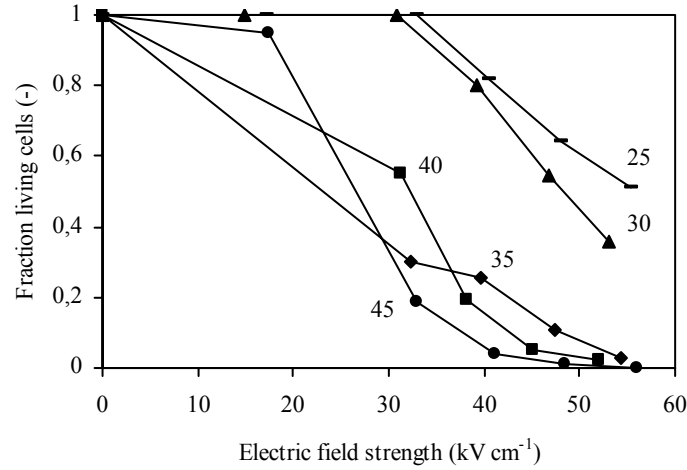
Figure 4.7 *L. plantarum* inactivation after application of 8 pulses of 2 μs at a temperature range from 25 to 45 °C.

In order to quantify the breakdown of *L. plantarum*, a model is proposed which incorporates both the electric field strength and the temperature effect. The decrease of the fraction of living cells (S) in time (dS/dt) is assumed to follow a first order process with a rate constant (k) which is dependent both on the applied electric field strength and the temperature.

$$\frac{dS}{dt} = -kS \Rightarrow k = \frac{-\ln(S)}{t} \tag{4.3}$$

The proposed first order model for k can be checked by fitting it to figure 4.5. This shows that it will underestimate values at short times, and overestimate values at longer times. Other more flexible inactivation models, like a Weibull model (Van Boekel, 2002), could also be applied, but further analysis showed that the conclusions with regard to the temperature and electric field strength dependency will not change significantly by this.

To describe the temperature and electric field dependency, is assumed that the rate constant is determined by two independent events; one determined by the temperature at a constant electric field strength, α(T), and one determined by the electric field strength at a constant temperature, β(E). It is assumed that the effects are multiplicative. One might hypothetically envisage this as a thermally dependent stochastic hydrophobic pore formation, followed by an electric field stimulated disruptive hydrophilic pore creation. But it must be stressed that very different mechanisms might as well show a multiplicative dependence of the inactivation rate on the temperature and electric field strength.

$$k = A \cdot \alpha(T) \cdot \beta(E) \tag{4.4}$$

The effect of temperature on the rate constant can be described by an Arrhenius equation using the activation energy ($G_{activation}$) and the thermal energy $k_b T$, where k_b is the Boltzmann constant ($8.62 \cdot 10^{-5}$ eV K^{-1}).

$$\alpha(T) = \exp\left(\frac{-G_{activation}}{k_b \cdot T}\right) \tag{4.5}$$

The effect of the electric field strength has been modelled by two different approaches. The first approach follows the model proposed by Huelsheger (Huelsheger *et al.*, 1981), which is often used for describing inactivation kinetics using PEF. It assumes that the inactivation rate is linear with the applied electric field strength above a critical electric field strength (E_{crit}). When the electric field strength is lower than the critical electric field strength, the inactivation rate is equal to 0.

$$\beta(E) = (E - E_{crit}) \tag{4.6}$$

The second model to describe the effect of the electric field strength on the inactivation kinetics uses a similar activation energy argument as in the Arrhenius equation. Instead of the dimensionless ratio of the activation energy over the thermal energy used in Arrhenius, an activation energy term over the local energy stored in the electric field over the membrane is used. This is proportional to the square of the electric field strength and hence the ratio with the square of an activation electric field strength is taken (E_{act}).

$$\beta(E) = \exp\left(-\left(\frac{E_{act}}{E}\right)^2\right) \tag{4.7}$$

A close inspection of the two models reveals that the functional behaviour of the two equations is quite similar for the range of the electric field strengths typically used in PEF studies. However, equation 4.7 will reach a plateau value for $E \gg E_{act}$, where the reaction rate is not energetically limited anymore. This would mean that the effect of increasingly higher voltages would be limited.

Table 4.1 Fit result for the combined temperature-electric field strength model

5 and 6 (critical E)		5 and 7 (activation E)	
A	$e^{24.0}$ µs^{-1}	A	$e^{28.3}$ µs^{-1}
G_{act}	0.77 eV	G_{act}	0.77 eV
E_{crit}	26.5 kV cm^{-1}	E_{act}	51.3 kV cm^{-1}
$V_{TM\,crit}$	6.0 V	$V_{TM\,act}$	11.5 V
SD	0.07	SD	0.07

For evaluation of both electric field inactivation models, the measured data were fitted to the combined temperature and electric field model; i.e. a combination of equation 4.5 and 4.6 and equation 4.5 and 4.7 (Table 4.1). The critical electric field strength model (Eq. 4.6) and activation electric field strength model (Eq. 4.7) both have 2 free parameters and give an equally adequate fit, based on the standard deviation (Table 4.1). The parity plots (Fig. 4.8) for the two models show that low inactivation rates are slightly overestimated, while faster rates are slightly underestimated.
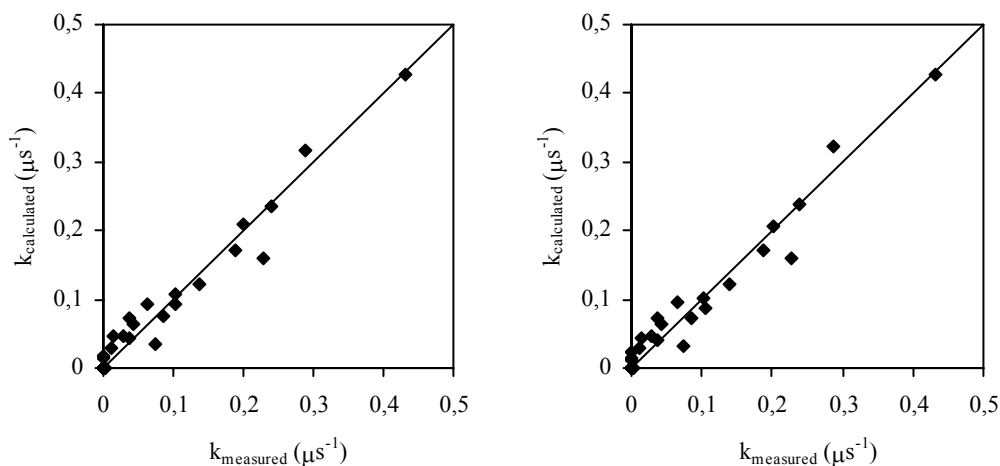
Figure 4.8 Parity plot for the model describing PEF inactivation with a critical electric field strength (left) and for the model describing PEF inactivation with an activation electric field strength (right) .

Since the first model is comparable to the Huelsheger model, a comparison of the critical electric field strength can be made to literature values. This shows that the determined critical electric field strength of 26.5 kV cm^{-1} is relatively high. In general, critical electric field strengths for microorganisms are in the range of several kV cm^{-1} (Huelsheger *et al.*, 1981). Electroporation usually starts at a transmembrane potential (Eq. 4.1) of approximately 1 V. If a radius of 3 µm is assumed, this implies a critical transmembrane potential of 6 V (Table 4.1), which is very high.

In order to test whether this could be a characteristic of the *L. plantarum* strain or a characteristic of the microreactor, a verification experiment has been performed on a colinear laboratory PEF setup with a diameter of 1 mm and a length of 3 mm (Pol, 2000). This measurement also revealed a high critical electric field strength of 27 kV cm^{-1}. This confirms that the high critical electrical field strength is caused by this *L. plantarum* strain in this medium and not by the microreactor. The exact reason for this high critical electric field strength is not known, but it should be noted that a high critical electric field will give problems in commercial applications, where high inactivation rates are desired.

The above models combined the electric field dependency with the temperature dependency. The validity of the Arrhenius model to describe the temperature dependency can be checked by fitting a reduced model at each temperature independently.

$$k = A_T \cdot \beta(E) \tag{4.8}$$

The factor A_T now includes the temperature effect. The Arrhenius model predicts a linear relation between the logarithmic of A_T and the inverse of the temperature.

$$\ln(A_T) = -G_{act} \cdot \frac{1}{T} + \ln(A) \tag{4.9}$$

Fitting of the critical electric field strength model and the model with the activation electric field strength for the electric field strength dependency, and thus to derive A_T for each temperature, shows linear behaviour for the temperature range of 25 to 45 °C, with $G_{act} = 1.2 \cdot 10^4$ K, $\ln(A) = 33.7$ and $R^2 = 0.94$ (Fig. 4.9). This shows that the Arrhenius model may indeed be used to describe the temperature dependent inactivation kinetics within the range from 25 to 45 °C.

The temperature dependency is not incorporated in kinetic PEF models of Abram *et al.* (Abram *et al.*, 2003), Peleg (Peleg, 1995) and Huelsheger *et al.* (Huelsheger *et al.*, 1981). Their model parameters are biased by the significant difference between the measured inlet and outlet temperatures, which are equipment and process dependent. In contrast, the temperature is unambiguously defined in the PEF micro reactor, which makes it possible to quantify the temperature effects in the PEF kinetics. The results above show that the fluid temperature is an important parameter, which cannot be neglected for a correct description of the whole PEF process. To correctly model a full scale PEF reactor, the proposed kinetic model could be expanded with a thermal process model in order to predict the inactivation as function of process parameters.
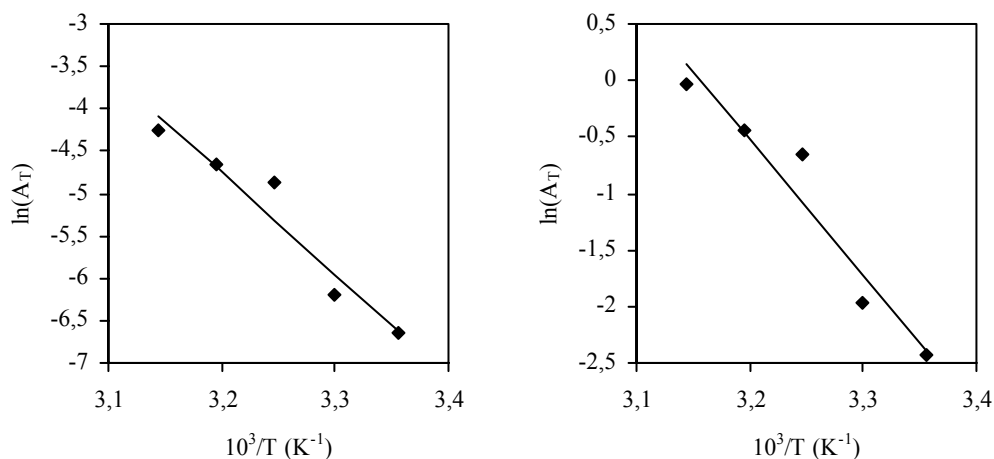
Figure 4.9 Arrhenius plots using a critical electric field strength model (left) and an activation electric field strength (right) to describe the electric field strength dependency.

4.4 Conclusion

This article shows that *L. plantarum* can be inactivated using a PEF microreactor. The specific advantage of the microreactor is the very good controllability of pulses and that temperature can be well controlled in contrast to laboratory or pilot scale equipment, which makes it very suitable to study the temperature effect. The high temperature controllability has been confirmed by a temperature measurement, which showed that the temperature increase in the microreactor is marginal compared to the energy input. The inactivation rate of a *L. plantarum* strain could be described by a combination of the Arrhenius model for the description of the temperature dependency, and a model using either a critical electric field strength or an activation electric field strength to describe the electric field dependency. The used *L. plantarum* strain turned out to be particularly resistant to PEF treatment at room temperature. The difference in inactivation performance between the micro fluidic and laboratory scale equipment could be attributed to the difference in temperature development, which has a strong influence on the PEF inactivation.

4.5 Acknowledgements

Chapter 5

Electroporation of yeast in a flow-through and a single-cell microdevice

Microtechnology offers the opportunity to study biological processes at the cellular level. One of these processes is electroporation; the inactivation of microorganisms by high electric field pulses. In this study, electroporation of yeast was studied using two different microdevices; a single-cell electroporation device, which allows visual observation of the electroporation process of one cell in time, and a flow-through electroporation device, which gives quantitative kinetic data based on a population of cells. The electroporation process was studied using the membrane-impermeable fluorescent DNA stain PI. Visual observation and flow cytometry measurements revealed that the electroporation process is a progressive process, since the application of more pulses showed an increased PI uptake. When the pulses were applied in rapid succession, the inactivation rates increased which is attributed to the avoidance of reversible pore formation closure. Inactivation behaviour in both devices was comparable and started at electric field strengths of 1.2 to 4 kV cm^{-1}.

5.1 Introduction

Application of an electric field pulse to a biological cell leads to reversible membrane damage at low electric field strengths (lower than 1 kV cm^{-1}) and inactivation of cells at high electric field strengths (generally higher than 1 kV cm^{-1}), a phenomenon known as electroporation. When an external electric field (E) is applied to a cell, a potential difference will arise over the cellular membrane, the transmembrane potential. This transmembrane potential (V_{TM}) is proportional to the cell radius (r) according to (Ho *et al.*, 1996)

$$V_{TM} = 1,5 \, r \, E$$

(5.1)

A transmembrane potential lower than ~1 V leads to reversible pore formation. This is extensively used for introduction of foreign molecules to cells, like DNA (Prasanna *et al.*, 1997), whereby the aim is to keep the transfected cell viable. When the transmembrane potential is increased to values above 1 V, the pore formation becomes irreversible, and the extensive membrane damage will inactivate the cells. This is used for the novel pasteurization method pulsed electric fields (PEF)(Knorr *et al.*, 2001).

The use of microengineered systems offers major advantages for the study of electroporation process. Since the electrode distances are very small, relatively low voltages already give high electric field strengths. This facilitates the control of the electrical pulses. Secondly, since the size of the channels is in the same order of magnitude as the cells, it is possible to follow the electroporation process online, during the application of the electrical pulses. Microtechnological electroporation devices can roughly be divided into two categories (Fox *et al.*, 2006); microdevices that trap cells in an integrated microstructure located between two electrodes and microdevices that lead the suspended cells through a treatment-zone where the electrical pulses are delivered. The cell trapping devices are particularly suitable for the qualitative, online observation of the electroporation process since the trapped cells will not move during the treatment (Valero *et al.*, 2005). However, they are less suitable for quantitative measurements since the electric field is inhomogeneous and the measurements are laborious and time consuming, but do provide information about the difference between individual cells. In contrast, the flow-through devices are very suitable for quantitative measurements since samples with larger amounts of cells can be collected after the electroporation process. However, qualitative measurements are hard to perform due to the continuous flow of cells during the application of the electrical pulses.

In this article, electroporation of *S. cerevisae* will be studied using two microdevices; a single cell trapping device and a flow-through PEF microreactor. Therefore it is possible to study the electroporation process both on single cell level and to accurately measure the average response of the ensemble of cells. The electric field distribution will be derived

from a finite element model, which makes a coupling between the measurements in the single cell device and the PEF microreactor possible. The electroporation process itself will be followed by fluorescent staining.

5.2 Materials and methods

5.2.1 Microdevices: layouts and fabrication

I. Single cell trapping device

The cell trapping device consists of two parallel channels that are connected by microholes with dimensions smaller than cells (Fig. 5.1). These microholes act as trapping sites for living cells by applying a pressure difference over the holes. The 50 μm wide top channels, the 20 μm wide bottom channel and the nine trapping sites with a width of 4 μm are etched by reactive ion etching (RIE) to a depth of 15 μm. The reservoirs are powderblasted from the backside of the silicon. On the whole substrate a silicon oxide layer is thermally grown to electrically insulate the conductive silicon. The channels are closed with a Pyrex wafer which allows the visualisation of the channels as well as the trapping and the electroporation process. The platinum electrodes are sputtered into the recess Pyrex wafer, followed by anodically bonding of the two substrates.
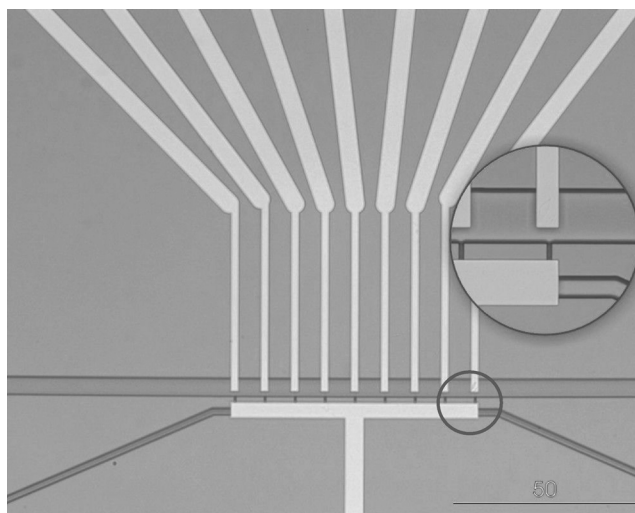
Figure 5.1 Image of the cell trapping device with electrodes integrated and a zoom of the trapping sites (4μm width)

II. PEF microreactor

The flow-through PEF microreactor was developed to study the PEF process in more detail (Fox *et al.*, 2005) (Fig. 5.2). It consists of a 50 μm deep channel with a 10 μm deep constriction. A 200 nm thick platinum electrode is placed at either side. This channel constriction acts as the treatment-zone for cell inactivation since it serves as an electrical resistance, concentrating the potential drop and thus creating a local high electric field strength. It was shown previously that this microreactor performs comparable to laboratory setups (Fox *et al.*, 2005) and that it is suitable for bacterial inactivation (Fox *et al.*, 2006).
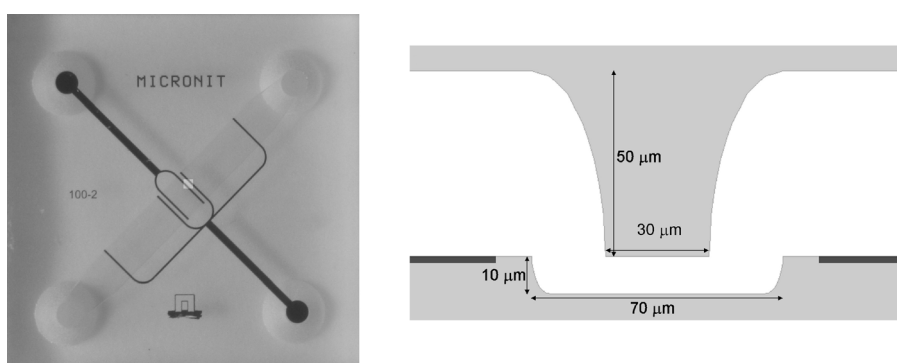
Figure 5.2 Image and schematic drawing of the PEF microreactor with dimensions.

5.2.2 Modelling the electric field distribution

The electric field distribution has been modelled both for the trapping device and the PEF microreactor, using finite element software (Femlab 3.0, Comsol, Sweden). The DC conductive medium model was used for a steady state situation, which solves Gauss' differential equation. The boundary conditions are considered as being electrical insulated, with the two electrodes being 1 V and grounded. The fluid has a conductivity of 0.1 S m^{-1}.

5.2.3 Experiments

I. Single cell trapping device

For the experiments performed with the cell trapping device, the chip was mounted on to an X–Y–Z translation stage in an inverted microscope (Leica DM IRM, Leica Microsystems, Wetzlar, GmbH, Germany). The microscope system is equipped with a mercury lamp, 20x, 40x, 50x, 63x objectives, and the fluorescence filter set (BP 450– 490, LP 515). In addition, a computer-controlled CCD camera (Leica DFC300 FX) is mounted in the microscope for

image recording. For the electroporation signal, a pulse generator (Avtech AVR-4-B-WUA) was directly connected to a specifically designed chip holder.

Experiments were started by filling the chip with buffer (5 mM HEPES, 6 mM NaCl solution with pH=7 and a conductivity of 0.1 S m^{-1}) by capillary forces. Then 100 μl of the buffer solution is added to all the reservoirs. To initiate the cell experiment the buffer solution in the top inlet reservoir is replaced by 100μl of the cell sample consisting of 0.01% (w/v) *S. cerevisae* suspended in HEPES buffer mixed with the fluorescent probe PI (Invitrogen, The Netherlands) at a concentration of 30 μM. The cells were forced to flow along the upper channel. A pressure gradient over the trapping sites to the lower channel was created by suction on the bottom access holes. As a result, some of the yeasts cells which flow in the upper channel are trapped at the trapping sites. Cells were electroporated using two different pulse widths (5 and 10 μs) and three different electric field strengths (6, 9 and 12 kV cm^{-1}). The degree of electroporation was optically monitored using the fluorescent staining as a result of the PI probe uptake.

II. PEF microreactor
For the inactivation experiments in the PEF microreactor, *S. cerevisae* was cultivated in the logarithmic growth phase from a 40 g L^{-1}, glucose, 5 g L^{-1} bacterial peptone, 5 g L^{-1} yeast extract solution and was washed twice. A syringe (Hamilton, USA) was filled with a 0.1% (w/v) yeast solution and mounted to a syringe pump (Harvard Scientific, USA). The syringe was connected to a specifically designed chip holder via a 100 micrometer diameter glass capillary (Polymicro, USA). Experiments were done with a peroxide sterilized setup, and started with the most intense treatment, going towards milder treatments to reduce recontamination after the treatment chamber. Treated samples were collected and cell inactivation was studied using plating and PI staining.

An experiment was performed in which 8 pulses of 5 μs were applied at electric field strengths ranging from 0 to 26 kV cm^{-1} to derive a working range for the inactivation experiments. Based on this experiment, inactivation experiments were done at electric field strengths of 3, 6, 9 and 12 kV cm^{-1} with pulse widths of 5 and 10 μs, where the number of pulses was varied from 0 to 40 pulses on average. For the study of reversible electroporation, an experiment was done with 5 μs pulses of 6 kV cm^{-1} where PI was already added to the cell solution in advance of the measurement and compared to an experiment where PI was added after treatment.

5.2.4 Probes and flow cytometry

The nuclear stain propidium iodide (PI) (Invitrogen, The Netherlands) was used as a cell impermeable membrane integrity indicator. PI will intercalate with the nuclear DNA, causing red fluorescence. However, it can only permeate through a cellular membrane if it is damaged. PI stained cells were incubated for 10 minutes after which flow cytometry (FCM) analysis was conducted. The FCM analyses were performed on a FACSCalibur flow cytometer (Becton Dickinson, USA), equipped with a 15 mW, 488 nm air-cooled argon ion

laser. PI fluorescence was measured using a long-pass filter of 670 nm (FL3). Forward scatter was collected with a diode detector, side scatter and fluorescence were collected with photomultiplier tubes. Forward scatter and side scatter was collected using a linear amplification, PI fluorescence was measured using logarithmic amplification. Data were analysed using CellQuest (Becton Dickinson, USA).

5.3 Results and discussion

5.3.1 Electric field distribution in cell trapping device and PEF microreactor

The electric field distribution in the microdevices has been modelled using finite element modelling software for a 2D situation (Fig. 5.3). The distribution in the cell trapping device clearly shows that the electric field is focussed at the site where the cell is trapped. The electric field strength in the upper channel is negligible compared to the electric field strength at the trapping site, so cells which are not trapped will not be affected.

Figure 5.3 Electric field strength distribution in the cell trapping device (left) and the PEF microreactor (right). Higher electric field strengths are depicted blacker. The electrodes are depicted in grey.

Analysis of the electric field strength distribution shows that a voltage difference of 1 V gives an electric field strength of 0.57 kV cm^{-1}. Since applied voltages are measured in following experiments, this factor has been used to calculate the electric field strength. As the trapping device consists of nine parallel trapping sites with one common grounded electrode (bottom electrode in Fig. 5.1), leakage of current from one trapping site to the other could occur. This could cause a high electric field strength at the neighbouring site. This has been studied in a multi-trapping site model. However, the effect proves to be negligible since the resistance between the high voltage electrode of a trapping site and the grounded electrode via a neighbouring site is much higher than the resistance between the electrodes of the same trapping site. Therefore, the current leakage and thus the electric field strength will be very small. Secondly, neighbouring electrodes are grounded to reduce the leakage current even more.
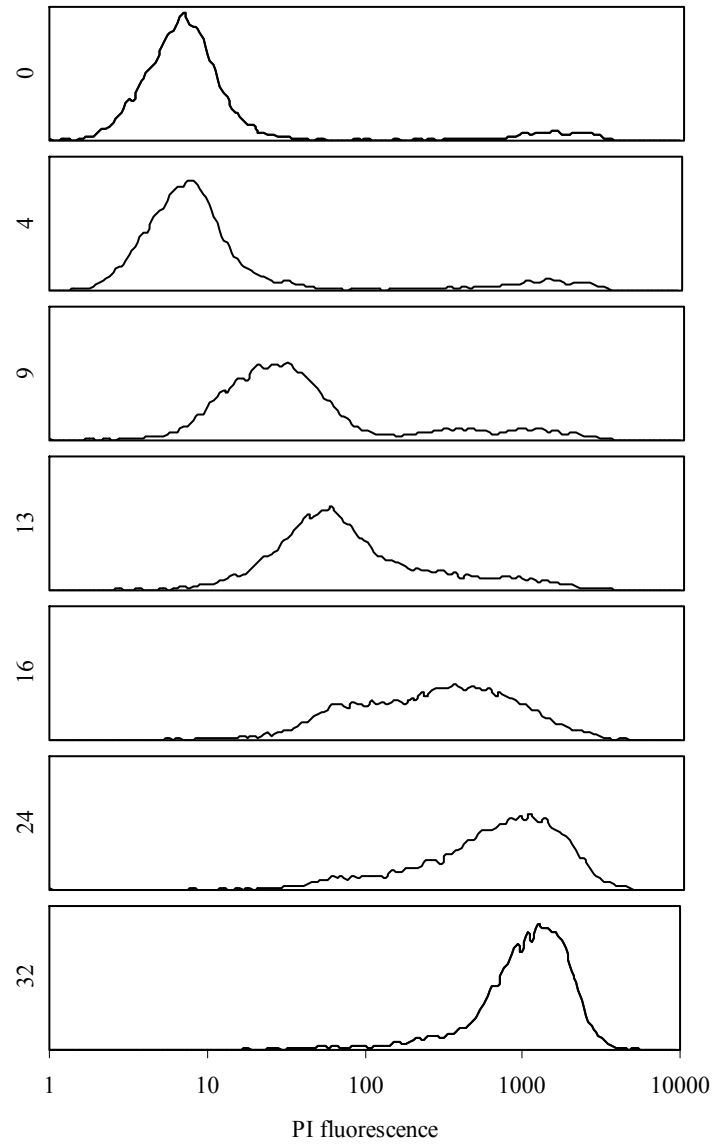
Figure 5.4 Fluorescence histogram of PI as measured with flow cytometry at increasing electric field strengths (electric field strength given at the left in kV cm^{-1}).

The electric field strength distribution has also been determined for the PEF microreactor (Fox *et al.*, 2005) (Fig. 5.3), which shows that the electric field is focussed at the treatment zone. A voltage difference of 1 V here gives an electric field strength of 0.14 kV cm^{-1}. This value is lower than the trapping device since the electrode distances are larger, but it is still much higher than comparable laboratory scale PEF equipment.

5.3.2 Flow cytometry and probing

Flow cytometric measurements of yeast inactivation were carried out using PI as a membrane integrity marker on samples obtained from the PEF microreactor. The FCM measurements (Fig. 5.4) show that application of increasing higher electric field strength pulses results in a higher average PI intensity. A similar pattern has been observed for the application of an increasing number of pulses. This indicates that the membrane is damaged more at higher treatment intensities (higher electric field strengths or more pulses), allowing more PI to enter the cell. When intact cells are compared to heat inactivated cells, two distinct populations can be distinguished (data not shown). Electroporated cells do not show these two distinct populations, but a more gradual increase of the PI fluorescence. This gradual increase of damage has been observed by others as well (Wouters *et al.*, 2001) and seems to be typical for electric field treated cells.

The electroporation of yeast in the single cell trapping device has also been studied using PI as a membrane integrity probe. In these measurements pulses were applied with a frequency of one pulse per minute and the fluorescence intensity was checked one minute after each pulse. These measurements showed a similar trend of gradual increase in the fluorescence intensity (Fig. 5.5).
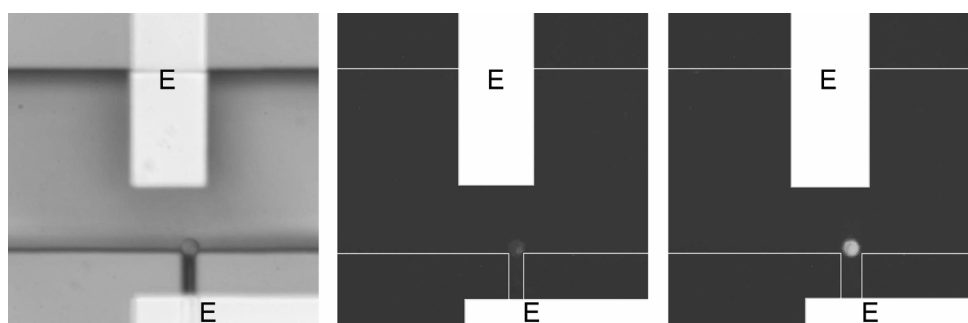

Figure 5.5 Light image and two fluorescent images of a trapped yeast cell PI response after 6 pulses and after 7 pulses of 10 μs and electric field strength of 9 kV cm^{-1}. The electrode structures and channel are drawn in the two fluorescent pictures. Electrodes are marked with E.

At the start of an experiment, trapped cells were not fluorescent, indicating that the cellular membrane was intact. After application of a certain amount of pulses, a relatively low fluorescent signal appeared, indicating that the membrane was damaged and PI could stain the cell. When a cell was inactivated by a pulse, it took approximately 30 seconds before a cell stained red. However, the application of one additional pulse gave a large increase in PI fluorescence with a very bright coloured nucleus, which indicates that the membrane was damaged more severely. This is in accordance with the flow cytometry measurements of the PEF microreactor samples where this effect was observed as a gradual fluorescent increase. Cells did not shrink significantly when being inactivated which indicates that the membrane is electroporated, but the three dimensional structure is still intact. Moreover, when pulses were applied to one trapping site, cells at a neighbouring trapping site did not show red fluorescent/PI uptake, which indicates that the electric field strength at that neighbouring site is negligible, as has been predicted by the electric field model.

5.3.3 Yeast inactivation as function of pulse width and number of pulses

Inactivation of yeast was carried out both in the cell trapping device and the PEF microreactor, with varying the electric field strength, pulse width and number of pulses. The effective range of the electric field strength was determined experimentally in the PEF microreactor at a constant average number of 8 pulses of 5 µs pulse width (Fig. 5.6). The measurement shows that yeast is strongly inactivated in the range of 3 to 12 kV cm^{-1}, where the process can be studied using PI as an indicator. Higher inactivation rates can be measured by counting the viability with plating, but these inactivation ranges are not measurable in the trapping device as only a single cell can be studied each time with PI fluorescence. Therefore, following experiments both in the PEF microreactor and the trapping device were conducted in the range of 3 to 12 kV cm^{-1}.
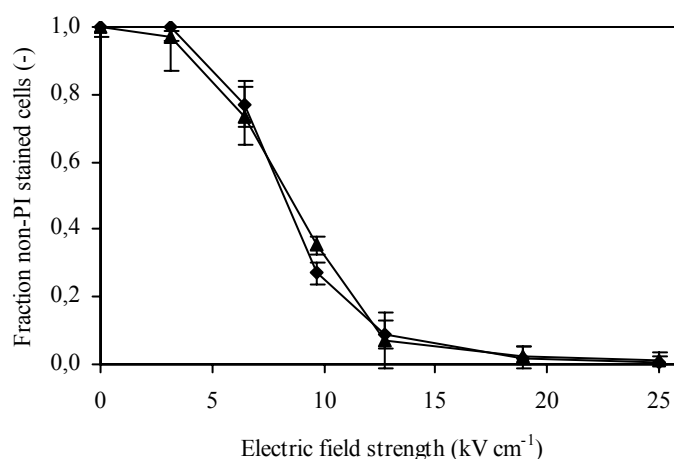
Figure 5.6 Effect of the electric field strength on the fraction of living cells after application of on average 8 pulses with a pulse width of 5 μs in the PEF microreactor, measured with flow cytometry (▲) and plate counting (♦).

For yeast inactivation experiments in the cell trapping device, pulses were delivered at a one minute interval to trapped cells. A cell was designated as inactivated when it showed red fluorescence due to PI uptake (Fig. 5.5). The duplo measurements in the cell trapping device showed fairly large differences (Fig. 5.7). This, most probably, has to do with the inhomogeneity of the electric field. In some measurements more than one cell was trapped at a trapping site, the measurements have been performed trapping sites which could have minor differences and trapping sites have been cleaned with ethanol between measurements, which could all affect slightly the electrode behaviour and electric field distribution. The increase in the pulse width had a large impact on the required number of pulses to achieve yeast inactivation. For example at 6 kV cm^{-1}, the number of pulses decreased from an average 17.5 to 6.5 pulses when the pulse width is doubled from 5 to 10 μs. In literature it is often reported that the required time constant to describe cell inactivation is the total treatment time, which is equal to the pulse width times the number of pulses (t = τ·n). It is therefore noteworthy that in these experiments a doubling of the pulse width gives somewhat more than a twofold reduction in the required number of pulses; i.e. the total treatment time at each electric field strength for 5 μs pulses seems to be higher than in case of 10 μs.

Figure 5.7 Number of pulses and total treatment time (τ·n) required to inactivate *S. cerevisae* in the cell trapping device using 5 μs (■, solid line to guide the eye) and 10 μs pulses(◊, dashed line to guide the eye). The PEF microreactor measurements, based on Eq. 2 and 3 are depicted in figure b (Δ).

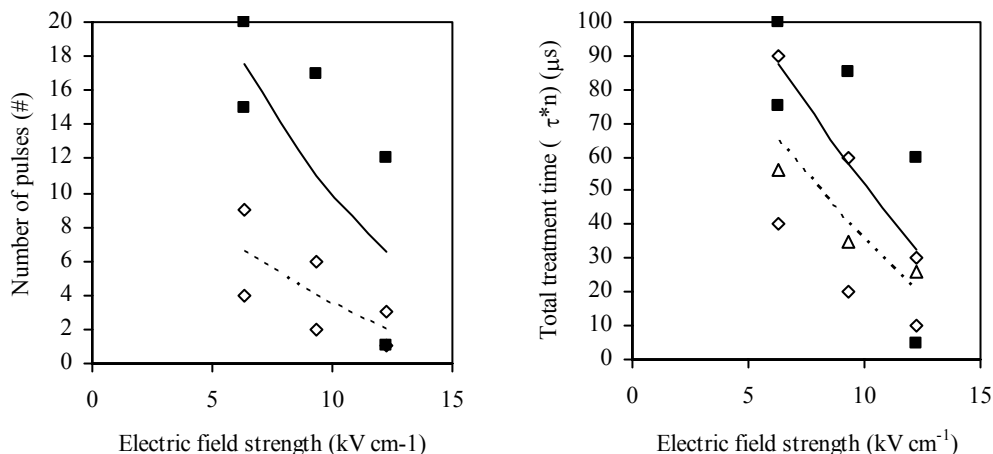The effect of the number of pulses in cell inactivation was also studied in the PEF microreactor with increasing number of pulses at similar electric field strengths to the ones used in the cell trapping device. The inactivation was measured both by flow cytometry (Fig. 5.8) and measuring by plating (Fig. 5.10). The flow cytometry measurements also show that increasing the pulse width gives stronger inactivation (Fig. 5.8). However when the inactivation is plotted, as the fraction of non-PI stained cells versus the total treatment time for the different electric field strengths, it is clear that the total treatment time is in this case a good parameter for the description of cell inactivation since the 5 μs pulse width measurements are in good agreement with the 10 μs pulse width measurements.

Figure 5.8 Inactivation of yeast versus the number of applied pulses and the total treatment time (τ·n) at 4 different electric field strengths (3(●), 6 (■), 9 (▲) and 12 (♦) kV cm^{-1}) and 2 different pulse widths (5 μs (open symbols, dashed line) and 10 μs (closed symbols, solid line)) as measured with flow cytometry.

To compare the cell trapping device and the PEF microreactor, it is (arbitrarily) assumed that the threshold measured in the study of the cell trapping device corresponds to a 50 % fraction of living cells. Based on this assumption and the model data generated in the next paragraph, a comparison has been made (Fig. 5.7b) between the two devices. This shows that the PEF microreactor equals the measurements with the 10 μs pulses in the cell trapping device. A disagreement is observed in the fact that the 5 μs pulses and 10 μs pulses behave similar in the PEF microreactor but not in the cell trapping device. However, the experimental setup of both experiments varied, since the pulses in the PEF microreactor were applied in a very short time frame (in the order of milliseconds), while the pulses in the cell trapping device were applied at one minute interval. In the cell trapping device, cells might therefore be able to partly recover after each single pulse, similar to reversible cell electroporation, while in the PEF microreactor the rapid pulses sequence lead to more

irreversible electroporation. This would imply that for the experiments in the cell trap device, the application of one single pulse of 10 μs is more effective in cell inactivation than two 5 μs pulses, since it includes an extra recovery time for the pores.

To check whether reversible electroporation could take place in the PEF microreactor, an experiment was performed where PI was added at forehand to the cell suspension. It that way cells would be stained immediately when electroporated, irrespective whether the pore formation would be partly reversible or not. This experiment was then compared to a control experiment where PI was added after PEF treatment to measure only irreversible electroporation. A comparison of the two experiments at 5 μs, 6 kV cm^{-1} (Fig. 5.9) shows that there is a fraction of cells which is PI positive when PI is present during treatment, but PI negative when added afterwards. A similar pattern has been observed for a 10 μs, 3 kV cm^{-1} experiment (data not shown). This is a strong indication that, despite the high field strengths applied, the electroporation is still partly reversible (20-40%) within a time scale of 10 minutes. The cells however do not stain PI positively after 10 minutes, indicating that they are still alive.
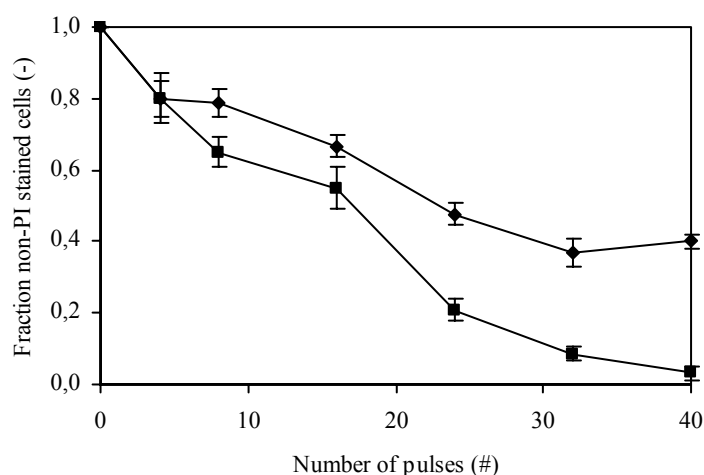
Figure 5.9 Inactivation of yeast measured with flow cytometry using 5 μs, 6 kV cm^{-1} pulses. PI is present in the medium during the PEF treatment (■) and PI is added after the PEF treatment(♦).

5.3.4 Modelling of the yeast inactivation

Yeast inactivation was also measured using plate counting as a viability measurement (Fig. 5.10). Plate counting is a more suitable measurement method for fractions lower than 10% living cells, since the measurements are done in a logarithmic fashion, opposed to the linear

PI measurements. The plate counting measurements show that the effect of the treatment time ($t=\tau \cdot n$) at a constant electric field strength can be described by first order kinetics

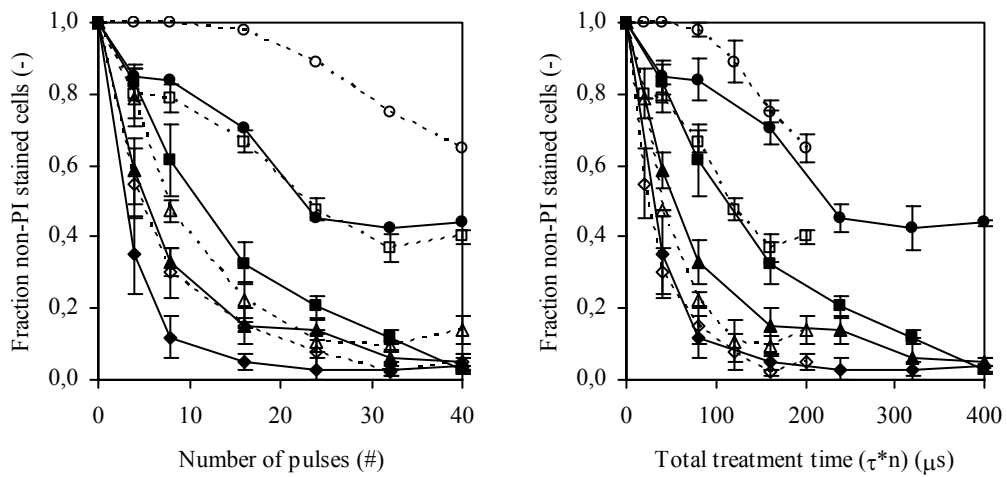$$\frac{dS}{dt} = -kS \Rightarrow k = \frac{-\ln(S)}{t} \tag{5.2}$$
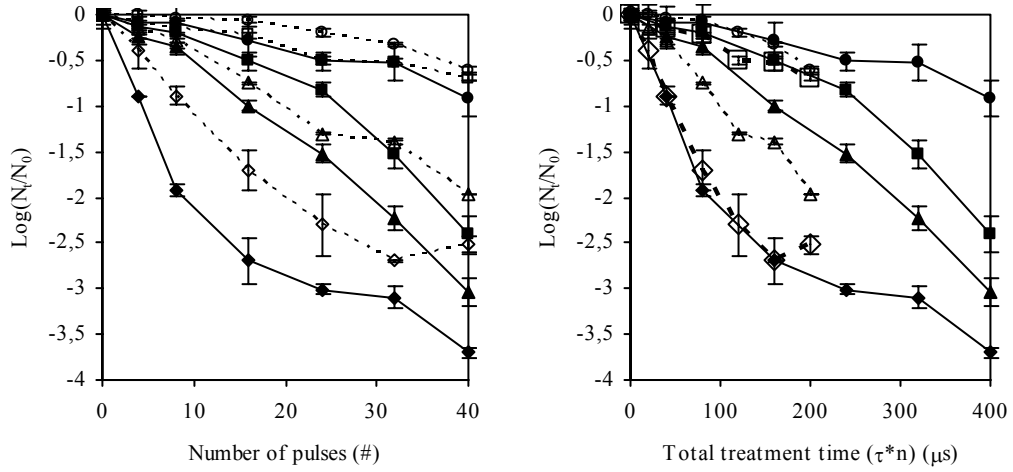
Figure 5.10 Inactivation of yeast versus the number of applied pulses and the total treatment time ($\tau \cdot n$) at 4 different electric field strengths (3($\bullet$), 6 ($\blacksquare$), 9 ($\blacktriangle$) and 12 ($\blacklozenge$) kV cm^{-1}) and 2 different pulse widths (5 µs (open symbols, dashed line) and 10 µs (closed symbols, solid line)) as measured with plating.

The effect of the electric field strength (E) on the fraction of living cells is often described by the empirical model proposed by Huelsheger (Huelsheger *et al.*, 1981) using a rate constant (A) and a critical electric field strength (E_{crit})

$$k = A \cdot (E - E_{crit}) \tag{5.3}$$

The viability measurements were fitted to these equations, showing that the inactivation can be described with a critical electric field strength of 1.2 kV cm^{-1} and a rate constant of $2.4 \cdot 10^{-3}$ µs^{-1} cm kV^{-1}. These values are in the same order of magnitude as values measured by other researchers (Zhang *et al.*, 1994; Qin *et al.*, 1995). The average diameter of the cultured yeast was 7.3 µm, as has been measured with a coulter counter. The critical electric field strength can be translated to a transmembrane potential (Eq. 5.1), giving a critical transmembrane potential of 0.7 V. This value is within the range of 0.5 to 1 V that is reported as being the range where electroporation of cells starts.

For the cell trapping device, similar inactivation constants can be derived. However, a time and an electric field strength have been measured, but no fraction living cells has been determined. If it is once again assumed that the fraction of living cells is 50% at the number of pulses that has been applied in the single cell electroporation device, a critical electric field strength of 4 kV cm^{-1} is calculated with a rate constant of $3 \cdot 10^{-3}$ μs^{-1} cm kV^{-1}. The critical transmembrane potential, based on this electric field strength, is 2.2 kV cm^{-1}. These values are in the same order of magnitude as in the PEF microreactor, which shows that the devices are well comparable. The small deviations with the PEF microreactor can be attributed to the fact that the fraction living cells has been assumed and the number of measurements is only 12, therefore giving larger standard deviations.

5.4 Conclusion

The inactivation of yeast by electric fields can be very well studied by combined measurements of a single cell trapping device and a PEF microreactor. The electroporation process was shown to be a progressive process, since staining with PI revealed that the fluorescent intensity increased gradually with increasing treatment (higher electric fields, longer pulse width or more number of pulses), observed both optically and with flow cytometry.

Applying pulses within a short period (e.g. milliseconds) is advantageous. Direct evidence was found that membrane recovery is reduced and that the effective irreversible pore formation favours cell inactivation. The electroporation process itself could be described by a combination of two models; a first order kinetics model for the description of the effect of the duration of the pulses of pulses and a Huelsheger-like model for the description of the electric field strength effect. This gave a critical transmembrane potential of 0.7 V for the PEF microreactor and 2.2 V for the trapping device, which is comparable to literature values. The two devices were very well comparable in their electroporation behaviour.

Chapter 6

Conceptual design of a mass parallelized PEF microreactor

For a large scale process aimed at e.g. 1 m^3 hr^{-1}, a PEF microreactor has to be mass parallelized. A conceptual design is proposed based on a microengineered microsieve with a highly defined pore geometry. The pores serve as a restriction to concentrate the voltage drop, and thus increasing the electric field strength. It is shown that the pore residence time can be utilized to define the total treatment time, which enables the use of constant (AC) power sources instead of pulsed power sources. A consequence of the reduced electrode spacing is that average current is inversely increased. The hereby emerging problem of electrolytic damage can be virtually eliminated by using a source frequency of 1 MHz.

The pore length is limited at small residence times by the maximal allowable pressure drop. For a good treatment homogeneity and process stability it is advisable to separate the electrodes from the microsieve, However, a relative close proximity of the electrode meshes to the microsieve is required keep the power efficiency up to reasonable levels, and at the same time to limit the required membrane area. The final design will always be a trade-off between the pore geometry, the pore size and the efficiency that has to be reached. This has been illustrated in an example case.

6.1 Introduction

Pulsed electric fields (PEF) is a novel pasteurization method, especially suitable for the pasteurization of fluid foods. Microorganisms are inactivated by applying short (10-300 μs), high electric field (10-60 kV cm^{-1}) pulses. These pulses induce a potential difference over the cellular membrane, which will cause pore formation in this membrane and eventually inactivation of the entire microorganism (Chang *et al.*, 1992).

The inactivation by PEF depends on several parameters, determined by the microorganism, the food matrix and the process. Microorganism related parameters involve the growth phase, type and size of the microorganism (Pothakamury *et al.*, 1996). The food matrix also influences the inactivation by determining for example the pH and conductivity (Barbosa-Canovas *et al.*, 1999). Typical process parameters that determine the inactivation are the electric field strength, the number of applied pulses, the pulse width and the temperature. Increasing the total treatment time (being the product of the pulse width and the number of pulses) will give higher inactivation rates. This can also be obtained by increasing the electric field strength and therefore the potential difference over the membrane. Performing PEF at higher temperatures will also increase the inactivation rate, which can be described by Arrhenius kinetics (Fox *et al.*, 2006).

This article discusses the conceptual scaling up of the pulsed electric field (PEF) pasteurization process using microtechnological structures. The advantages and disadvantages of the microtechnological system relative to already existing PEF systems will be discussed and possible ways to scale up microtechnological PEF systems will be treated.

6.2 Existing PEF reactors

Several different designs have been proposed for PEF treatment chambers, which can be categorized in three groups: crossfield, radial and cofield chambers. Crossfield chambers are designed such that the direction of the electric field is perpendicular to the flow of the food. This is applied by Dunn *et al.* (Dunn *et al.*, 1987) (Fig. 6.1a) who used a chamber consisting of two parallel plate electrodes where the fluid could flow in between. The electrodes were separated from the product by membranes to avoid contamination by electrolysis products. Radial chambers consist of an inner electrode centred in a grounded tube. Fluid will flow through the tube while pulses are applied by the inner electrode. This will give a radial electric field distribution. An example of a larger scale radial chamber is the design of Belloso *et al.* (Martin-Belloso *et al.*, 1997) (Fig. 6.1b). However, a radial chamber could also be regarded as a special case of a crossfield design.
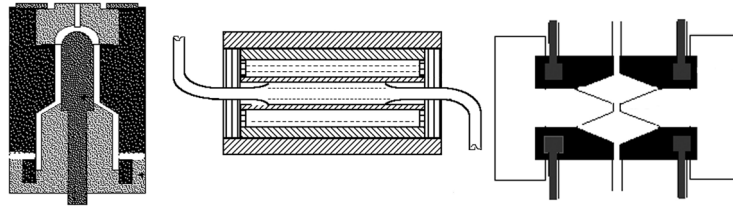
Figure 6.1 Example of a radial PEF treatment chamber (Martin-Belloso *et al.*, 1997), a crossfield chamber (Dunn *et al.*, 1987) and a cofield design (Yin *et al.*, 1997).

The direction of the electric field is equal to the fluid flow direction in cofield chambers, which is for example applied in the pilot scale PEF equipment (Yin *et al.*, 1997; Roodenburg *et al.*, 2002) (Fig. 6.1c). It basically consists of two metal tubes (one grounded and one high voltage), separated by an isolator. Fluid flows through the tubes and the isolator and is treated in the region of the isolator. In general, cofield designs seem to be more reliable, since no high electric field strengths are present at the electrode surface, therefore reducing the chance of electrode damage.

Existing PEF equipment faces several challenges. First of all, by applying an electric field, ohmic heating of the fluid will take place. Although inactivation of microorganisms using PEF improves at higher temperatures (Pothakamury *et al.*, 1996; Heinz *et al.*, 2003; Fox *et al.*, 2006), the fluid temperature should not rise too much, since temperature sensitive food ingredients should be unaltered by this pasteurization method. Besides the increase of the average temperature, the local temperature distribution in the treatment chamber gives local hot spots. This effect is non-linear, since the conductivity is increasing with temperature. Hot spots will result in an inhomogeneous treatment, which might damage both the product and the treatment chamber and could even trigger the formation of local vapour bubbles.

A second challenge is the highly specific electric equipment required for pulsing. Severe constrains apply for the switches in the pulsing equipment, which have to be fast and be able to handle the high voltages (more than 20 kV) and high currents. (Roodenburg *et al.*, 2002). To obtain a short square pulses, dedicated pulse forming networks have to be designed to transform the switched output (de Haan *et al.*, 2002).

Due to the interfacial charge transfer between electrodes and food product, electrolysis is inevitable in the commonly applied DC pulsed systems. The electrolysis of water and electrode material creates another challenge for PEF applications. If the fluid flow is high enough, the electrolytic products, hydrogen and oxygen, will stay dissolved. However, when gas bubbles are formed, arching will occur because the internal electric field strength will readily excess the ionization threshold. Therefore, gas formation should be avoided at all times since it can heavily damage the treatment chamber. It is also clear that the

electrode lifetime will be finite, due to electrolytic dissolution of the metal ions and erosion due to food particles (Roodenburg *et al.*, 2005).

PEF laboratory research is usually performed with PEF treatment chambers of a few millimetres, whereas pilot scale PEF treatment chamber have a typical size of a few centimetres. Aspect ratios of the treatment chamber should be larger than 1.5 to guarantee the treatment of all the passing fluid (Fiala *et al.*, 2001; Morren *et al.*, 2003). Microfluidic structures, with sizes in the 1-100 micrometer scale, offer various advantages to large size structures, such as a very predictable, most times laminar flow, fast heat exchange and a small distance between electrodes, which implies that only low voltages are needed to obtain high electric field strengths.

In recent years, new microfluidic electroporation devices have been designed, aimed at the analysis of the electroporation process, transfection or inactivation of cells (Fox *et al.*, 2006). Most microtechnological structures are aimed at analytical applications, since the advantages, like a small sample size, high separation efficiencies and a high sensitivity, are obvious. However, large scale applications aimed at production, like the pasteurization of fluid foods with microtechnological PEF structures, are less obvious since large quantities of fluid have to be treated. Nevertheless, in this article we will explore the possibilities to upscale the micro PEF reactor concept, with the aim to investigate whether some of the mentioned challenges that faces the current full scale PEF approach can be solved.

6.3 Scaling up the PEF microreactor

In the process industry, scaling up from laboratory scale equipment to pilot or commercial scale is usually done by enlarging all the involved dimensions. This approach will not work in microtechnology, since the specific advantages of microtechnology, such as fast mixing or fast heat exchange, are specifically related to the small size. Scaling up should therefore be done by mass parallelization of the microtechnological structure; i.e. scaling up by number instead of scaling up by size. However, massive parallelization of the current existing microfluidic devices would be highly impractical. The microtechnological PEF reactor described by Fox *et al.* (Fox *et al.*, 2005) can be taken as an example. Its compact design is based on a 1 mm wide and 50 µm deep channel with constrictions between successive electrodes, which concentrates the electric field; i.e. a cofield reactor design. The flow in one chip is around 0.5 ml hr^{-1}. An aimed production of 1 m^3 hr^{-1} should require the use of 2 million of these devices in parallel.

In general, microtechnological research tools are expensive to make, as it is labour-intensive work, resulting in a small amount of microchips. For large quantities, the production processes can be automated, thereby significantly reducing the processing costs per chip as has been readily proven by the microelectronic industry. However, the material costs would remain roughly the same, and since about 1 cubic meter of dedicated borofloat

glass wafers is required for the two million devices, the material costs of such a device will be rather exorbitant in comparison to current pilot scale PEF equipment.

A more sophisticated, integrated design is required, where the channel density in the system is maximal and a minimal amount of micro-engineered material is used to direct the flow. Two types of approaches are conceivable, one where the fluid flow is parallel to the wafer, and alternatively one where the fluid flow is directed perpendicular to the wafer. The first approach is used in micro-reactors, micro-mixers and micro engineered heat exchangers designed for treatment of reasonable volumes (Ehrfeld *et al.*, 2000). This is a logical choice for processes that are inherently ruled by the chemical kinetics, or transfer rates between adjacent streams, since the minimally required residence time can only be met by channels of sufficient length. The second approach is used in microsieves and membranes (Van Rijn, 2004) which are characterized by a massive throughput due to the limited path length in the thin membrane. Their application in filtration and emulsification does not require a certain residence time within the constricted flow zone. The inherently required minimal treatment time for electroporation is also very short, in the order of 10 to 100 microseconds. Therefore we think that the most effective route for massive parallel micro PEF reactors is a design based on the flow trough principle of a microsieve.

6.4 Electrical aspects

Microsieves are microengineered membranes which have a highly defined pore structure and size which dimensions can be adjusted to desired specifications. (Kuiper 2000)(Van Rijn, 2004) The top layer consists of non conducting silicon nitride, which is supported by a silicon support structure. The membrane can serve as a mass parallelized microreactor with electrodes placed above and beneath it. The pores serve as the parallel constrictions which focus the electric field.

A PEF treatment chamber can conceptually be regarded as a water column between two electrodes. Pulses will be applied to this water column between the electrodes. A PEF microsieve can be regarded as a water column where the length is reduced up to the membrane thickness (Fig. 6.2). Based on this representation, the electrical regime for a PEF microsieve can be deducted.
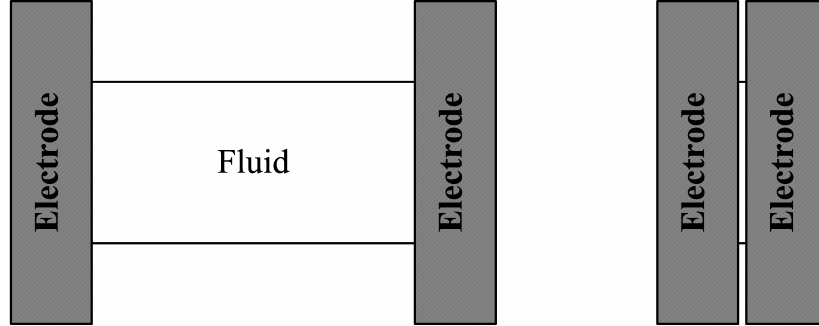
Figure 6.2 Conceptual picture of a large scale (left hand side) and microtechnological PEF treatment chamber (right hand side). The electrodes are hatched, while the fluid column is white.

The microbial inactivation kinetics dictates two of the process parameters, i.e. the treatment time and the electric field strength. The electric current (I) during pulsing is the product of the electric field strength (E), the flow through area (A) and the medium conductivity (σ)

$$I = E \, \sigma \, A \tag{6.1}$$

Since the conductivity is determined by the type of product, and the electric field strength required by the inactivation kinetics, the current through in a PEF microsieve reactor will be comparable to a pilot scale reactor, since the electrode area remains roughly the same. The voltage that has to be applied (V) will reduce significantly, since it scales linearly with the electrode distance or, in this case, the treatment chamber length (h).

$$V = \frac{E \, h}{\varepsilon} \tag{6.2}$$

This voltage needs to be corrected for the power efficiency (ε) (see §6.8), which is the fraction of total power (P_{total}) that is dissipated in the treatment chamber (P_{tc}). The power efficiency is only dependent on the chamber geometry (relative dimensions) and not on the chamber size (absolute dimensions).

$$\varepsilon = \frac{P_{tc}}{P_{total}} \tag{6.3}$$

The residence time in the PEF microsieve will be drastically smaller, since the chamber length will be much shorter. The residence time will equally decrease with the length. If the microsieve thickness gets about a factor 10^2 smaller pulse frequencies have to increase a factor 10^2 to obtain similar inactivation. Existing pulseforming networks have duty cycles around 100 to 1000 Hz (Roodenburg *et al.*, 2002). In this case, pulse repetition frequencies

around 10-100 kHz would be required. The residence time could in principle be increased by increasing the flow through area of the PEF microsieve, i.e. the number of pores. If a pilot scale PEF reactor would have a diameter of 1 cm and the residence time of a 10^2 times scaled down microreactor needs to be equal, this would give membrane surface areas in the order of several square decimetres to a square meter. In general, this is not much membrane surface. However, the microengineered membranes are costly to produce.

Since the residence times in the pores can be controlled by changing the number of pores or flow rates, the residence times can also be kept very short (e.g. in the range of 10 μs-1 ms). This offers the most promising way of controlling the pulse width, since a continuous electrical signal can be applied, using the residence time to determine the time that a microorganism is treated. Therefore, there is no need anymore for dedicated pulsers, which makes the electrical design of a PEF reactor much easier. Secondly the required membrane area will be much smaller, since very short residence times are required. To summarize the changes in the electrical regime, it can be said that a switch to a PEF microsieve will involve a switch from a high voltage, pulsed system to a low voltage, continuous system with an equal peak current, but a higher average current.

6.5 Energy use and dissipation

The total amount of dissipated energy per volume of treated product (ΔH), assuming pure ohmic behaviour in a continuously operating PEF microsieve, is described by

$$\Delta H = \frac{E^2 \sigma t}{\varepsilon} \tag{6.4}$$

Since ΔH is only determined by food product properties (through σ), and inactivation kinetics (through the electric field strength E and the treatment time t), and not by the dimensions of the treatment chamber, the energy use in a PEF microreactor will be equal to the energy use in a large scale reactor.

Since the energy use will not differ in a microreactor and a large scale reactor, the temperature rise due to ohmic heating will be equal. However, it should be noted that the heat transport in the microreactor will be much faster due to the small distances. In large scale equipment, local hotspots can be present due to the design of the treatment chamber. In the microstructure, the temperature distribution inside the treatment chamber will be much more equal due to this fast heat transport, which is beneficial for the treatment homogeneity, product quality and process stability.

6.6 Pulse width

With the application of a continuous electrical signal to the parallelized PEF reactor, care should be taken that it does not result in a continuous, and therefore much higher production of electrolytic products. This hydrolysis might trigger gas bubble formation, which will disturb the electric field distribution, induce arching and thereby heavily damage the electrodes. Furthermore, the rate of electrode corrosion might also increase significantly.

The use of bipolar pulses will lead to a (partial) reverse reaction of the hydrolysis products if the frequency is high enough. From practice (Fox *et al.*, 2006), it is known that electrolysis is not observed at frequencies higher than 1 kHz. If the net current is zero, the electrodes will stay pH neutral, and will the electrolytic corrosion of the electrode be reduced. Therefore, bipolar signals, like for example AC voltages are preferred (Morren *et al.*, 2003). The rate of electrolysis during a pulse depends on the applied electric potential over the Debye double layer formed at the wetted electrode surface. An electrode in a fluid environment can be electrically regarded as a Debye double layer capacitance and an electrolytic resistance in parallel. The fluid in between the electrodes is regarded to be an ohmic resistance. If a pulse is applied, the Debye double layer is first charged, followed by an electrolytic current through the parallel resistor. If the alternating pulse period is small enough, the minimal redox potential that is needed to start electrochemical reaction will not be reached.

For a sinusoidal continuous signal, the repetition period should be several times shorter than the residence time to be sure that passing cells will meet the maximum applied voltage. Since the residence time will be 10 to 100 μs, frequencies higher than 10 to100 kHz need to be applied.

In addition to the fact that the frequency should not be too low, it should also not be too high, since the cellular membrane needs to be charged for the electroporation process. At frequencies higher than approximately 10 MHz, the charging will only happen partially and thus the transmembrane voltage will be lower. It has been tested in practice (Fox *et al.*, 2006) that for a pulsed system using square wave pulses down to pulse widths of 300 ns (1.7 MHz) a regular electroporation process is observed. Therefore we conclude that an AC signal around 1 MHz is fast enough to eliminate the electrolysis at the electrode surface, while still slow enough to cause electroporation of a bacterial membrane.

6.7 Pressure

Microsieves are delicate membranes which can only withstand a limited deflection force. The flow of the liquid through small pores will create a pressure drop. The pressure drop over a pore with a diameter (d) and a pore height (h) in a microsieve caused by a flow (ϕ) with a viscosity (η) and a fluid density (ρ)is described by (van Rijn *et al.*, 1995; Kuiper, 2000)

$$\Delta P = \phi\left(\frac{24\eta}{d^3}\right)\left(1+\frac{16h}{3\pi d}\right)\left(1-f(\kappa)\right)+\frac{4\rho}{\pi^2 d^4}\phi^2 \qquad (6.5)$$

The term $24\eta/d^3$ describes the resistance of a pore in an infinitely thin membrane. The term $1+16h/3\pi d$ is an addition for the pore length while the term $1-f(\kappa)$ corrects for the synergistic effect of all the pores lying in a square array on a membrane with a porosity κ. The function $f(\kappa)$ can be described by

$$f(\kappa) = \sum_{i=1} a_i \kappa^{i+0.5} \qquad (6.6)$$

with $a_1 = 0.894$, $a_2 = 0.111$ and $a_3 = 0.066$. At the entrance of the pore an extra pressure drop will arise to the acceleration of the fluid, which is known as the Bernoulli effect. This kinetic energy is generally dissipated to heat at the exit and the term $(4\rho/\pi^2 d^4)\phi^2$ in equation 6.5 is a correction for this pressure drop.

When the behaviour of the pressure as a function of the pore diameter is inspected with a fixed pore aspect ratio of 2 (Fig. 6.3), it is observed that the pressure is increasing with increasing pore diameter. This is in contrast with regular membrane operation, where a pressure reduction is noticed with increasing pore diameter. However, regular membrane operations are controlled by setting a certain flow rate. In his case, the residence time in a pore is set. At larger pore diameters and hence longer pores, the flow rate will increase rapidly since the residence time has to be kept constant, thereby causing a pressure increase. Similarly, the pressure will rapidly increase with a decreasing residence time, since the flow rate will increase inversely.
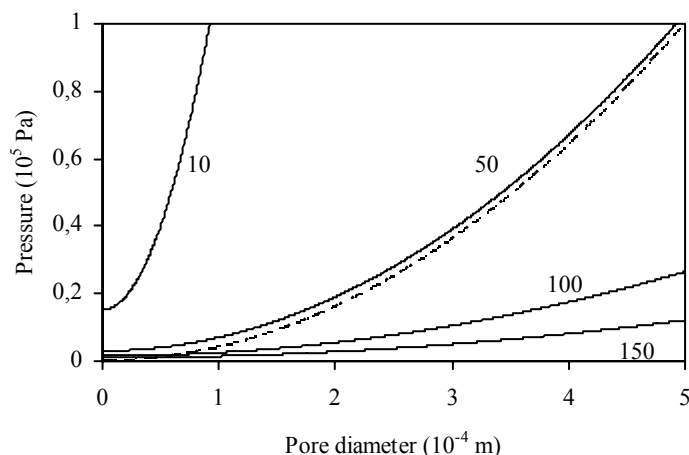
Figure 6.3 Pressure over the membrane as a function of the pore diameter at a fixed residence time of 10, 50,100 and 150 μs with the pore height being twice the pore diameter. One case of the 50 μs residence time (---) is shown where only the last (Bernoulli) term has been used for calculation. The membrane porosity was set at 5 %.

A closer inspection of equation 6.5 shows that the main factor that determines the pressure is the last term; i.e. the pressure difference over the membrane is mainly caused by Bernoulli effect. The resistance caused by the membrane itself is less important. Since the flux ϕ is determined by the residence time of fluid in the pore(τ) and the pore volume (with a pore length h), the last term can be rewritten to

$$\Delta P = \frac{\rho}{4}\left(\frac{h}{\tau}\right)^2 \tag{6.7}$$

This implies that the porosity and pore diameter are not the main ruling parameters, but that the pressure drop scales with the square of the fluid velocity (h/τ). The pressure is therefore quadratically increasing with a decreasing residence time. Given a required flux of 1 m³/hr and a minimal treatment time of 10 μs, a maximal pressure drop of 1 bar will be reached at a maximal pore length of 200 μm. At a treatment time of 100 μs, this will already be 2 mm.

6.8 Electrodes

Different electrode designs can be applied to a scaled-up PEF microreactor. Micromechanical techniques (e.g. sputtering) enable the deposition of a metal layer on the microsieve surface itself. This will be advantageous for the electric efficiency since hardly

any field will be present outside the pore, thereby making the process energy efficient. However, a problem might be the inhomogeneous electric field strength distribution. At the entrance of the pore, a very high local electric field strength will exist at the electrode edge. This can damage the electrode surface and thereby disturb the field distribution. Besides, the electrode is attached to the membrane, thereby making it impossible to replace the electrode after damage. Since the costs of a microsieve will be relatively high, the latter is a considerable disadvantage. Secondly, a conducting particle which accidentally blocks a pore will receive a local high power density which will ultimately lead to a local shortcut.

The electrode can also be placed at a short distance from the membrane, e.g. being a metal wire mesh or specially designed metal electrode structure. This structure can be potentially replaced and will be placed in a zone with a much lower electric field strength. With the electrodes oriented at a distance from the microsieve, the maximal electrical current through a blocked pore will be limited by the resistance of the surrounding fluid, thereby reducing the risk of damage. However, the electric energy losses outside the pores can become quite significant.

A PEF microsieve could be operated in a cross-flow mode, where fluid is flowing through the membrane and along the membrane, and a dead end filtration mode. Cross-flow looks interesting at first sight, since there will be less problems with fouling of the membrane as the fluid flow along the membrane will remove particles. However, the pressure and electrode distance to the membrane will give operational problem. It is essential that the transmembrane pressure is constant, since different pressures will give different residence times, which in turn will lead to different treatment and unequal heating of the product. This could probably be solved by using the uniform transmembrane pressure concept (Sandblom, 1975; Saboya *et al.*, 2000).

A dead end concept with the electrodes being fine wire meshes or structured metal membranes which are positioned at a constant distance to the microsieve also looks promising. The transmembrane pressure and electrode distance can be kept constant. The electrode distance has to be large enough in order to restore a constant fluid flow profile behind the electrode mesh. Therefore it should have a minimal distance to the membrane of at least a couple times the pore separation distance.
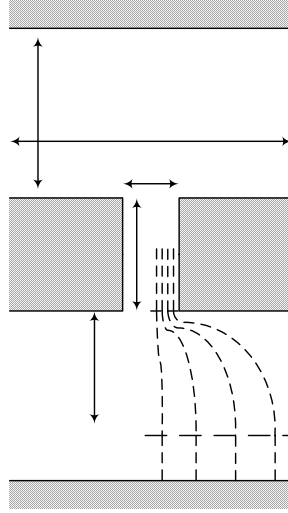
Figure 6.4 Schematic representation of a pore in a membrane with the sizes and resistance contributions.

An electrode oriented above the microsieve will give energy losses. The energy efficiency in a setup with the electrode oriented above the membrane can be described using dimensionless numbers (Fig. 6.4).

$$\varepsilon = \frac{\alpha_{pore}}{(\alpha_{feed} - 1)\sqrt{\kappa_r} + \dfrac{1}{\sqrt{2 - \kappa_r}} + \alpha_{pore}} \qquad (6.8)$$

where the dimensionless pore aspect ratio (α_{pore}) is described by

$$\alpha_{pore} = \frac{h}{d} \qquad (6.9)$$

the dimensionless feed channel aspect ratio (α_{feed}) by

$$\alpha_{feed} = \frac{H}{D} \qquad (6.10)$$

and the radial porosity (κ_r) by

$$\kappa_r = \frac{d^2}{D^2} \qquad (6.11)$$

Equation 6.8 is derived in appendix 6.1. Inspection of the efficiency at an increasing porosity (Fig. 6.5) shows that the efficiency reaches a maximum efficiency at infinitely small porosities. The efficiency is decreasing with an increasing porosity. This increasing porosity implies an increase in the amount of pores per surface area. Therefore, the relative pore resistance will decrease, resulting in a lower power efficiency. The energy efficiency also decreases rapidly with an increasing feed aspect ratio. This decrease is caused by the increase in the bulk dissipation. This dependency is stronger than the porosity dependency.
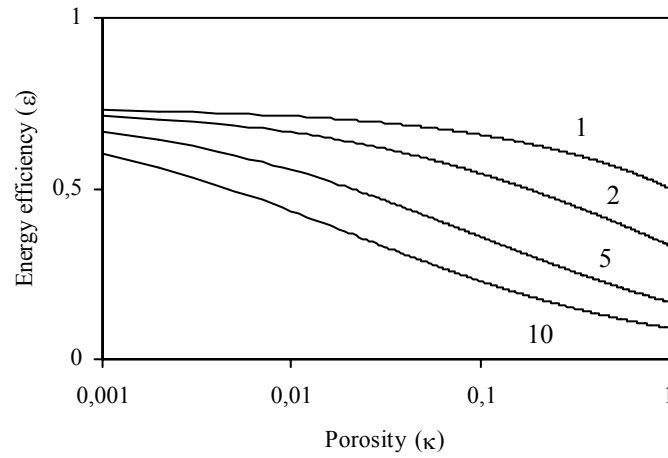
Figure 6.5 Power efficiency of a PEF microsieve as a function of the porosity for a feed aspect ratio (α_{feed}) of 1, 2, 5 and 10 at a pore aspect ratio (α_{pore}) of 2.

The maximum efficiency at the limit-to-zero porosity is equal to

$$\varepsilon = \frac{\alpha_{pore}}{\frac{1}{\sqrt{2}} + \alpha_{pore}} \qquad (6.12)$$

This relation shows (Fig. 6.6) that high pore aspect ratios are advantageous for the energy efficiency; a pore aspect of 1.5 can lead to an energy efficiency of 67 %, whereas a pore aspect ratio of 3 can already reach an efficiency of 81%. However, larger pore aspect ratios will involve higher voltages to reach the required electric field strength since the pore length will increase, and more important, it is a technological challenge (though not impossible) to create a straight pore with an aspect ratio of more than 10.

A minimal energy efficiency of about 50% is desired in a PEF reactor, which compares up to 80% for existing PEF equipment. At lower efficiencies the heat generated in the PEF microsieve will be so high that the thermal effect will overshadow the electrical effects.
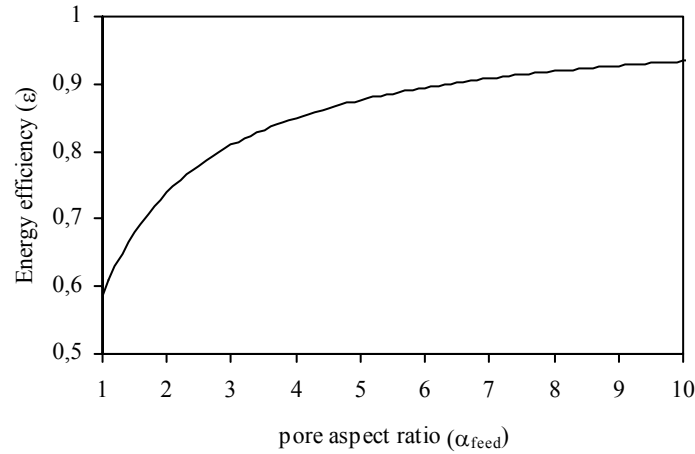
Figure 6.6 Maximum energy efficiency that can be reached at different pore aspect ratios.

6.9 Design window

Based on the information given above, a working range can be deducted for the operation of a PEF microsieve. First of all the practical limitations for the pore aspect ratio and the maximum pressure load are considered. These limits are plotted in figure 6.7a, to show the available design space in pore diameter and aspect ratio. As said before, the aspect ratio has to be larger than 1.5 to obtain a uniform electric field and will be smaller than 10 because of manufacturing constraints. This is depicted by line 1. Line 2 depicts the pressure limitation of 1 bar, as described by equation 6.7. This leaves a design window for the pore diameter and pore aspect ratio.

A similar plot can be made for the membrane area and feed aspect ratio when a point is chosen in the design window in the left figure of figure 6.7 (denoted with X). The feed aspect ratio will be larger than 2 to ensure a good electric field distribution and flow properties (line 3). The maximum membrane area is limited to about 1 dm^2 for a standard wafer (line 4). The required membrane area (A_m) is determined by the required flux (ϕ), residence time (τ), the pore length (h) and porosity (κ).

$$A_m = \frac{\tau\phi}{\kappa h} \qquad\qquad (6.13)$$
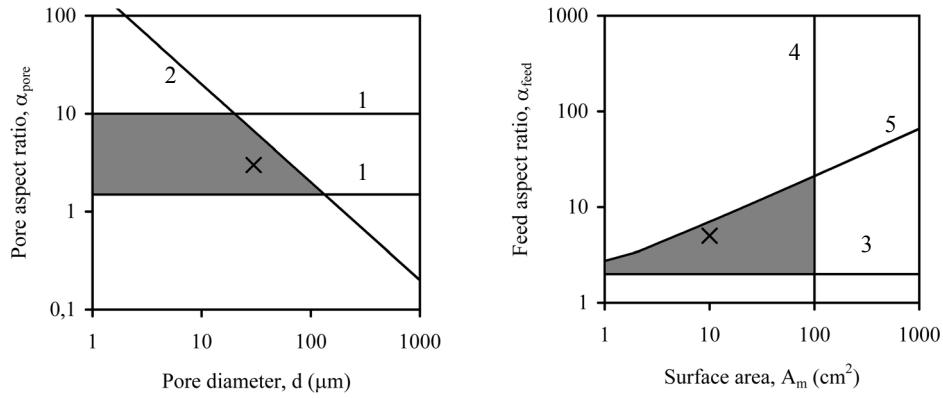
Figure 6.7 Design space for the pore diameter and pore aspect ratio (left) and the membrane surface area and the feed aspect ratio (right). The right figure is based on the point marked X in the left figure.

The maximal feed aspect ratio is limited by the energy efficiency requirement of 50% (Eq. 6.8). Based on the pore diameter and pore aspect ratio chosen, this will determine the design window for the membrane surface area and the feed aspect ratio. An example for the operating values for a PEF microsieve based on this figure is given in table 6.1.

In practice, the pore diameter will be chosen as large as possible, since the risk of fouling will be as low as possible. Nevertheless, it is advisable to incorporate a filtration step in advance of the PEF microsieve to remove fouling.

91

Table 6.1 Parameters for microsieve size

Parameter	Symbol	Value
Pore height	h	90 μm
Pore diameter	d	30μm
Electrode-microsieve distance	H	0.85 mm
Pore aspect ratio	α_{pore}	3
Feed aspect ratio	α_{feed}	5
Efficiency	ε	57%
Microsieve area	A_m	10 cm^2
Flow	ϕ	1 m^3 hr^{-1}
Transmembrane pressure	ΔP	0,2 bar
Viscosity	η	10^{-3} Pa s
Density	ρ	10^3 kg m^{-3}
Residence time	τ	10 μs
Porosity	κ	3.1 %
Electric field strength	E	30 kV cm^{-1}
Voltage	V	475 V

6.10 Conclusion

In this article the conceptual design for a mass parallelized PEF microreactor is discussed. A promising design is a microtechnologically created microsieve, of which the pores serve as a resistance for the concentration of the voltage drop. A large advantage for a PEF microsieve is the ability to use the residence time in the treatment chamber as the pulse duration; i.e. a continuous voltage difference can be applied which makes the electrical design much easier. The shift to a PEF microsieve will be a shift from a high voltage, pulsed system to a low voltage, non-pulsed system at an equal peak current.

The pressure drop over the membrane will be relative low for small pore size, and increase for larger pore sizes, since the residence time needs to be kept constant and therefore the flow rate increases rapidly. It should be noted that the pressure drop over the membrane is not limiting if the residence times is longer than 10 μs and the membrane is thinner than 200 μm.

The electrodes can best be separated from the microsieve, making the setup more flexible. However, this will cause an energy efficiency loss. The electrode configuration should therefore be taken into account. It can be concluded that a mass parallelized PEF microreactor will give different operating regimes from a pilot scale PEF plant. An example was given, which showed the possible operating regime for a PEF microsieve. The pore diameter should be chosen as large as possible, to minimize the risk of blockage.

Nevertheless, it is advisable to incorporate a filtration step in advance of the PEF microsieve to remove any particles. Because of this, it will most probably not serve as a substitution for large scale equipment, but as a complement to the currently available PEF designs.

This study shows that outscaling of a microfluidic device such as for PEF is possible. The total system surface is relatively small, which may imply that the design might be economically realistic. This remains to be evaluated practically in the future, however.

6.11 Acknowledgments

Appendix Power efficiency in a PEF membrane reactor

The energy efficiency of mass parallelized membrane PEF reactor can be approximated using an axisymetric model (Fig. 6.4). This can be done with dimensionless numbers since the power efficiency is not determined by the absolute size.

The energy efficiency can be described as the fraction of the total power dissipated in the pore. Since the current through a series of resistors is equal, the resistances can be used as a measure for the power. The total resistance can be regarded as a series of resistances consisting of the pore resistance, the bulk feed resistance and a resistance describing the entry effect

$$\varepsilon = \frac{P_{tc}}{P_{total}} = \frac{R_{pore}}{R_{pore} + 2(R_{bulk} + R_{entry})} \qquad (A6.1)$$

The pore and bulk resistance can be described using a parallel plate geometry

$$R_{pore} = \frac{4\alpha_{pore}}{\sigma\pi d} \qquad (A6.2)$$

$$R_{bulk} = \frac{4\alpha_{feed} - 2}{\sigma\pi D} \qquad (A6.3)$$

The entry effect is determined for a layer with a height equal to the half of the diameter of the feed layer. The rest is considered bulk resistance.

The entry effect has been modelled using a finite element model consisting of a cylinder with a voltage difference over the two flat sides and a very thin membrane in the middle with one pore in the centre. If the pore diameter is equal to the cylinder diameter (i.e. there is no membrane present), the lowest resistance (R_{open}) is reached. The resistance will rise when the pore diameter becomes smaller (R_{entry}), which can be described by the relative conductance of the setup (γ):

$$\gamma = \frac{R_{open}}{R_{entry}} \qquad (A6.4)$$

It was derived that the relative conductance (γ) is a function of the membrane porosity.

$$\gamma^2 + (1-\kappa)^2 = 1 \tag{A6.5}$$

R_{open} can be described using the parallel plate relation.

$$R_{open} = \frac{2}{\sigma \pi D} \tag{A6.6}$$

Substitution of equation A6.1 to A6.6 gives the power efficiency.

$$\varepsilon = \frac{\alpha_{pore}}{(\alpha_{feed} - 1)\sqrt{\kappa_r} + \dfrac{1}{\sqrt{2 - \kappa_r}} + \alpha_{pore}} \tag{A6.7}$$

This equation has been validated using a finite element model for the whole setup. Three radial porosities with a varying feed channel dimension were modelled. The comparison in figure A6.1 shows and excellent agreement between the analytical model and the finite element simulation.
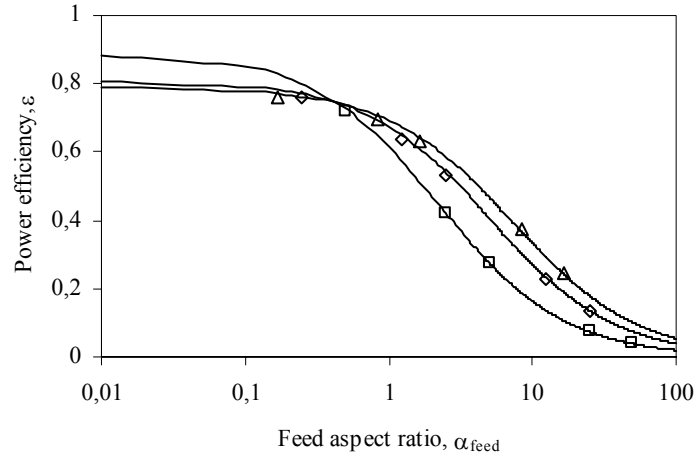

Figure A6.1 Energy efficiency in a parallelized PEF microreactor using an analytical model (solid lines) and a finite element model (points) at a radial porosity of 0.25 ($\square$), 0.06 ($\Diamond$) and 0.03 (Δ).

References

Abram, F., J. P. P. M. Smelt, R. Bos and P. C. Wouters (2003). "Modelling and optimization of inactivation of Lactobacillus plantarum by pulsed electric field treatment." *Journal of Applied Microbiology* **94**(4): 571-579.

Andersson, H. (2003). "Microfluidic devices for cellomics: a review." *Sensors and actuators. B, Chemical* **92**(3): 315-325.

Andersson, H. (2004). "Microtechnologies and nanotechnologies for single-cell analysis." *Current opinion in biotechnology* **15**(1): 44-49.

Baer, D. R., P. E. Burrows and A. A. El-Azab (2003). "Enhancing coating functionality using nanoscience and nanotechnology." *Progress in Organic Coatings* **47**(3-4): 342-356.

Barbosa-Canovas, G. V., M. M. Gongora-Nieto, U. R. Pothakamury and B. G. Swanson (1999). PEF induced biological changes. *Preservation of foods with pulsed electric fields*. S. L. Taylor. San Diego, Academic Press. **1:** 76.

Barbosa-Canovas, G. V., M. M. Gongora-Nieto, U. R. Pothakamury, B. G. Swanson, G. V. Barbosa-C novas, M. M. Gongora-Nieto, U. R. Pothakamury and B. G. Swanson (1999). *Preservation of foods with pulsed electric fields*. San Diego, Academic Press.

Barbosa-Canovas, G. V. and Q. H. Zhang (2001). *Pulsed electric fields in food processing. Fundamental aspects and applications*. Lancaster, Technomic Publishing company, inc.

Becker, H. and C. Gärtner (2000). "Polymer microfabrication methods for microfluidic analytical applications." *Electrophoresis* **21**(1): 12-26.

Beebe, S. J., P. M. Fox, L. J. Rec, L. K. Willis and K. H. Schoenbach (2003). "Nanosecond, high-intensity pulsed electric fields induce apoptosis in human cells." *The FASEB journal* **17**(9).

Belghiti, K. E. and E. Vorobiev (2004). "Mass transfer of sugar from sugar beets enhanced by pulsed electric fields." *Food and bioproducts processing* **82**(3): 226-230.

Bessoth, F. G., A. J. deMello and A. Manz (1999). "Microstructure for efficient continuous flow mixing." *Analytical communications* **36**(6): 213.

Brody, J. P. and P. Yager (1997). "Diffusion-based extraction in a microfabricated device." *Sensors and Actuators A: Physical* **58**(1): 13.

Bruin, G. J. M. (2000). "Recent developments in electrokinetically driven analysis on microfabricated devices." *Electrophoresis* **21**(18): 3931-3951.

Cabrera, C. R. and P. Yager (2001). "Continuous concentration of bacteria in a microfluidic flow cell using electrokinetic techniques." *Electrophoresis* **22**(2): 355-362.

Chang, D. C., D. C. Chang, B. M. Chassy, J. A. Saunders and A. E. Sowers (1992). Structure and dynamics of electric field-induced membrane pores as revealed by rapid-freezing electron microscopy. *Guide to electroporation and electrofusion*. San Diego, Academic Press, Inc. **1:** 9.

Chang, D. C., B. M. Chassy and J. A. Saunders (1992). *Guide to electroporation and electrofusion*. San Diego, Academic Press.

Chen, N., K. H. Schoenbach, J. F. Kolb, R. J. Swanson, A. L. Garner, J. Yang, R. P. Joshi and S. J. Beebe (2004). "Leukemic cell intracellular responses to nanosecond electric fields." *Biochemical and biophysical research communications* **317**: 421-427.

Clague, D. S. and E. K. Wheeler (2001). "Dielectrophoretic manipulation of macromolecules: the electric field." *Physical review E* **6402**(2): 6605.

Davalos, R., Y. Huang and B. Rubinsky (2000). "Electroporation: bio-electrochemical mass transfer at the nanoscale." *Microscale thermophysical engineering* **4**: 147-159.

de Haan, S. W. H. and P. R. Willcock (2002). "Comparison of the energy performance of pulse generation circuits for PEF." *Innovative Food Science & Emerging Technologies* **3**(4): 349.

Dimitrov, D. S. and A. E. Sowers (1990). "Membrane electroporaton -- fast molecular exchange by electroosmosis." *Biochimica et Biophysica Acta (BBA) - Biomembranes* **1022**(3): 381-392.

Doh, I. and Y.-H. Cho (2005). "A continuous cell separation chip using hydrodynamic dielectrophoresis (DEP) process." *Sensors and Actuators A: Physical* **121**(1): 59-65.

Dunn, J. and J. S. Pearlman (1987). High pulsed voltage systems for extending the shelf life of pumpable food products. United States**:** 1.

Efremov, N. M., B. Y. Adamiak, V. I. Blochin, S. J. Dadashev, K. I. Dmitriev, V. N. Semjonov, V. F. Laevashov and V. F. Jubashev (2000). "Experimental investigation of the action of pulsed electric discharges in liquids on biological objects." *IEEE transactions on plasma science* **28**: 224-229.

Ehrfeld, W., V. Hessel and H. Loewe (2000). *Microreactors: new technology for modern chemistry*. Weinheim, Wiley-VCH Verlag.

Eshtiaghi (2002). "High electric field pulse pretreatment: potential for sugar beet processing." *Journal of food engineering* **52**(3): 265.

Fiala, A., P. C. Wouters, H. F. M. van den Bosch and Y. L. M. Creyghton (2001). "Coupled electrical-fluid model of pulsed electric field treatment in a model food system." *Innovative food science and emerging technologies* **2**: 229-238.

Fox, M. B., D. C. Esveld, H. C. Mastwijk and R. M. Boom (2006). "Inactivation of L. plantarum in a PEF microreactor. The effect of pulse width and temperature on the inactivation." *Innovative Food Science & Emerging Technologies* ***Submitted for publication***.

Fox, M. B., D. C. Esveld, A. Valero, R. Luttge, H. C. Mastwijk, P. V. Bartels, A. van den Berg and R. M. Boom (2006). "Electroporation of cells in microfluidic devices: a review." *Analytical and Bioanalytical Chemistry* **385**(3): 474-485.

Fox, M. B., E. Esveld, R. Luttge and R. Boom (2005). "A new pulsed electric field microreactor: comparison between the laboratory and microscale." *Lab on a chip* **5**(9): 943-948.

Gao, J., X. F. Yin and Z. L. Fang (2004). "Integration of single cell injection, cell lysis separation and detection of intracellular constituents on a microfluidic chip." *Lab on a chip* **4**: 47-52.

Glaser, R. W., S. L. Leikin, L. V. Chernomordik, V. F. Pastushenko and A. I. Sokirko (1988). "Reversible electrical breakdown of lipid bilayers: formation and evolution of pores." *Biochimica et biophysica acta* **940**: 275.

Guijt, R. M., A. Dodge, G. W. K. v. Dedem, N. F. d. Rooij and E. Verpoorte (2003). "Chemical and physical processes for integrated temperature control in microfluidic devices." *Lab Chip* **3**: 1.

Hamilton, W. A. and A. J. H. Sale (1967). "Effects of high electric fields on microorganisms II Mechanism of action of the lethal effect." *Biochimica et biophysica acta* **148**: 789-800.

Haswell, S. J. (1997). "Development and operating characteristics of micro flow injection analysis systems based on electroosmotic flow." *Analytica Chimica Acta* **122**: 1R-10R.

Heinz, V., S. Toepfl and D. Knorr (2003). "Impact of temperature on lethality and energy efficiency of apple juice pasteurization by pulsed electric fields treatment." *Innovative Food Science & Emerging Technologies* **4**(2): 167.

Ho, S. Y. and G. S. Mittal (1996). "Electroporation of cell membranes: A review." *Critical reviews in biotechnology* **16**(4): 349.

Ho, S. Y., G. S. Mittal and J. D. Cross (1997). "Effects of high electric field pulses on the activity of selected enzymes." *Journal of food engineering* **31**: 69-84.

Hope, M. J., M. B. Bally, G. Webb and P. R. Cullis (1985). "Production of large unilamellar vesicles by a rapid extrusion procedure. Characterization of size distribution, trapped volume and ability to maintain a membrane potential." *Biochimica et biophysica acta* **812**: 55.

Huang, Y. and B. Rubinsky (1999). "Micro-electroporation: improving the efficiency and understanding of electrical permeabilization of cells." *Biomedical microdevices* **2**(2): 145-150.

Huang, Y. and B. Rubinsky (2001). "Microfabricated electroporation chip for single cell membrane permiabilization." *Sensors and actuators A* **89**: 242-249.

Huang, Y. and B. Rubinsky (2003). "Flow-through micro-electroporation chip for high efficiency single-cell genetic manipulation." *Sensors and actuators A* **104**: 205-212.

Huang, Y., N. S. Sekhon, J. Borninski, N. Chen and B. Rubinsky (2003). "Instantaneous, quantitative single-cell viability assessment by electric evaluation of cell membrane integrity with microfabricated devices." *Sensors and actuators A* **105**: 31-39.

Huelsheger, H., J. Potel and E. G. Niemann (1981). "Killing of bacteria with electric pulses of high field strength." *Radiation and environmental biophysics* **20**: 53.

Hunter, R. J. (1980). Zeta potential in colloid science: Principles and applications. London, Academic Press.

Jankowski, J. A., S. Tracht and J. V. Sweedler (1995). "Assaying single cells with capillary electrophoresis." *Trends in Analytical Chemistry* **14**(4): 170-176.

Khine, M., A. Lau, C. Ionescu-Zanetti, J. Seo and L. P. Lee (2005). "A single cell electroporation chip." *Lab on a chip* **5**: 38-43.

Knorr, D., A. Angersbach, M. N. Eshtiaghi, V. Heinz and D. Lee (2001). "Processing concepts based on high intensity electric field pulses." *Trends in food science & technology* **12**(3&4): 129-135.

Kuiper, S. (2000). Development and application of microsieves. Enschede, The Netherlands, University of Twente.

Lee, S.-W. and Y.-C. Tai (1999). "A micro cell lysis device." *Sensors and Actuators A: Physical* **73**(1-2): 74-79.

Lelieveld, H. L. M. (2005). PEF - A food industry's view. *Novel food processing technologies*. **141:** 145-156.

Lettieri, G.-L., A. Dodge, G. Boer, N. F. d. Rooij and E. Verpoorte (2003). "A novel microfluidic concept for bioanalysis using freely moving beads trapped in recirculating flows." *Lab on a chip* **3**(1): 34-39.

Li, P. C. H. and D. J. Harrison (1997). "Transport, manipulation and reaction of biological cells on-chip using electrokinetic effects." *Analytical chemistry* **69**: 1564-1568.

Lin, C.-H., C.-H. Tsai and L.-M. Fu (2005). "A rapid three-dimensional vortex micromixer utilizing self-rotation effects under low Reynolds number conditions." *Journal of Micromechanics and Microengineering*(5): 935.

Lin, Y. C., C. M. Jen, M. Y. Huang, C. Y. Wu and X. Z. Lin (2001). "Electroporation microchips for continuous gene transfection." *Sensors and Actuators B* **79**: 137-143.

Lin, Y. C., M. Li, C. S. Fan and L. W. Wu (2003). "A microchip for electroporation of primary endothelian cells." *Sensors and actuators A* **108**: 12-19.

Lin, Y. C., M. Li and C. C. Wu (2004). "Simulation and experimental demonstration of the electric field assisted electroporation microchip for in vitro gene delivery enhancement." *Lab on a chip* **4**: 104-108.

Loomis-Husselbee, J. W., P. J. Cullen, R. F. Irvine and A. P. Dawson (1991). "Electroporation can cause artifacts due to solubilization of cations from the electrode plates." *Biochemical Journal* **277**: 883-885.

Lu, H., M. A. Schmidt and K. F. Jensen (2005). "A microfluidic electroporation device for cell lysis." *Lab on a chip* **5**: 23-29.

Lubicki, P. and S. Jayaram (1997). "High voltage pulse application for the destruction of the gram-negative bacterium Yersinia enterocolitica." *Bioelectrochemistry and bioenergetics* **43**: 135-141.

Lundqvist, J. A., F. Sahlin, M. A. Aberg, A. Stroemberg, P. S. Eriksson and O. Orwar (1998). "Altering the biochemical state of individual cultured cells and organelles with ultramicroelectrodes." *Proceedings of the national academy of sciences USA* **95**: 10356-10360.

MacInnes, J. M. (2002). "Computation of reacting electrokinetic flow in microchannel geometries." *Chemical Engineering Science* **57**(21): 4539-4558.

Martin-Belloso, O., H. Vega-Mercado, B. Qin, F. J. Chang, G. V. Barbosa-Canovas and B. G. Swanson (1997). "Inactivation of Escherichia coli suspended in liquid egg using pulsed electric fields." *Journal of food processing and food preservation* **21**: 193.

Mastwijk, H. C. and P. V. Bartels (2004). "Pulsed electric field (PEF) processing in the fruit juice and dairy industries." *The international review of food science and technology*: 106-108.

Mayer, L. D., M. J. Hope and P. R. Cullis (1986). "Vesicles of variable sizes produced by a rapid extrusion procedure." *Biochimica et biophysica acta* **858**(1): 161.

Mazurek, B., P. Lubicki and Z. Staroniewicz (1995). "Effect of short HV pulses on bacteria and fungi." *IEEE transactions on dielectrics and electrical insulation* **2**: 418-425.

McClain, M. A., C. T. Culbertson, S. C. Jacobson, N. L. Allbritton, C. E. Sims and J. M. Ramsey (2003). "Microfluidic devices for the high-throughput chemical analysis of cells." *Analytical chemistry* **75**: 5646-5655.

Min, S., Z. T. Jin, S. K. Min, H. Yeom and Q. H. Zhang (2003). "Commercial-scale pulsed electric field processing of orange juice." *Journal of food science* **68**(4): 1265-1271.

Morren, J., B. Roodenburg and S. W. H. de Haan (2003). "Electrochemical reactions and electrode corrosion in pulsed electric field (PEF) treatment chambers." *Innovative Food Science & Emerging Technologies* **4**(3): 285.

Mueller, K. J., V. L. Sukhorukov and U. Zimmermann (2001). "Reversible Electropermeabilization of Mammalian Cells by High-Intensity, Ultra-Short Pulses of Submicrosecond Duration." *Journal of Membrane Biology* **184**(2): 161-170.

Munce, N. R., J. Li, P. R. Herman and L. Lilge (2004). "Microfabricated system for parallel single-cell capillary electrophoresis." *Analytical chemistry* **76**: 4983-4989.

Nedelcu, S. and J. H. P. Watson (2004). "Size separation of DNA molecules by pulsed electric field dielectrophoresis." *Journal of Physics D: Applied Physics* **37**(15): 2197-2204.

Neumann, E., A. E. Sowers, C. A. Jordan, E. Neumann, A. E. Sowers and C. A. Jordan (1989). *Electroporation and electrofusion in cell biology*. New York, Plenum press.

Nolkrantz, K., C. Farre, A. Brederlau, R. I. D. Karlsson, C. Brennan, P. S. Eriksson, S. G. Weber, M. Sandberg and O. Orwar (2001). "Electroporation of Single Cells and Tissues with an Electrolyte-filled Capillary." *Analytical chemistry* **73**(18): 4469-4477.

Olofsson, J., K. Nolkrantz, F. Rytssen, B. A. Lambie, S. G. Weber and O. Orwar (2003). "Single-cell electroporation." *Current opinion in biotechnology* **14**: 29-34.

Orla-Jensen, S. (1919). *The lactic acid bacteria*. Copenhagen, Host & Son.

Pakhomov, A. G., A. Phinney, J. Ashmore, K. Walker, J. F. Kolb, S. Kono, K. H. Schoenbach and M. R. Murphy (2004). "Characterization of the cytotoxic effect of high-intensity, 10-ns duration electrical pulses." *IEEE transactions on plasma science* **32**(4): 1579-1586.

Peleg, M. (1995). "A model of microbial survival after exposure to pulsed electric fields." *Journal of the science of food and agriculture* **67**(1): 93.

Pol, I. E. (2000). "Pulsed-electric field treatment enhances the bactericidal action of nisin against Bacillus cereus." *Applied and environmental microbiology* **66**(1): 428-430.

Pol, I. E. (2001). Improved applicability of nisin in novel combinations with other food preservation factors.

Pothakamury, U. R., H. Vega, Q. H. Zhang, G. V. Barbosa-Canovas and B. G. Swanson (1996). "Effect of growth stage and processing temperature on the inactivation of E. coli by pulsed electric fields." *Journal of food protection* **59**(11): 1167.

Prasanna, G. L. and T. Panda (1997). "Electroporation: basic principles, practical considerations and applications in molecular biology." *Bioprocess engineering* **16**: 261-264.

Prins, M. W. J. (2001). "Fluid control in multichannel structures by electrocapillary pressure." *Science* **291**(5502): 277-280.

Qin, B. L., F. J. Chang, G. V. Barbosa-Cánovas and B. G. Swanson (1995). "Nonthermal inactivation of S. cerevisiae in apple juice using pulsed electric fields." *Lebensmittel-Wissenschaft und -Technologie* **28**(6): 564-568.

Reyes, D. R., D. Iossifidis, P. A. Auroux and A. Manz (2002). "Micro total analysis systems. 1. Introduction, theory, and technology." *Analytical chemistry* **74**(12): 2623-2636.

Reyns, K. F. M. A., A. M. J. Diels and C. W. Michiels (2004). "Generation of bactericidal and mutagenic components by pulsed electric field treatment." *International journal of food microbiology* **93**(2): 165-173.

Rice, K. C., B. A. Firek, J. B. Nelson, S.-J. Yang, T. G. Patton and K. W. Bayles (2003). "The Staphylococcus aureus cidAB Operon: Evaluation of Its Role in Regulation of Murein Hydrolase Activity and Penicillin Tolerance." *J. Bacteriol.* **185**(8): 2635-2643.

Roodenburg, B., J. Morren, H. E. Berg and S. W. H. de Haan (2005). "Metal release in a stainless steel Pulsed Electric Field (PEF) system: Part I. Effect of different pulse shapes; theory and experimental method." *Innovative Food Science & Emerging Technologies* **6**(3): 327-336.

Roodenburg, B., J. Morren, H. E. Berg and S. W. H. de Haan (2005). "Metal release in a stainless steel pulsed electric field (PEF) system: Part II. The treatment of orange juice; related to legislation and treatment chamber lifetime." *Innovative Food Science & Emerging Technologies* **6**(3): 337-345.

Roodenburg, B., J. Morren, S. W. H. de Haan, H. A. Prins and Y. L. M. Creyghton (2002). Modelling a 80 kV pulse source for pulsed electric fields. *PEF, 10th Power electronics and motion control conference (PEMC)*. Croatia.

Ross, D., M. Gaitan and L. E. Locascio (2001). "Temperature Measurement in Microfluidic Systems Using a Temperature-Dependent Fluorescent Dye." *Analytical chemistry* **73**: 4117.

Ryttsen, F., C. Farre, C. Brennan, S. G. Weber, K. Nolkrantz, K. Jardemark, D. T. Chiu and O. Orwar (2000). "Characterization of Single-Cell Electroporation by Using Patch-Clamp and Fluorescence Microscopy." *Biophys. J.* **79**(4): 1993-2001.

Saboya, L. V. and J. L. Maubois (2000). "Current developments of microfiltration technology in the dairy industry." *Lait* **80**: 541-553.

Sale, A. J. H. and W. A. Hamilton (1967). "Effects of high electric fields on microorganisms. I Killing of bacteria and yeasts." *Biochimica et biophysica acta* **148**: 781-788.

Sale, A. J. H. and W. A. Hamilton (1968). "Effects of high electric fields on micro-organisms III Lysis of erythrocytes and protoplasts." *Biochimica et biophysica acta* **163**: 37-43.

Sandblom, R. M. (1975). Filtering process. USPTO. United States.

Schasfoort, R. B. M. (1999). "Field-effect flow control for microfabricated fluidic networks." *Science* **286**(5441): 942-945.

Schneider, M. A., T. Maeder, P. Ryser and F. Stoessel (2004). "A microreactor-based system for the study of fast exothermic reactions in liquid phase: characterization of the system." *Chemical engineering journal* **101**(1-3): 241-250.

Schoenbach, K. H., S. J. Beebe and E. S. Buescher (2001). "Intracellular effect of ultrashort electrical pulses." *Bioelectromagnetics* **22**: 440-448.

Schoenbach, K. H., F. E. Peterkin, R. W. Alden, III and S. J. Beebe (1997). "The effects of pulsed electric fields on biological cells: Experiments and applications." *IEEE transactions on plasma science* **25**(2): 284-292.

Sensoy, I., Q. H. Zhang and S. Sastry (1996). "Inactivation kinetics of Salmonella dublin by pulsed electric field." *Journal of food process engineering* **20**: 367.

Seo, J., C. Ionescu-Zanetti, J. Diamond, R. Lal and L. P. Lee (2004). "Integrated multiple patch-clamp array chip via lateral cell trapping junctions." *Applied physics letters* **84**(11): 1973-1975.

Sepulveda, D. R., M. M. Gonogora-Nieto, M. F. San-Martin and G. V. Barbosa-Canovas (2005). "Influence of treatment temperature on the inactivation of Listeria innocua by pulsed electric fields." *Lebensmittel-Wissenschaft und Technologie* **38**(2): 167-172.

Serpersu, E. H. and T. Y. Tsong (1984). "Activation of electrogenic Rb+ transport of (Na,K)-ATPase by an electric field." *J. Biol. Chem.* **259**(11): 7155-7162.

Serpersu, E. H., T. Y. Tsong and K. Kinosita (1985). "Reversible and irreversible modification of erythrocyte membrane permeability by electric field." *Biochimica et biophysica acta* **812**(3): 779-785.

Stacey, M., J. Stickley, P. M. Fox, V. Statler, K. H. Schoenbach, S. J. Beebe and E. S. Buescher (2003). "Differential effects in cells exposed to ultra-short, high intensity electric fields: cell survival, DNA damage, and cell cycle analysis." *Mutation research* **542**: 65-75.

Stuart, J. N. and J. V. Sweedler (2002). "Single-cell analysis by capillary electrophoresis." *Analytical and bioanalytical chemistry* **375**: 28-29.

Suehiro, J., T. Hatano, M. Shutou and M. Hara (2005). "Improvement of electric pulse shape for electropermeabilization-assisted dielectrophoretic impedance measurement for high sensitive bacteria detection." *Sensors and Actuators B: Chemical* **109**(2): 209-215.

Suehiro, J., M. Shutou, T. Hatano and M. Hara (2003). "High sensitive detection of biological cells using dielectrophoretic impedance measurement method combined with electropermeabilization." *Sensors and Actuators B: Chemical* **96**(1-2): 144-151.

Suehiro, J., R. Yatsunami, R. Hamada and M. Hara (1999). "Quantitative estimation of biological cell concentration suspended in aqueous medium by using dielectrophoretic impedance measurement method." *Journal of Physics D: Applied Physics* **32**(21): 2814-2820.

The Associated Press (August 18, 2005). "Press release: Juice company returns after FDA setback, Genesis utilizes pasteurization alternative in order to reopen."

Tsong, T. Y. and K. Kinosita (1985). "Use of voltage pulses for the pore opening and drug loading and the subsequent resealing of red blood cells." *Bibl. Haematol. (Basel)* **51**: 108-114.

Valero, A., F. Merino, F. Wolbers, R. Luttge, I. Vermes, H. Andersson and A. van den Berg (2005). "Apoptotic cell death dynamics of HL60 cells studied using a microfluidic cell trap device." *Lab on a chip* **5**(1): 49-55.

Van Boekel, M. J. A. S. (2002). "On the use of the Weibull model to describe thermal inactivation of microbial vegetative cells." *Int. J. Food Microbiol.* **74**: 139-159.

Van Rijn, C. J. M. (2004). Nano and micro engineered membrane technology, Elsevier.

van Rijn, C. J. M. and M. C. Elwenspoek (1995). "Micro filtration membrane sieve with silicon micromachining for industrial and biomedical applications." *IEEE Micro mechanical systems*: 83-87.

Verpoorte, E. (2002). "Microfluidic chips for clinical and forensic analysis." *Electrophoresis* **23**(5): 677-712.

Voldman, J., R. A. Braff, M. Toner, M. L. Gray and M. A. Schmidt (2001). "Holding Forces of Single-Particle Dielectrophoretic Traps." *Biophys. J.* **80**(1): 531-541.

Vrouwe, E. X., R. Luttge and A. v. d. Berg (2004). "Direct measurement of lithium in whole blood using microchip capillary electrophoresis with integrated conductivity detection." *Electrophoresis* **25**(10-11): 1660-1667.

Washizu, M. (2005). "Biological applications of electrostatic surface field effects." *Journal of Electrostatics* **63**(6-10): 795-802.

Wheeler, A. R., K. Morishima, D. W. Arnold, A. B. Rossi and R. N. Zare (2000). *Proceedings of micro-TAS*: 25-28.

Wong, P. K., T.-H. Wang, J. H. Deval and C.-M. Ho (2004). "Electrokinetics in micro devices for biotechnological applications." *IEEE/ASME transactions on mechatronics* **9**(2): 366-376.

Wouters, P. C. (1999). "Effects of pulsed electric fields on inactivation kinetics of Listeria innocua." *Applied and environmental microbiology* **65**(12): 5364-5371.

Wouters, P. C., I. Alvarez and J. Raso (2001). "Critical factors determining inactivation kinetics by pulsed electric field food processing." *Trends in food science & technology* **12**(3): 112.

Wouters, P. C., A. P. Bos and J. Ueckert (2001). "Membrane Permeabilization in Relation to Inactivation Kinetics of Lactobacillus Species due to Pulsed Electric Fields." *Appl. Environ. Microbiol.* **67**(7): 3092-3101.

Yeom, H., G. A. Evrendilek, Z. T. Jin and Q. H. Zhang (2004). "Processing of yoghurt-based products with pulsed electric fields: Microbial, sensory and physical evaluations." *Journal of food processing and food preservation* **28**(3): 161-178.

Yeung, E. S. (1999). "Study of single cells by using capillary electrophoresis and native fluorescence detection." *Journal of Chromatography A* **830**(2): 243-262.

Yin, Y., Q. H. Zhang and K. S. Sudhir (1997). High-voltage pulsed electric field treatment chambers for the preservation of liquid food products, The Ohio State University.

Zabzdyr, J. L. and S. J. Lillard (2001). "New approaches to single-cell analysis by capillary electrophoresis." *Trends in Analytical Chemistry* **20**(9): 467-476.

Zhang, Q. H., A. Monsalve-Gonz lez, B. Qin, G. V. Barbosa-Canovas and B. G. Swanson (1994). "Inactivation of Saccharomyces cervisiae in apple juice by square-wave and exponential-decay pulsed electric fields." *Journal of food process engineering* **17**: 469.

Summary

Pulsed electric fields (PEF) is a novel, non-thermal pasteurization method which uses short, high electric field pulses to inactivate microorganisms. These high electric field pulses are usually in the order of 2 to 300 μs wide with an electric field strength of 10 to 50 kV cm^{-1}. The advantage of a pasteurization method like PEF compared to regular heat pasteurization is that the taste, flavour, texture and nutritional value are much less affected. At the moment, the PEF process faces several challenges, to which microtechnology could be an aid. Microtechnology is the field of research where very small structures (in the order of micrometers) are created in materials like glass or silicon, using modern micromachining techniques.

To generate the high electric field pulses, very high voltage pulses are required. This complicates the design of equipment for pulsing. In microtechnological channels, the distances are much smaller, which implies that much lower voltages are required. Therefore, more conventional (and cost effective) electrical equipment can be used, and the pulsing can be better controlled. Secondly, fluid will heat in the PEF process due to ohmic heating. Since the surface-to-volume area in microtechnological devices is much larger than in regular PEF chambers and since the distances are much smaller, the generated heat can be removed much faster. This makes a separation of the electric field inactivation kinetics and heat inactivation kinetics possible. This thesis describes the state-of-art in microfluidic electroporation (Chapter 2), the design of a PEF microreactor and inactivation experiments on several model systems (Chapter 3-5) and the conceptual design of an upscaled PEF microreactor (Chapter 6).

In chapter 2, a literature review is done on the microfluidic devices that have been designed to study the process of electroporation. The devices can be divided in three categories; devices for analysis, transfection or pasteurization. High electric field strengths were created by the close proximity of the electrodes or by creating a constriction in between the electrodes, which focuses the electric field. Detection is usually done by fluorescent labelling or impedance measurement. Most devices have been focussed at the electroporation process itself, but integration with separation and detection methods is expected. Especially single cell content analysis is expected to be a valuable addition to the microfluidic chip concept. Furthermore, microdevices can enhance the research in intracellular electroporation by using advanced pulse schemes.

Chapter 3 describes the design of a new microreactor dedicated for PEF and the comparison with a laboratory-scale setup. The PEF microreactor consists of a flow-through channel with a constriction where the electric field is focussed. Compared to a laboratory-scale setup, 25 times lower voltages were required to obtain the same electric field strength due to the close electrode spacing. A finite element model showed that the electric field intensity is very homogeneous throughout the channel, which is crucial for pasteurization processes. Experiments where artificial vesicles, loaded with carboxyfluorescein, were

electroporated showed that the maximum transmembrane potential adequately described the electroporation processes both in the microreactor and the laboratory-scale setup, although the length scales are different. Electroporation started at a transmembrane potential of 0.5 V, reaching a maximum fraction of electroporated vesicles of 51% at a transmembrane potential of 1.5 V. The partial electroporation was shown not to be a result of the heterogeneity of the vesicles or the electric field.

Chapter 4 describes the inactivation of *L. plantarum* by pulsed electric fields (PEF) in a microfluidic reactor. Temperature measurements were carried out using the fluorescent intensity dependency of Rhodamine B on temperature. It was demonstrated that the temperature increase due to the ohmic heating of the fluid during treatment is marginal, thereby making this an excellent device for decoupling temperature and electric field effects during PEF. Flow cytometry measurements showed that the electroporation of cells by PEF is a gradual effect. Reducing the pulse width at equal energy inputs did not result in a change in inactivation. Higher temperatures showed strongly increased inactivation rates. The effect of the temperature and the electric field strength could be described by a model that combines an Arrhenius equation for temperature dependency with either a Huelsheger equation or an activation energy based model for electric field dependency.

In chapter 5, the electroporation of yeast was studied using two different microdevices; a single-cell electroporation device, which allows visual observation of the electroporation process of one cell in time, and the PEF microreactor, which gives quantitative kinetic data based on a population of cells. The electroporation process was studied using the membrane-impermeable fluorescent DNA stain PI. Visual observation and flow cytometry measurements revealed that the electroporation process is a progressive process, since the application of more pulses showed gradually more PI uptake, and thus higher fluorescent intensities. When the pulses were applied in a short time interval, the inactivation rates increased, which was attributed to the prevention of partial membrane recovery between the pulses. The inactivation behaviour in both devices was comparable. The inactivation started at electric field strengths of 1.2 to 4 kV cm^{-1}.

Several potential advantages were already mentioned for a PEF microreactor, but for a large scale process aimed at e.g. 1 m^3 hr^{-1}, the microreactor has to be mass parallelized. In chapter 6, a conceptual design is proposed based on a microengineered microsieve with a highly defined pore geometry. The pores serve as a restriction to concentrate the voltage drop, and thus increasing the electric field strength. It is shown that the pore residence time can be utilized to define the total treatment time, which enables the use of constant (AC) power sources instead of pulsed power sources. A consequence of the reduced electrode spacing is that average current is inversely increased. The hereby emerging problem of electrolytic damage can be virtually eliminated by using a source frequency of 1 MHz. The pore length is limited at small residence times by the maximal allowable pressure drop.

For a good treatment homogeneity and process stability it is advisable to separate the electrodes from the microsieve, However, a relative close proximity of the electrode meshes to the microsieve is required keep the power efficiency up to reasonable levels, and at the same time to limit the required membrane area. The final design will always be a trade-off between the pore geometry, the pore size and the efficiency that has to be reached. This has been illustrated in an example case.

Samenvatting

Toepassing van gepulseerd elektrische velden (PEF) is een nieuwe, non-thermische pasteurisatiemethode waarbij korte pulsen met een hoge elektrische veldsterkte worden gebruikt om micro-organismen te inactiveren. Deze pulsen zijn over het algemeen 2 tot 300 µs lang en hebben een veldsterkte van 10 tot 50 kV cm^{-1}. In tegenstelling tot de gebruikelijke hitte pasteurisatiemethoden tast PEF de smaak, geur, textuur en voedingswaarde van producten minder aan. Op het moment zijn er een aantal beperkingen aan het PEF proces, waarbij microtechnologie een oplossing zou kunnen bieden. Microtechnologie is het onderzoeksveld waarbinnen zeer kleine structuren (in de orde grootte van micrometers) worden gemaakt in materialen zoals glas of silicium.

Om pulsen van een hoge veldsterkte te genereren zijn hoog voltage pulsen nodig. Hiervoor zijn zeer gespecialiseerde pulsers nodig. In microtechnologische kanalen zijn de afstanden veel kleiner, waardoor veel lagere voltages nodig zijn. Daardoor kan conventionele (en dus goedkopere) elektrische apparatuur gebruikt worden en de pulsen kunnen beter gecontroleerd worden. Ten tweede zal vloeistof opwarmen tijdens het PEF proces door ohmse opwarming. Omdat de oppervlakte-volume verhouding in een microtechnologische chip veel groter is, en omdat de afstanden veel kleiner zijn, kan de warmte veel sneller afgevoerd worden. Omdat het systeem daardoor nog nauwelijks opwarmt, kan de kinetiek van de elektrisch veld inactivatie gescheiden worden van warmte inactivatie effecten. Dit proefschrift behandelt microtechnologische elektroporatie (hoofdstuk 2), het ontwerp van een nieuwe PEF microreactor en inactivatie experimenten met verscheidene modelsystemen (hoofdstuk 3-5) en besluit met een conceptueel ontwerp van een opgeschaalde PEF microreactor (hoofdstuk 6).

In hoofdstuk 2 wordt een literatuuroverzicht gegeven van de verschillende microchips die ontworpen zijn om het elektroporatieproces te bestuderen. Deze microchips kunnen in drie categorieën ingedeeld worden: microchips voor analyse, voor transfectie of voor pasteurisatie. Hoge elektrische veld sterktes worden verkregen door een kleine elektrode afstand of door een vernauwing tussen de elektrodes te creëren waar het elektrisch veld gefocust wordt. Detectie wordt meestal gedaan door fluorescente labelling of door impedantiemetingen. De meeste microchips zijn ontworpen voor de bestudering van het elektroporatieproces zelf, hoewel integratie met scheidings- en detectietechnieken in de toekomst wordt verwacht. Dit zou het mogelijk maken een analyse te verrichtten van bepaalde componenten uit één enkele cel.

Hoofdstuk 3 beschrijft het ontwerp van een nieuwe microreactor speciaal ontworpen voor het PEF proces en een vergelijking van de werking met een bestaande laboratoriumschaal opstelling. De PEF microreactor bestaat uit een kanaal met een vernauwing waar het elektrische veld in geconcentreerd wordt. Door de kleine elektrode afstand is er, vergeleken met een laboratoriumopstelling, een 25 keer lager voltage nodig om een gelijke veldsterkte te bereiken. Een eindige-element model laat zien dat het elektrische veld homogeen is in het

kanaal, wat cruciaal is voor het PEF proces. Er zijn experimenten gedaan met kunstmatige vesicles, gevuld met fluorescente kleurstof (carboxyfluorescein). Deze experimenten laten zien dat de maximum transmembraan potentiaal het elektroporatieproces goed beschrijft, hoewel de lengteschalen sterk verschillen. Elektroporatie begint bij een transmembraan potentiaal van 0.5 V, totdat een maximum fractie van 51% wordt geëlektroporeerd bij een transmembraanpotentiaal van 1.5 V. Deze gedeeltelijke elektroporatie wordt niet veroorzaakt door een heterogeniteit van de vesicles of het elektrische veld.

Hoofdstuk 4 beschrijft de inactivatie van de melkzuur bacterie *L. plantarum* in de microreactor bij verschillende elektrische regimes en temperaturen. De temperatuur in de microreactor is gemeten door de temperatuursafhankelijkheid van de fluorescentie intensiteit van Rhodamine B te gebruiken. De temperatuursstijging door ohmse verhitting is klein, waardoor de microreactor zeer geschikt is voor het ontkoppelen van temperatuurs- en elektrische effecten tijdens het PEF proces. Door middel van flowcytometrie metingen is aangetoond dat elektroporatie een gradueel proces is. Een reductie van de pulsduur bij een gelijke energietoevoer geeft geen verschil in inactivatie. De effecten van de temperatuur en het elektrische veld kunnen worden beschreven door een model dat een Arrhenius vergelijking (voor het temperatuurseffect) combineert met een Huelsheger vergelijking of een activeringsenergie gebaseerd model (voor de elektrische veld afhankelijkheid).

In hoofdstuk 5 is de elektroporatie van gist bestudeerd in twee verschillende microchips: een chip om een enkele cel te meten, waarbij het elektroporatie proces van een enkele cel visueel gevolgd kan worden in de tijd, en de PEF microreactor, waarbij kwantitatieve data gegenereerd kunnen worden gebaseerd op een populatie van cellen. Het elektroporatie proces is bestudeerd door cellen te kleuren met de fluorescente DNA kleurstof PI, die niet door het celmembraan heen kan tenzij het membraan beschadigd is. Visuele observatie en flowcytometrie metingen laten zien dat elektroporatie een progressief proces is, omdat het toedienen van meer pulsen leidt tot hogere intensiteiten en dus een hogere opname. Meer cellen werden geïnactiveerd wanneer pulsen in een kort tijdsbestek werden toegediend. Dit wordt waarschijnlijk veroorzaakt doordat het celmembraan bij lange tussenposen gedeeltelijk kan herstellen. De inactivatie in de twee microchips is vergelijkbaar, en begint bij elektrische veldsterktes van 1.2 tot 4 kV cm^{-1}.

Een aantal voordelen van een PEF microreactor zijn al genoemd, maar voor een proces op grote schaal waarbij bijvoorbeeld 1 m^3 hr^{-1} moet worden verwerkt, moet de microreactor geparalleliseerd worden. In hoofdstuk 6 wordt een conceptueel ontwerp gegeven dat gebaseerd is op een microzeef met een nauw gedefinieerde poriegrootte. De poriën dienen als een vernauwing om het potentiaalverschil te concentreren en dus de elektrische veldsterkte te verhogen. De verblijftijd in de poriën kan gebruikt worden om de behandeltijd te bepalen, waardoor constante (wissel)stroom bron gebruikt kan worden in plaats van een gepulseerde energiebron. Een resultaat van de kleine elektrodeafstand is dat de gemiddelde stroom omgekeerd evenredig toeneemt. Hierdoor zouden elektroden beschadigd kunnen raken, maar dit kan ondervangen worden door frequenties van 1 MHz te gebruiken. De porielengte wordt bij korte verblijftijden gelimiteerd door de maximum drukval die het membraan kan weerstaan. Om het proces stabiel te houden en een homogene behandeling te garanderen, wordt er geadviseerd om de elektroden gescheiden te

houden van het microzeef oppervlak. Ze moeten wel in de buurt van de poriën blijven om het proces energie efficiënt en het membraan oppervlak klein te houden. Het uiteindelijke ontwerp zal daardoor altijd een balans zijn tussen de poriegeometrie, de poriegrootte en de gewenste energie efficiëntie. De vrijheden in de parameterkeuzen bij het ontwerpzijn afgebakend; het ontwerp is geïllustreerd met een voorbeeld.

Het proefschrift voor de niet-wetenschapper

Pulsed electric fields (PEF): hoe cellen gedood worden door een elektrisch veld

De hedendaagse consument wil graag levensmiddelen kopen die vers smaken en gezond zijn, maar daarnaast ook nog lange tijd houdbaar. Vaak worden levensmiddelen lang houdbaar gemaakt door ze kort te verhitten om bacteriën (of andere cellen die voor het bederf zorgen) te doden. Een dergelijke manier van conserveren (pasteuriseren) leidt echter tot vermindering van kwaliteit. Neem bijvoorbeeld sinaasappelsap. Iedereen die wel eens verse sinaasappelsap perst weet dat dit anders smaakt dan de sinaasappelsap uit de supermarkt. Het sinaasappelsap uit het pak is veel langer te bewaren, maar bevat bijvoorbeeld minder vitamine C. Deze veranderingen worden onder andere veroorzaakt door het verhitten.

De levensmiddelenindustrie is daarom op zoek naar andere methoden om de bacteriën te doden zonder dat ander eigenschappen van het product veranderen. Eén van de nieuwe veelbelovende technieken is PEF (pulsed electric fields). Hierbij worden de bacteriën gedood door zeer korte elektrische schokken door het product te sturen. Bacteriën worden daarbij als het ware geëlektrocuteerd. De hoeveelheid vitamine C in het verse sinaasappelsap wordt nauwelijks beïnvloed. Dit geldt ook voor andere vitamines, eiwitten en andere stoffen. Deze techniek is vooral geschikt voor de pasteurisatie van vloeistoffen, zoals vruchtensappen of melkproducten.

Om het principe van PEF te begrijpen, is het nodig om te kijken hoe een bacterie eruit ziet. Een bacterie kan voorgesteld worden als een ballon. Hij bestaat uit een celmembraan (de ballon) waarbinnen alle andere onderdelen (organellen) liggen. Wanneer er een spanning van slechts enkele volts over de bacterie staat, ontstaat er een gaatje in het membraan (de ballon wordt lek geprikt). De cel zal dit niet overleven. Het probleem is echter dat een bacterie heel klein is. Om dan toch nog een paar volt verschil over de bacterie te hebben, moeten er in de apparatuur pulsen met een heel hoog voltage gegeven worden (zie figuur). Voor grootschalig PEF worden voltages van meer dan 15000 volt gebruikt! Ter vergelijking: uit het stopcontact komt 220 volt.
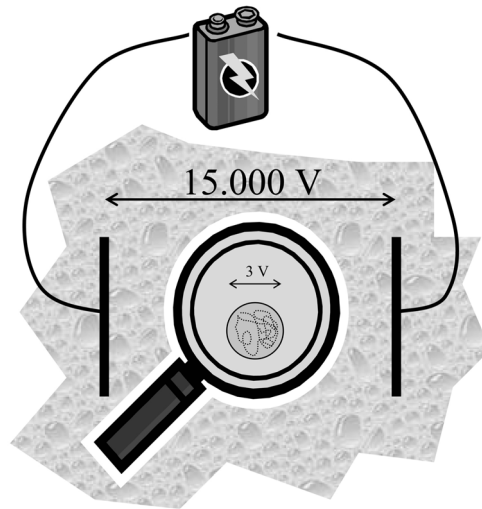
Uit het stopcontact komt echter de hele tijd stroom, terwijl er bij PEF gepulst wordt. Wanneer je stroom zet op een vloeistof, wordt de vloeistof namelijk warm. Wanneer je dit continu zou doen, zou het levensmiddel binnen een fractie van een seconde gaan koken. Daarom worden bij PEF pulsen gegeven. Deze pulsen duren erg kort: 2 tot 300 microseconden. Een microseconde is één miljoenste seconde. Een puls duurt dus 0.000002 tot 0.0003 seconde. Ter vergelijking: knipperen met je ogen duurt 0.05 seconde, de schaatswereldrecords worden gemeten met honderdste secondes (0.01 seconde); een elektrische puls bij PEF duurt dus nog duizend keer zo kort.

Om korte pulsen van zo'n hoog voltage te geven, is specialistische apparatuur nodig. Daarbij is de kans dat het mis gaat ook reëel. Wanneer er bijvoorbeeld luchtbelletjes in het vruchtensap zitten, kunnen er vonken ontstaan op de plaats waar het sap behandeld wordt, waardoor in het slechtste geval de apparatuur zwaar kan beschadigen. Ook kunnen de elektroden, de draadjes die de elektriciteit naar het sap brengen, zwaar beschadigen.

Wanneer een heel klein kanaaltje gebruikt zou worden, kan je een heel laag voltage gebruiken, in tegenstelling tot de grootschalige apparatuur. Hiermee zou het in principe mogelijk zijn om bacteriën af te doden met een huis-tuin-en-keuken batterij. Deze kleine kanaaltjes kunnen gemaakt worden met behulp van microtechnologie.

Microtechnologie

In de jaren tachtig van de vorige eeuw zijn grote vooruitgangen geboekt in de computerchip industrie. Er zijn allerlei technieken ontwikkeld waardoor buitengewoon kleine structuren gemaakt kunnen worden in bijvoorbeeld glas of silicium. Deze wetenschap wordt ook wel microtechnologie genoemd, omdat de structuren afmetingen hebben die een paar

micrometer (tot 100 micrometer) groot zijn. Dit is dus ontzettend klein! Ter vergelijking zijn in een tabel de afmetingen van een paar bekende structuren gegeven.

Structuur	Afmeting
Mier	2 tot 25 millimeter = 2000 tot 25000 micrometer
Speldeknop	1.5 millimeter = 1500 micrometer
Dikte vaneen zwarte haar	56 tot 180 micrometer
Dikte van een blonde haar	17 tot 50 micrometer
Aluminiumfolie (dikte)	6 tot 20 micrometer
Rode bloedcel	6 tot 8 micrometer
Bacterie	1 tot 10 micrometer

Microtechnologische kanaaltjes kunnen dus dunner zijn dan een haar, of even klein als aluminiumfolie. De microtechnologie is zo ver gevorderd dat het nu mogelijk is om kleine kanaaltjes te maken, hierdoor vloeistoffen te laten stromen, en ook nog eens eigenschappen van die vloeistof te meten. Zo is het bijvoorbeeld mogelijk om met een dergelijk systeem het suikergehalte te meten van bloed, waarvoor je veel minder dan een druppel bloed nodig hebt. Microtechnologie wordt momenteel al veel toegepast in inktjet printers, om kleine druppeltjes inkt te maken die op het papier terechtkomen, en in airbags, om te meten of er een botsing plaatsvindt.

Opbouw van het proefschrift

In dit proefschrift is een combinatie gemaakt van PEF en microtechnologie. Het tweede hoofdstuk bestaat uit een literatuuronderzoek; het derde, vierde en vijfde hoofdstuk beschrijven eigen onderzoeksresultaten en in het zesde hoofdstuk wordt de opgedane kennis gebruikt voor een nieuw ontwerp van een industriële PEF microreactor.

In het tweede hoofdstuk is aan de hand van de wetenschappelijke literatuur gekeken wat voor types microchips er al zijn ontworpen om gaatjes in cellen te maken met elektrische velden. De bestaande microchips konden in drie categorieën ingedeeld worden:
1.   microchips om het effect van elektrische velden op cellen te bestuderen
2.   microchips waarbij stoffen in een cel kunnen worden gebracht met een elektrisch veld
3.   microchips om cellen mee te doden

Bij de eerste categorie kijkt men wat er gebeurt met een cel wanneer er een elektrisch veld op gezet wordt. Omdat een microchip kanaaltjes kan hebben met verschillende afmetingen waarbij er enkele groter zijn dan een cel, maar ook enkele die kleiner zijn dan een cel, is het nu mogelijk om één cel te "vangen" in een chip, en onder de microscoop deze ene cel te bestuderen wanneer men een elektrisch veld erop zet. Wanneer men een niet al te sterk elektrisch veld op cellen zet, zullen deze beschadigd raken, maar uiteindelijk kunnen herstellen en blijven leven. Wanneer de cellen beschadigd zijn en er dus gaatjes in het membraan zitten, is het mogelijk om moleculen zoals DNA of een kleurstof in een cel te brengen, waardoor een cel bijvoorbeeld gekleurd kan worden. Dit wordt gedaan met chips uit de tweede categorie. De derde categorie richt zich op het doden van cellen, zoals

gebruikt wordt bij PEF. Hierbij worden sterkere elektrische velden gebruikt dan in chips van de tweede categorie, om te voorkomen dat de cellen zich kunnen herstellen.

In het derde hoofdstuk beschrijven we hoe we een microchip hebben ontworpen die bestaat uit een kanaaltje dat 1 millimeter breed is en 7 millimeter lang (nog goed zichtbaar). Het kanaaltje is echter maar 50 micrometer diep, met vernauwingen die slechts 10 micrometer diep zijn. Nog minder dan een haar dus. Het uiteindelijke ontwerp is onder andere bepaald met behulp van berekeningen op de computer. Met deze chip zijn 25 keer lagere voltages nodig als met een PEF apparaat voor een laboratorium. Wanneer je dus eerst 5500 volt nodig had, kan je nu al vooruit met 220 volt uit het stopcontact. Tenslotte is er gekeken of deze chip zich hetzelfde gedraagt als een laboratoriumopstelling. Dit bleek het geval te zijn, wat betekent dat de onderzoeksresultaten in de microchip goed vergelijkbaar zijn met resultaten in andere, grotere apparatuur.

Het vierde hoofdstuk gaat over het doden van bacteriën in de microchip. Hierbij is er vooral gekeken naar het effect van de temperatuur waarbij de elektrische velden worden toegepast. Wanneer er een elektrisch veld aangelegd wordt in vloeistof en er een electrische stroom door de vloeistof loopt, wordt de vloeistof warmer, net zoals een gloeilamp ook warm wordt. Omdat de microchip zo klein is, is het relatief eenvoudig om de temperatuur goed te controleren. Dit komt doordat er heel veel oppervlakte is in vergelijking tot het volume. Vergelijk het met een kopje heet water dat staat af te koelen. Het water zal veel sneller afkoelen wanneer je het over de tafel uitgiet, omdat dezelfde hoeveelheid water nu over een veel groter oppervlak uitgespreid is, terwijl de hoeveelheid water toch gelijk is. Dit is in een microchip ook het geval; een microchip heeft naar verhouding heel veel oppervlak, waardoor vloeistof heel snel afkoelt. Met de gebruikte microchip kon de temperatuur zeer goed gecontroleerd worden, waardoor we heel nauwkeurig de elektrische effecten konden meten. Hieruit bleek onder andere dat PEF in stapjes gebeurt; je kunt een vloeistof met cellen een elektrische puls geven, en daardoor zal een aantal cellen dood gaan, maar door meer pulsen te geven gaan er veel meer cellen dood. Daarbij gaat het doden van bacteriën ook veel beter bij hogere temperaturen. Bij 45 °C gaan er veel meer cellen dood dan bij kamertemperatuur. Dit zijn temperaturen die nog altijd veel lager zijn dan de temperaturen die gebruikt worden bij normale warmte pasteurisatie.

In het vijfde hoofdstuk is er gekeken naar het doden van gistcellen in twee verschillende microchips: de microchip die hierboven beschreven is, waarin een heleboel cellen tegelijk worden behandeld, en een microchip waarin het mogelijk om één gistcel te vangen, een puls te geven en vervolgens te kijken wat er dan met deze cel in de tijd gebeurt (zoals ook beschreven in het tweede hoofdstuk). Hierbij werd een oranje kleurstof gebruikt, waarmee gekeken kon worden of een cel dood of levend was. In de eerste microchip zagen we dat meerdere pulsen ervoor zorgden dat meer cellen dood gingen. In de tweede microchip zagen we dat één cel meer oranje werd naarmate er meer pulsen gegeven werden, wat aangeeft dat meerdere pulsen toenemende schade aanrichten bij een cel. Verder was het gedrag in beide microchips goed vergelijkbaar. Door vergelijken van de twee onderzoeksmethoden werd getoond dat de pulsen snel achter elkaar gegeven moeten worden omdat er anders een gedeeltelijk herstel van het celmembraan optreedt. Daarmee

hebben we op twee verschillende manieren aangetoond, dat meer pulsen leiden tot een betere behandeling (meer bacteriën gedood).

Door een microchip kan slechts een kleine hoeveelheid vloeistof stromen. De vraag is dan ook hoe we de kennis, die we in het onderzoek hebben opgedaan kunnen toepassen op een grotere schaal. Om grote hoeveelheden vloeistof te behandelen kunnen er zeer veel microtechnologische kanaaltjes naast elkaar worden gebruikt. Het slimst is het om ie kanaaltjes dwars door een dikke(re) plak silicium of glas te maken. Je kan dan erg veel kanaaltjes vlak naast elkaar plaatsen, terwijl de aan- en afvoer van vloeistof gemakkelijk is. Dat kan, door een recent ontwikkelde microzeef te gebruiken. Dit is een plaat met daarin een heleboel kleine gaatje naast elkaar. Het geheel vormt een zeef, maar met gaatjes die in de orde van 1 tot 50 μm zijn. In hoofdstuk zes is er een theoretisch ontwerp geschetst van zo'n PEF microzeef, en geanalyseerd onder welke voorwaarden het zou kunnen werken. Je kan bijvoorbeeld niet een te grote druk op het systeem zetten, omdat de zeef dan kapot kan gaan. Een andere voorwaarde is dat het systeem elektrisch efficiënt moet zijn. Het is niet goed om maar een paar procent van de elektrische energie te gebruiken om de cellen te doden omdat er dan teveel warmte wordt geproduceerd. Door rekening te houden met dit soort beperkingen was het mogelijk om vuistregels te geven waarmee de dimensies van een grootschalige PEF microreactor kunnen worden bepaald.

Het hierboven beschreven onderzoek in dit proefschrift was een eerste aanzet om te kijken wat de mogelijkheden van PEF in microtechnologische kanaaltjes zijn. Het is nog maar de vraag of dit ooit zal worden toegepast in de industrie. Dit proefschrift toont echter duidelijk aan dat het mogelijk is om bacteriën te doden in een microreactor, ook op productieschaal, wat de belangrijkste zaken zijn waarmee rekening gehouden moet worden bij het ontwerp en wat de potentiële voordelen zijn.

Nawoord

Vier jaar een promotieonderzoek doen… Dit klinkt in het begin heel erg lang, maar als ik er achteraf op terugkijk is de tijd ontzettend snel gegaan. Van de ene onderzoeksvraag rol je in de andere vraag, en dan blijken vier jaren erg kort te duren! Dat het allemaal zo snel leek te gaan, kwam natuurlijk ook voor een groot deel door iedereen om me heen.

Remko, aan enthousiasme geen gebrek. Wanneer ik dacht vast te zitten en de resultaten weinig reden tot juichen gaven wist jij te laten zien dat er veel mogelijk was met de resultaten. Als jij en Erik met z'n tweeën in een discussie over modellen raakten was net alsof je in een achtbaanrit beland raakte. Dat was echt ontzettend stimulerend! Bedankt voor je begeleiding deze vier jaren. Ik vind het een eer jou als promotor te hebben!

Erik, ontzettend bedankt voor alle tijd en moeite die ook jij in dit proefschrift hebt gestoken. Ik ken weinig mensen die zo creatief zijn! Het aantal nieuwe ideeën en Mathcad modelletjes was soms overstelpend. We hadden nog jaren door kunnen gaan met het onderzoeken van nieuwe elektrisch veld effecten op cellen in microchips.

Paul, copromotor, zonder jou als initiator bij A&F had dit project niet plaatsgevonden. Ik heb de gesprekken over dit onderzoek, onderzoek in het algemeen en alle andere dingen die zoal voorbij kwamen ontzettend gewaardeerd! Hennie, je was een wandelende PEF encyclopedie. Ook de experimentele hulp is ontzettend van pas gekomen! Harald, bedankt voor de hulp met de labschaal experimenten. Irene, jouw kennis over het PEF-en van bacteriën kwam ontzettend goed van pas bij de *Lactobacillus* experimenten.

Dit project was een samenwerking met de Universiteit Twente. Ana, should I write this in Dutch or English? I will do it in English for your convenience, although I should keep talking Dutch to you, so you can practice (and your Dutch is already quite good!). I think we succeeded in getting a nice object of study with the yeast. The experiments in both of our systems have resulted a nice article! Good luck with your own promotion!

Regina, bedankt voor je inzet voor dit project. Jouw microtechnologie kennis heeft voor een belangrijk deel het ontwerp bepaald van de microreactor. Albert, volgens mij kan je dagenlang voorbeelden uit je mouw blijven schudden van microtech toepassingen. Bedankt voor de samenwerking! Jan, bedankt voor het maken van de chips. Ronny, bedankt dat jullie bij Micronit ook chips voor me hebben gemaakt.

De houder voor de chips werd gemaakt door de werkplaats. Hans en Hans, ik kon altijd weer met kleine en grotere praktische vragen langskomen. Dat heeft me een hoop tijd bespaard!

Wouter, het was een hoop werk om die vesicles een beetje reproduceerbaar te maken! Ondanks alle problemen heb je echter goed doorgezet en een mooi afstudeerverslag

119

afgeleverd. Jouw metingen op lab schaal met vesicles zijn dan ook terechtgekomen in het derde hoofdstuk. En alle kennis van PEF die je hebt oppgedaan komt bij je baan dus ook nog van pas! Gert, het was een hele kunst om een mooi confocaal volume te krijgen, maar onder het motto "Als ge het niet wit, kit" lukte het uiteindelijk toch om de temperatuur confocaal te meten. Jouw metingen zijn uiteindelijk niet direct teruggekomen, maar het meetprincipe is wel gebruikt in hoofdstuk vier. Wouter, Gert, bedankt voor alle werk!

Ciska, Eira en Karin, ik heb het ontzettend leuk gevonden om de Canada reis samen met jullie te organiseren. Hoewel het ons financieel en organisatorisch af en toe knap lastig werd gemaakt, is het toch een geslaagde AIO reis naar Canada geworden! Eira, bedankt dat je paranimf wil zijn!

Sybrand, Ruurdtje, Jan-Willem, de jaarlijkse barbecues zijn een activiteit die we vol moeten blijven houden! Syb, bedankt dat je mijn paranimf wil zijn.

Natuurlijk heb ik niet alleen op de vakgroep op een kamer gezeten. Detmer en Ronald, de sponzenboys, toen ik begon op de vakgroep werd ik door jullie verwelkomd op de kamer met de opmerking dat niemand het langer dan een half jaar met jullie uit had gehouden. Uiteindelijk zaten jullie niet meer op de kamer toen ik vertrok... Het was erg leuk met alle gesprekken over nutteloze onderwerpen zoals Spongebob en hoe je een wereldkaart op moet hangen. Daniël, Koen en Marieke, jullie vulden de plaatsen alweer gauw op en zorgden voor een hoop nieuwe gezelligheid met Chiel Montagne, Zeeuws meisje foto's en kameretentjes.

En natuurlijk zijn er nog een heleboel ander collega's. Gerben, een ski vakantie met zoveel sneeuw (en zoveel Schnappi) had ik nog niet eerder meegemaakt! Sandra, in het begin stond ik veel hoger op de burgelijkheidsladder, maar uiteindelijk naderden we elkaar toch weer erg dicht. Jan-Willem, ik hoop dat je blij was met je twee elanden in je opstelling. Het stond erg gezellig met de kerstdagen. Maarten, het was een mooie vakantie in Zuid-Afrika. We blijven nog we even tot elkaar veroordeeld bij het NIZO! Eduard, bedankt voor de discussies over microtechnologische structuren en de eindeloze stroom nutteloze, maar leuke feitjes. Sebastiaan Haemers, je hebt je lab en apparatuur weer voor jezelf. Het was gezellig om samen op een lab experimenten te doen! Marieke B., Sebastiaan Hoekema, Julita, Jan, Cynthia, Tim, Jeroen, Mark, Rene, Maartje, Janneke, Marleen, Hylke, Olivier, Hadi, Maurice, Marjoleine, Jeroen en iedereen die ik nu nog vergeet, bedankt voor de leuke tijd bij proceskunde! Joyce, Hedy, zonder jullie zou de vakgroep niet blijven draaien. Bedankt voor alle hulp met de administratieve klussen!

Thies en Gerry, jullie belangstelling was altijd motiverend. Thies, ik denk dat er weinig mensen zijn die het proefschrift zo uitgebreid hebben gelezen! Ingrid en Erwin, de Senegal vakantie was precies de goede voorbereiding om te beginnen aan het laatste stuk van het promotietraject!

Pap, mam, vier jaar lang deed ik onderzoek wat misschien niet altijd even duidelijk was voor jullie. Met de lekensamenvatting is daar wel verandering in gekomen! Deze is mede door jullie hulp geworden zoals hij is. Bart, Michiel, dit was dus waar ik vier jaar aan heb

gewerkt Jullie hadden er allemaal altijd vertrouwen in dat er een proefschrift kwam. Bedankt voor deze steun!

Mirjam, als laatste en allerbelangrijkste wil ik jou bedanken. Als ik het even niet zag zitten beurde je me op, als je het idee had dat het niet opschoot spoorde je me aan. Hoewel je zelf geen promotie zou willen doen, zou dit proefschrift er zonder jou niet hebben gelegen! Er zitten vele avonden en weekenden in, maar vanaf nu kunnen we weer leuke dingen gaan doen in de weekenden en blijft er weer meer tijd over. Laten we er de komende jaren een mooie tijd van maken!

Curriculum vitae

Martijn Fox werd op 13 augustus 1978 geboren te Eindhoven. In 1996 behaalde hij zijn gymnasiumdiploma aan het Lorentz Lyceum in Eindhoven. In september 1996 begon hij zijn opleiding bioprocestechnologie aan Wageningen Universiteit, waar hij de technologische specialisatie volgde. Hij deed een afstudeervak bij de leerstoelgroep proceskunde en via proceskunde bij het Rijksinstituut voor volksgezondheid en milieu. Gedurende een half jaar deed hij een stage bij Chalmers University in Göteborg, Zweden. Hij studeerde in november 2001 af. Van januari 2002 tot en met maart 2006 werkte hij als promovendus bij de sectie proceskunde van Wageningen Universiteit op het project "Electric field mediated processes" in samenwerking met Agrotechnology and food innovations en de Universiteit Twente. Vanaf mei 2006 in hij werkzaam als scientist bij de afdeling processing van NIZO food research.

Training activities

Discipline specific activities
Unified approach to mass transfer, OSPT, 2004
Numerical methods in chemical engineering, OSPT, 2005
Short Course on Microsystems Technology, Montreux, 2004
Cleanroom course Mesa+, UTwente, 2003
Nanotech 2004, Montreux, Switzerland, 2004 (presentation)
Micronanoconferentie, 2005 (presentation)
2nd, 3rd, 4th and 5th Netherlands Process Technology Symposium, 2002-2006

General courses
Scientific writing, CENTA, 2004
PhD student week VLAG, 2002
Career perspectives, WGS, 2005
Teaching and supervising MSc students, OWU, 2002

Optionals
Brainstorm week Food and Bioprocess Engineering Group, 2003
Brainstorm week Food and Bioprocess Engineering Group, 2005
PhD trip Process Engineering, South Africa, 2002
PhD trip Process Engineering, Canada, 2004